NTNU
Norwegian University of
Science and Technology

# Experimental Investigation of Vertical Forces in Pure Sway Motion for a Free Surface Roll Damping Tank

Eirik Hereid Spilde

Summary of Thesis Objective

NTNU
Norwegian University of
Science and Technology

MASTER THESIS IN MARINE HYDRODYNAMICS

SPRING 2016

FOR

Stud.techn. Eirik Hereid Spilde

Roll-damping tanks

The candidate shall perform model experiments with a roll-damping tank. In the tests the student shall analyze how the vertical forces in sway depend on:

- the excitation amplitude
- excitation frequency
- tank filling ratio

Special focus should be paid to the frequencies close to the eigenfrequency. If possible the student shall come up with a formula expressing the vertical forces based on the above mentioned parameters.

In the thesis the candidate shall present his personal contribution to the resolution of the problem within the scope of the thesis work. Theories and conclusions should be based on mathematical derivation and logic reasoning identifying the various steps in the deduction. The

original contribution of the candidate and material taken from other sources shall be clearly defined. Work from other sources shall be properly referenced. The candidate should utilize the existing possibilities for obtaining relevant literature. The thesis should be organized in a rational manner to give a clear exposition of results, assessments and conclusions. The text should be brief and to the point, with a clear language.

The thesis shall contain the following elements: A text defining the scope, preface, list of contents, summary, main body of thesis, conclusions with recommendations for further work, list of symbols and acronyms, references and appendices. All figures, tables and equations shall be numerated. It is supposed that Department of Marine Technology, NTNU, can use the results freely in its research work by referring to the student's thesis. The thesis deadline is June 10.

<div align="center">

Håvard Holm

Professor/supervisor

</div>

Clarification of Individuality

I hereby assure that I wrote this thesis independently, autographically and without using any other sources than stated

08/06/2016 Eirik Spilde

_____

Date / Signature

Eirik Hereid Spilde

eirik.spilde@gmail.com

Preface

As part of earning a Master of Science degree at the Norwegian University of Science and Technology a master thesis must be written. The following work is a result of that, and constitutes to the graduation of the 2-year master program in Marine Technology-hydrodynamics.

In this thesis roll damping tanks are addressed, more specifically a free surface tank. Roll damping tanks are roll motion dampening systems for ships. When a ship rolls there is a coupling of both roll and sway motion. If the ship is equipped with a roll damping tank there will be a dampening of the motions, given appropriate conditions. This is due to the counteracting moment produced by the motion of water in the tank. Finding a relationship between the forces that arise in such tank due to the motion of water, and parameters such as water filling level, excitation amplitude, and excitation frequency have -to the best of knowledge- not been investigated before. If such a relationship is found it will make it possible to predict the forces that arise if several of the parameters are known. Hence, the topic in this thesis involves the examination of the vertical forces that develop in pure sway motion of a free surface tank, to see if they depend on the above mentioned parameters.

I would like to thank Prof. Håvard Holm for his knowledge and excellent guidance through this period. Furthermore, I would like to thank Einar Ueland for his help with Matlab. My understanding of the program was close to nonexistent, and without his superior knowledge this thesis would not have been doable.

Lastly, I would also like to thank my parents, and my little brother. Without their support the completion of this master program would not have been possible.

Eirik Hereid Spilde

Trondheim, 8 June 2016

Summary

In this thesis the objective was to perform experiments in pure sway motion of a model roll damping tank, to try and locate a connection between the vertical forces that develop in such condition, and several influential parameters such as excitation frequency, excitation amplitude and water filling level. The frequency spectrums of the vertical forces that develops at these differing parameters were instrumental in the investigation. If a relationship existed, it was attempted to get a full mathematical description of this connection.

First an in depth investigation of the theoretical aspects of a free surface roll damping tank was performed. Here important subjects were discussed, such as the different main roll damping tank configurations available. Furthermore, as a free surface tank was the main area of focus, the thesis goes on to perform a thorough theoretical investigation of the function and design of such a tank. Lastly, as the tank was a model of a full scale version, the thesis proceeds to discuss different theoretical aspects related to scaling in a hydrodynamic problem.

After a thorough literature review of the free surface tank, the proceeding chapters goes on to discuss the overall setup, and the general preparation procedure applied before the experimental investigation. Described first is the model rig and the instrumentation applied in the setup. Then, the experiment strategy used when conducting the investigation is explained, as well as the preparation procedure of the equipment in the setup. Finally, the thesis proceeds to describe the filtering procedure, including the study performed of the accuracy of the experimental data; as part of ensuring that the results are trustworthy these procedures were necessary.

In the closing chapters of this thesis the post-processing of the experimental data is performed. Here the results are analyzed, and it is found that a connection exists between the vertical forces and the parameters tested. A full mathematical description was not established, however, the relationship was partially expressed by a Gaussian model which were a function of the excitation frequency.

Sammendrag

Målet i denne oppgaven var å utføre eksperimenter i ren svai bevegelse for en modell rulledempingstank, for å prøve å finne en sammenheng mellom de vertikale krefter som utvikler seg i en slik tilstand, og flere innflytelsesrike parametere som eksitasjonsfrekvens, eksitasjonsamplitude og vannpåfyllingsnivå. Frekvensspektrene til de vertikale kreftene som utvikles under eksitasjon ved de ulike parameterne var instrumentale i undersøkelsen. Dersom et forhold eksisterte, ble det forsøkt å få en fullstendig matematisk beskrivelse av denne forbindelsen.

Først ble det utført en grundig gjennomgang av de viktigste teoretiske aspektene ved en fri overflate rulledempingstank. Her ble det diskutert viktige temaer som for eksempel hvilke hoved rulledempingstank konfigurasjoner som er tilgjengelig. Videre, ettersom en fri overflate rulledempingstank var hovedtemaet i undersøkelsen, ble funksjon og design av en slik tank diskutert. Til slutt, ettersom tanken var en modell av en fullskala versjon, fortsetter oppgaven med å diskutere ulike teoretiske aspekter knyttet til skalering i et hydrodynamisk problem.

Etter en gjennomgang av den viktigste teorien til en fri overflate rulledempingstank, tar de følgende kapitlene for seg oppsettet som ble brukt under testingen, samt de generelle forberedelser som ble gjennomført før den eksperimentelle undersøkelsen. Først blir modellriggen og instrumenteringen beskrevet. Deretter blir strategien som brukes ved gjennomføring av undersøkelsen forklart, så vel som forberedelsesprosedyren til utstyret som ble anvendt. Til slutt fortsetter oppgaven med å beskrive filtreringen, inkludert inspeksjonen som ble utført av nøyaktigheten til de eksperimentelle dataene; som en del av å sikre pålitelige resultater var disse prosessene nødvendig å gjennomføre.

I de avsluttende kapitlene til denne avhandlingen blir etterbehandlingen av de eksperimentelle dataene utført. Her blir resultatene analysert, og det blir avdekket at et forhold eksisterer mellom de vertikale kreftene og parameterne som ble testet. En fullstendig matematisk beskrivelse av dette forholdet ble ikke etablert, istedenfor ble det delvis uttrykt ved hjelp av en Gaussisk formel som var en funksjon av eksitasjonsfrekvensen.

List of Contents

List of Figures

List of Tables

Nomenclature

a Acceleration $[m/s^2]$

A_{44} Added mass coefficient in roll $[Nms^2/rad]$

a_n Gaussian coefficient [-]

B_{44} Damping coefficient in roll $[Nms/rad]$

β Frequency ratio [-]

b_n Gaussian coefficient [-]

b Tank breadth $[m]$

c_r Critical damping coefficient $[Nms/rad]$

c Damping coefficient $[Nms/rad]$

c_n Gaussian coefficient [-]

C_{44} Restoring coefficient in roll $[Nm/rad]$

D Diameter $[m]$

$e^{(x)}$ Exponential [-]

ε_t Phase angle $[rad]$

ε_v Relative elongation $[m]$

E_v Volume elasticity $[N/m^2]$

$\forall_{ship}$ Water displacement from ship hull $[m^3]$

F_e	Elastic forces in the fluid $[N]$
f	Excitation frequency $[Hz]$
F	Force $[N]$
F_N	Froude number [-]
$f(x)$	Gaussian function of x
F_g	Gravitational Forces $[N]$
F_i	Inertia forces $[N]$
F_p	Pressure Forces $[N]$
F_4^{exc}	Roll excitation moment due to incident waves $[Nm]$
F_s	Surface Forces $[N]$
F_4^t	Tank roll moment $[Nm]$
$F(f)$	Total vertical force [N]
F_v	Viscous Forces $[N]$
g	Acceleration of gravity $[m/s^2]$
$\overline{\Delta GM}_T$	Quasi-steady decrease in transverse metacentric height $[m]$
$\overline{GM}_T$	Transverse metacentric height $[m]$
h	Water depth $[m]$
I_{tank}	Area moment of the water line in the tank $[m^4]$
I_{44}	Inertia coefficient in roll $[Nms^2/rad]$

J	Advance coefficient [-]
K_{ta}	Tank roll moment amplitude [Nm]
k	Wave number [m^{-1}]
L	Length [m]
λ	Scale [-]
l	Tank length [m]
λ	Wave length [m]
μ	Fluid viscosity coefficient [Ns/m^2]
M	Moment [Nm]
M	Structural mass [kg]
n	Constant, positive integer [-]
n	Rate of revolution [s^{-1}]
$\ddot{n}_4$	Roll acceleration [rad/s^2]
n_{4a}	Roll amplitude [rad]
n_4	Roll angle [rad]
$\dot{n}_4$	Roll velocity [rad/s]
ω	Angular frequency of excitation [rad/s]
ω_1	Lowest natural frequency [rad/s]
ω_n	Natural frequencies [rad/s]

ω_0	Natural frequency of a one-degree system $[rad/s]$
P	Pressure $[N/m^2]$
ρ	Fluid density $[kg/m^3]$
R	Radius $[m]$
r_i	Residual [-]
Re	Reynolds number [-]
S	Summed square of residuals [-]
σ	Surface tension $[N/m]$
T_1	Highest natural period $[s]$
T_n	Natural periods $[s]$
t	Time $[s]$
U	Velocity $[m/s]$
ξ	Damping ratio [-]
y_i	Observed response value [-]
$\hat{y}_i$	Predicted response value [-]

Abbreviations

COG   Centre of Gravity

DLF   Dynamic Load Factor

FFT   Fast Fourier Transform

HMS   Her Majesty's Ship

SS   Steam Ship

AD   Analogue to Digital

CF   Curve-Fitting

1. Introduction

Ship stability has been a challenging topic since the construction of the first floating vessel. The stability of a ship is defined as its ability to prevent lateral motions, or roll motions. A ship may experience roll motion in many ways. For instance, an incorrectly placed COG will result in a highly unstable ship.

In early days (1700th century etc.) when the propulsion system of a ship consisted of sails, the most durable method to maintain ship stability - both in calm waters and in heavy sea states - was to construct a ship that was heavier in the bottom than in the top. This was accomplished by designing a ship hull with a bulb shaped cross section, and loading it with ballast.

As time passed significant changes were introduced to the development and design of ships. The most noticeable design change was that sails were replaced by steam engines. As a result, this obviously led to large changes in the transverse stability of ships in general. The consequence of this stability change was greater roll motion. To counteract this stability, it was necessary to develop countermeasures.

In the late 1800s William Froude's research on roll motion led to the development of bilge keels, which increased the hydrodynamic resistance, resulting in less rolling. However, as more knowledge about hydrodynamics was acquired, more advanced and more responsive approaches to prevent roll motion were investigated. These approaches included both active and passive motion stabilization designs. In present days, multiple active and passive designs for improving roll instability have been tested and confirmed. This includes everything from bilge keels, roll damping tanks and skegs, to counterweights, adjustable fins, gyrostabilizers etc. Roll damping tanks are the topic in this thesis, and will be discussed further.

1.1. Motivation and Objective

When a ship rolls there is a coupling of both roll and sway motion. If the ship is equipped with a roll damping tank, and given appropriate conditions, sloshing of the water in the tank will occur. This sloshing has the potential to create large dynamic and hydrostatic forces. Subsequently, the effectiveness of the tank depends on several parameters. This can be parameters such as excitation amplitude, excitation frequency and water filling level. The arrangement of these parameters will decide whether the tank contribute to damping, do nothing at all, or enhance the motion. However, - to the best of knowledge - something which has not been examined before, is finding a method for predicting the forces and moments that arise during such motion. This would be practical in any situation, given that such a method exists. Since this topic has not been examined before, there exists no restrictions on where to begin.

For instance, the vertical forces that arise during excitation in pure sway motion of a free surface tank is an interesting topic. By varying several of the parameters, such as excitation amplitude, excitation frequency and water filling level, the vertical forces will change. To be able to predict these vertical forces that develop in pure sway, a connection that relates the forces to the different parameters must be found. Consequently, the objective in this thesis is to investigate if a possible connection exits by performing several experiments where these parameters are varied. The frequency spectrums of the vertical forces are of interest in this investigation. If similarities exist it will be attempted to extrapolate a more specific equation based on several of the parameters capable of predicting the vertical forces present in pure sway.

1.2.   Thesis Structure

This thesis contains nine main chapters. The first chapter is an introduction to the present work ahead. In the second chapter the theoretical aspects of a roll damping tank are discussed to give insight and understanding of their function and purpose.

The experimental procedure starts in chapter three and ends in chapter six. In chapter three the sloshing rig, and model free surface tank used for the experiments is presented. Furthermore, the instrumentation that is used is explained. In chapter four the experiments are planned, and the execution strategy for the experiments is explained. Additionally, the calibration procedure of the instrumentation, as well as zeroing is described. In chapter five the pre-processing of the experimental data is clarified. This chapter explains the filtering procedure of the experimental data. Furthermore, it addresses why it is important to acquire an adequate recording length of the tests. Lastly, in chapter six the post-process of the experimental data presented. This chapter includes the analysis of the frequency spectrums, and it includes the curve-fitting procedure to locate a similarity in the results.

After the experimental procedure have been listed and explained the final chapters, chapter seven to nine, concludes the thesis. In chapter seven an error analysis is performed. When conducting model experiments there are many factors that affect the end results, some can be controlled, others can't. This chapter summarizes those topics. In chapter eight the conclusion for the thesis is presented, and finally, in chapter nine future work regarding this topic is discussed.

2. Background and Theoretical Basis

Presented in the following chapter is a summary of relevant literature for a roll damping tank. First a little background on why roll damping tanks came to be is described, followed by a description of the two main versions of a roll damping tank. Furthermore, a discussion of the theoretical background of a free surface tank such as design and function is presented. These sections describe how the different dimensions of such a tank is decided, to multiple natural periods, the purpose of a hydraulic jump and the theory behind damping. Finally, scaling in general and scaling of a free surface tank is discussed.

2.1. Roll Damping Tank Configurations

When it comes to roll motion stability using water tanks there are two specific configurations available. The first is the free surface tank, and the second is the U-tube tank. These two types come in both passive and active form, where active devices stabilize the vessel by continuously counteracting the response from the environment using automatic control systems, and passive devices, which do not have any automatic control systems, and rely solely on the motion of the water in the tank to help stabilize the vessel.

2.1.1. Free Surface Tank

Passive roll damping tanks were the first to arrive the main reason being that they required less advanced technology to operate. As stated by Moaleji & Grieg (2007) the first legitimate type of passive roll stabilizing device was the free surface tank. According to Perez & Blanke (2012) one of the earliest attempt of using such a tanks was due to the ship HMS Inflexible

(1876) and questions raised about the ships stability. This ship was designed so that if her un-armored ends were compromised; the buoyancy of the armored center section would keep her afloat. In fact, in 1878 according to Goodrich (1968) the committee on the Inflexible presented a study on the damaged stability[1] of the ship, in which they concluded that if a limited number of the un-armored compartments were flooded with water, and the water level was low enough, the flooded compartments would actually contribute to an increase in roll righting power. The results from these experiments lead to the ship being fitted with permanent water chambers in the un-armored compartments in 1880. These water chambers were, as mentioned earlier, an early attempt of a free surface tank.

To fully verify the function of the free surface tank additional experiments on the HMS Inflexible were carried out by Watts and Froude in 1882, and they tested the tanks with different water depths. They concluded that the roll damping for the HMS Inflexible was optimal when the tanks were about half-full. The explanation behind Watts and Froude's conclusion was that at 50% water filling the ratio between the lowest natural frequency mode of the tanks at this filling level, and the natural frequency of the ship was close one. Thus, when the excitation frequency was equal to the natural frequency of the ship, and thereby the lowest natural frequency of the water in the tank, resonance at this mode would occur producing a great counteracting roll moment (Moaleji & Grieg, 2007).

It can be noted that today it is said that a good water level benchmark for an effective operating free surface tank is 60% of total tank volume. This is because several experiments through time have concluded that the first natural period at 60% filling gives the largest counteracting roll moment. This roll moment is the result of a hydraulic jump. A Hydraulic jump is a quite distinctive condition of the water motion, and occur at excitation frequencies near and at the lowest natural frequency when shallow water conditions are satisfied. Hydraulic jump will be discussed later in section 2.2.2 (Moaleji & Grieg, 2007).

In free surface tanks without restrictions severe sloshing could be an issue. Hence, damping grids might be included in the design. When roll motion is exerted on a ship with a free

---

[1] Damaged stability is when the hull of a ship has been compromised leading to a change in the ships COG (Pettersen, 2007).

surface tank the fluid in the tank will flow form one side to the other. As stated by Akyildiz & Ünal (2005) this phenomenon is called sloshing and occurs in partially filled tanks, like a free surface tank. The severity of sloshing depends on the tank geometry, depth of the liquid, and amplitude and nature of the tank motions. For severe sloshing water will impact the roof of the tank introducing saturation of the tank's roll damping effect, and the tank will lose it purpose as roll damping device. Thus, by including damping grids the water movement is restricted to a certain amount, lowering the possibility for saturation.
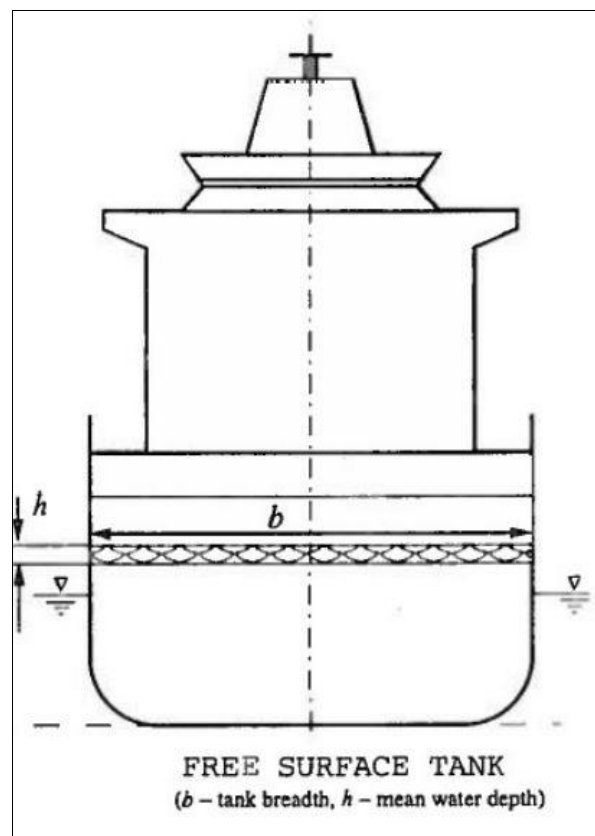

Figure 1 Free surface tank (Faltinsen O. M., 1990)

In modern ship design the most effective location for a free surface tank is close to the bridge, or above the center of rotation (COG). The main reason being that the roll motion is higher further away from this location. Thus, by installing the tank in a position above the COG it is more effective, and it can be reduced in size compared to if it was installed below the center of rotation.

The disadvantage of this concept is the reduced stability due to a reduced transverse metacentric height $\overline{GM}_T$. For instance, during slow sway motions/roll motions the shifted mass of water will have opposite effect and can contribute to the vessel capsizing.

2.1.2.   U-Tube Tank

The U-tube tank solved the problems related to sloshing, the reduced stability and the dangers presented by the shifting of water mass during slow sway/roll motions. The first U-tube tank was developed by Frahm (1911). It consisted of two reservoirs that were connected at the bottom by a water duct. They were also connected at the top by an air duct. The purpose of the air connection (duct) between the two reservoirs was so to allow free oscillation of the water in the tanks. Additionally, the air duct was equipped with throttling valves that enabled throttling or even stop of the airflow. This provided - to some level - the possibility to adjust the oscillations of the water in the tanks to the condition of the sea, but not as effective as an active system. Moreover, it gave the option to stop the movement of water between the tanks by simply blocking the air connection with the valves. In so doing the air to flow freely between the reservoirs and the movement of the water was significantly reduced. Since air is compressible the precision of the control was not perfect - the water would not be completely still - but the movement of the fluid could be regarded as negligible. This type of U-tube tank designed by Frahm was classified as an air controlled passive roll damping tank. Presented Figure 2 is an illustration of Frahm's U-tube tank on the SS Ypiranga.
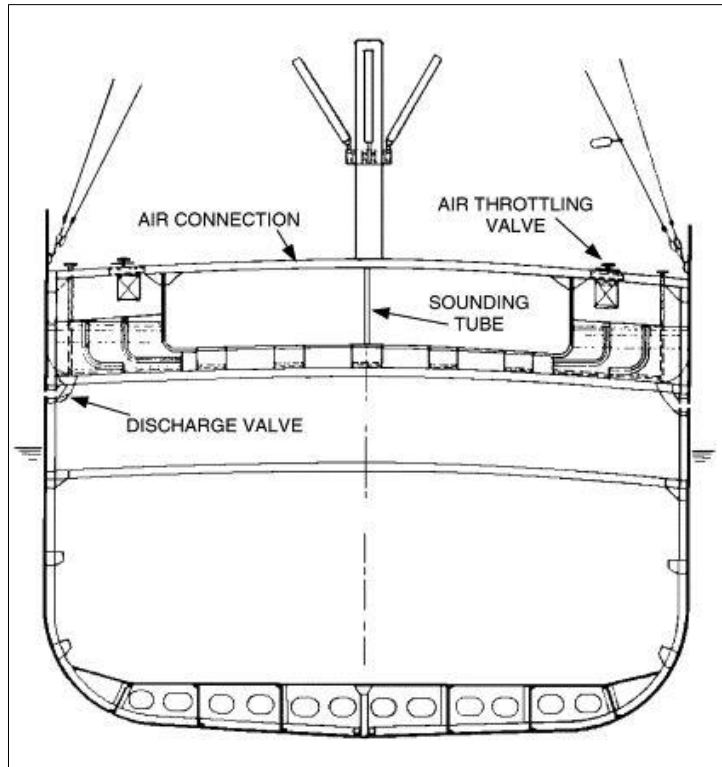
Figure 2 Frahm's U-tube tank on SS Ypiranga (Moaleji & Grieg, 2007)

There were also drawbacks with the passive U-tube tank designed by Frahm. For instance, Biles (1925) determined that there was only considerable roll reduction at resonance frequency. The roll was increased at other frequencies. Biles stated that this was a result of no active controls to manipulate fluid velocity in the tank. Hence, the transfer of water was mainly dependent on the rolling motion. By being dependent on the rolling motion to start the transfer of water, the inertia of water has a much larger effect on the tanks ability to dampen the roll motion at other frequencies than the natural frequency.

In modern days the U-tube tanks still apply the same concepts as the one suggested by Frahm, the difference is that most tanks today include active systems to operate it more efficiently. Hence, the delay due to waters inertia could be circumvented as the system would always be one step ahead of it.

2.2. Function of a Free Surface Tank

The objective in this master thesis incorporates a model of a free surface tank. Hence, In the following section the function of a free surface tank will be discussed.

2.2.1. Natural Periods in a Free Surface Tank

The natural frequency or Eigen frequency is the frequency at which a system oscillates in the absence of any driving force or damping force. For free surface tanks there are several natural frequency modes at which the fluid in the tank oscillates. These modes are characteristic wave patterns. When calculating these modes non-viscous fluid motions are assumed (Pettersen, 2007).

The relationship between any period (T) and the frequency (ω) is defined as:

$$T = \frac{2\pi}{\omega} \tag{1}$$

From the explanation above the natural periods for water in a free surface roll damping tank with an arbitrary water depth is then defined as (Pettersen, 2007):

$$T_n = 2\pi / \sqrt{\left(\frac{\pi n}{b} \text{gtanh}\left(\frac{\pi n}{b} h\right)\right)} \tag{2}$$

where n is a positive integer varying with time, g is the gravity constant, b is the tank breadth and h is the water depth in the tank. Since increasing n in the equation gives lower period values, it can be concluded that T_1 represents the highest natural period of the system, or lowest natural frequency (Pettersen, 2007).

Furthermore, from Pettersen (2007) the wavelength in a free surface tank is given as:

$$n\lambda = 2b \tag{3}$$

From these equations it is logical that n = 1, which is the mode with the highest natural period (T_1) or lowest natural frequency of the tank, will give the largest hydrostatic and dynamic forces and therefore the largest counteracting roll moment. This fact is demonstrated well in *Figure 3*.
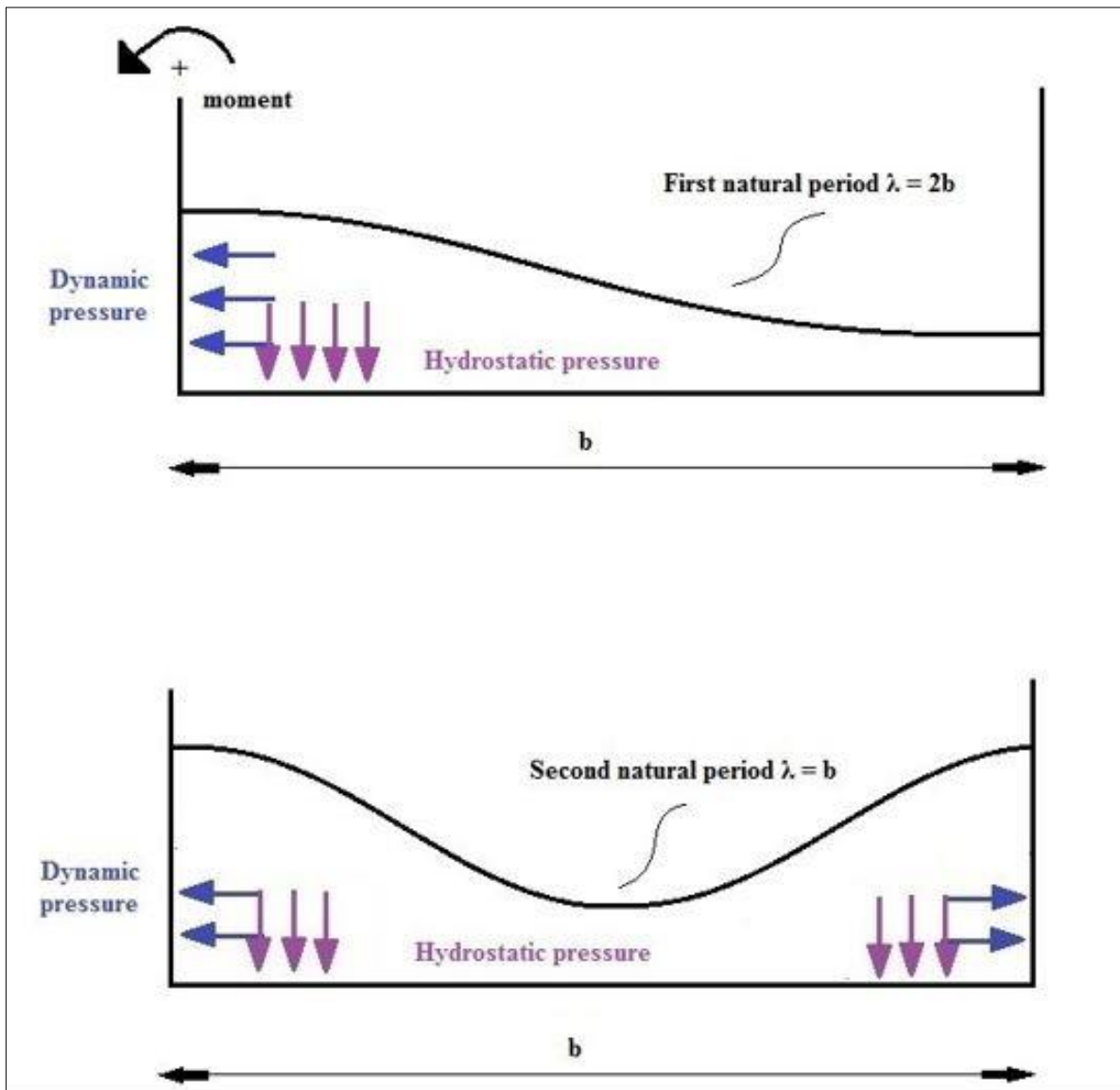

Figure 3 Example of some natural periods in a tank

As seen from the figure, when n = 1 most of the water is concentrated on one side of the tank. Hence, this mode gives the counteracting roll moment.

By tuning the water depth, you can change the natural frequencies of the tank. Hence, the tank can have an infinite number of natural frequencies. This fact is also clearly demonstrated in Figure 4 below which is based on equation (2). Consequently, a free surface tank is well suited for ships with a wide range of loading conditions (the natural period of a ship depends on the "stiffness" of the ship which varies with loading condition).
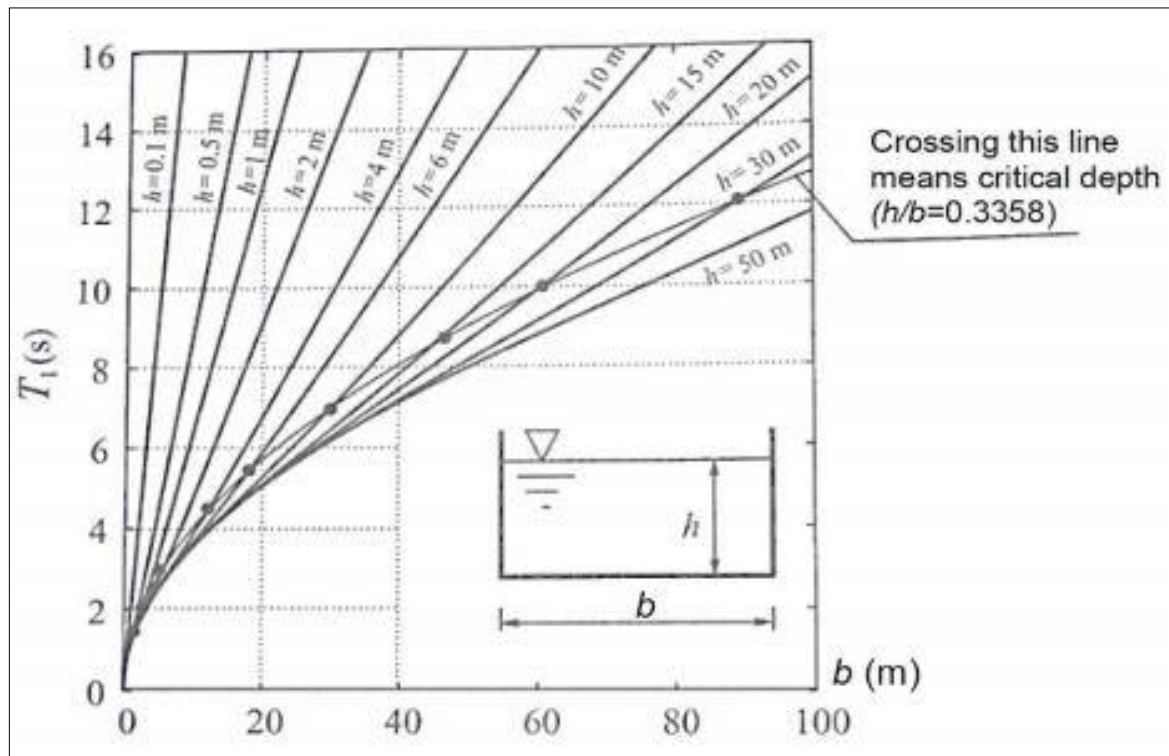
Figure 4 Natural sloshing period for a rectangular tank versus the tank breadth for different filling levels (Faltinsen & Timokha, 2009)

2.2.2.   Hydraulic Jump in a Free Surface Tank

As stated by Verhagen & Van Wijngaarden (1965), if a tank containing a fluid are exposed to forced oscillations and $\frac{h}{b} \ll 1$, where b is the tank breadth and h is the fluid depth, the motions of the fluid can be described by linear or non-linear shallow water theory depending on the frequency of oscillation.

According to the linear shallow water theory the amplitude of the wave elevation of the fluid in the tank is proportional to $\{\cos\left(\frac{\pi\omega}{2\omega_n}\right)\}^{-1}$, where ω is the angular frequency of the excitation and ω_n is the natural frequencies given as:

$$\omega_n = \frac{\pi n}{b} \sqrt{gh} \qquad (4)$$

where g is the gravitational acceleration.

As the equation for the amplitude of the wave elevation shows, at frequencies close to the resonance frequencies (mode 1,2…) the wave amplitude goes towards infinity. In conclusion, when $\omega \approx \omega_n$ the theory is no longer valid. Hydraulic jump, which occurs at excitation frequencies close to and at the lowest natural frequency (ω_1) of the tank, assuming shallow water conditions, is therefore a non-linear phenomenon based on non-linear shallow water theory. It should be noted that the excitation amplitude must also be larger than a threshold value in order for the jump to transpire. This theory is formed from the theory for one-dimensional gas flow under similar resonance conditions by Chu & Ying (1963). Refer to paper by Verhagen & Van Wijngaarden (1965) for a more detailed description.

In short the requirements for a jump to occur are shallow water conditions, the forcing frequency must be close to or at the lowest natural frequency and the excitation amplitude must be larger than a threshold value. This hydraulic jump will then have a great effect on the fluid transfer by producing a great counteracting roll moment. The larger the roll angle (excitation amplitude) of the tank the greater the hydraulic jump and thereby the counteracting roll moment. However, if the angle is too great the water will reach the top of the tank leading

12

to saturation. As previously mentioned saturation means that the effects from roll damping die out. Furthermore, as stated by Van den Bosch & Vugts (1966), the roll moment is not increasing linearly with the roll amplitude. The reason being that the strength of the hydraulic jump is proportional to the square root of the roll amplitude. Presented in Figure 5 is a visualization of a hydraulic jump.
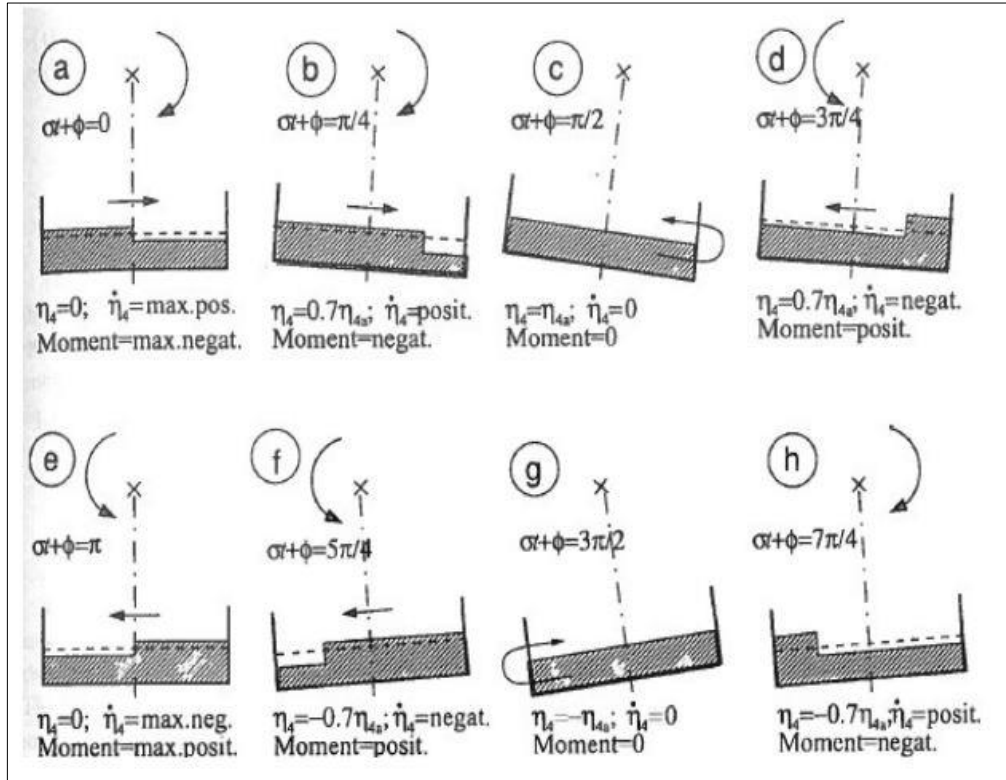

Figure 5 Position of hydraulic jump during one period of roll at resonance (Faltinsen & Timokha, 2009)

In Figure 5 a harmonic roll motion with frequency equal to the lowest natural frequency of the tank is excited. From Faltinsen & Timokha (2009) The roll angle n_4 is given as:

$$n_4 = n_{4a} \sin(\omega t) \tag{5}$$

and the angular roll velocity $\dot{n}_4$ is given as:

$$\dot{n}_4 = \omega n_{4a} \cos(\omega t) \tag{6}$$

Almost a full roll period is illustrated in Figure 5. As the figure shows the position of the jump changes over time. In position (a) the roll angle n_4 of the tank is zero, and the hydraulic jump is at the middle of the tank. As $n_4 = 0 \rightarrow \omega t = 0$. From this it is observed that maximum positive angular roll velocity is achieved in position (a). The moment at this position is therefore also at its maximum, and as the arrow around the center of roll indicates, the moment is negative and counteracting the positive roll motion. The same is true for position (e), however the maximum angular roll velocity is negative and the resulting maximum moment is positive.

A hydraulic jump in a free surface tank will always occur at excitation frequencies close to and at the natural frequency of the tank if shallow water conditions are satisfied and if the excitation amplitude is larger than a threshold value.

2.2.3.   Damping in a Free Surface Tank

To understand the damping effect on a ship caused by an anti-rolling tank, information about the hydrodynamic roll moment produced by the flow of water in the tank is needed. The rectangular tank from Figure 5 is applied. Regular incident waves are assumed. As previously stated the roll angle and roll angular velocity for the tank were given as:

$$n_4 = n_{4a} \sin(\omega t) \tag{7}$$

$$\dot{n}_4 = \omega n_{4a} \cos(\omega t) \tag{8}$$

From Faltinsen & Timokha (2009) the roll moment produced by the water in the tank is then given as:

$$F_4^t = K_{ta} \sin(\omega t + \varepsilon_t) \tag{9}$$

$$F_4^t = K_{ta} \sin(\omega t) \cos(\varepsilon_t) + K_{ta} \cos(\omega t) \sin(\varepsilon_t) \tag{10}$$

$$F_4^t = \frac{K_{ta}}{n_{4a}} \cos(\varepsilon_t) n_4 + \frac{K_{ta}}{\omega n_{4a}} \sin(\varepsilon_t) \dot{n}_4 \tag{11}$$

Furthermore, from Faltinsen & Timokha (2009) the uncoupled roll equation in regular waves for a ship without bilge keels and equipped with such a tank is given as:

$$(I_{44} + A_{44})\ddot{n}_4 + B_{44}\dot{n}_4 + C_{44}n_4 = F_4^{exc} + F_4^t \tag{12}$$

Where $I_{44}\ddot{n}_4$ is the ships moment of inertia in roll, $A_{44}\ddot{n}_4$ is the ships added moment in roll, $B_{44}\dot{n}_4$ is the ships damping moment in roll due to external wave generation, $C_{44}n_4$ is the ships restoring moment in roll, F_4^{exc} is the roll excitation moment due to incident waves and finally, F_4^t which is the extra excitation moment on the ship caused by the water in the free surface tank. Equation (12) can be written as:

$$(I_{44} + A_{44})\ddot{n}_4 + \left(B_{44} - \frac{K_{ta}}{\omega n_{4a}} \sin(\varepsilon_t)\right)\dot{n}_4 + \left(C_{44} - \frac{K_{ta}}{n_{4a}} \cos(\varepsilon_t)\right)n_4 = F_4^{exc} \tag{13}$$

As seen from equation (13) the damping contribution from the free surface tank on the ship roll motion comes from the damping coefficient $\frac{K_{ta}}{\omega n_{4a}} \sin(\varepsilon_t)$. Furthermore, it is observed from equation (13) that maximum damping effect is achieved when there is a 90° phase difference between the motion of the water in the tank and the rolling motion of the ship. At this phase difference the frequency ratio between the excitation frequency and natural frequency is equal to one. Thus, this phase difference is the reason why the roll moment

15

produced by the tank during resonant sloshing of mode one is able to function as a stabilizing/damping moment on the ships rolling motion.

To better identify how the ratio between excitation frequency and natural frequency influence the response of a system a factor has been derived. This factor is called the dynamic load factor (DLF). A one-degree system is used as an example. For a damped system this factor is given as:

$$DLF = \frac{1}{\sqrt{(1 - \beta^2)^2 + (2\xi\beta)^2}} \tag{14}$$

where β is the frequency ratio and ξ is the damping ratio.

The frequency ratio β is defined as:

$$\beta = \frac{\omega}{\omega_0} \tag{15}$$

The damping ratio ξ is defined as:

$$\xi = \frac{c}{c_r} \tag{16}$$

where c is the damping coefficient and c_r the critical damping coefficient.

In *Figure 6* the dynamic load factor for a one-degree damped system (one natural frequency mode) is presented as a function of frequency ratio β for different damping ratios ξ.

Figure 6 Dynamic load factor as a function of frequency ratio β for given damping ratios ξ (Larsen, 2015)

As a recurring observation from Figure 6 the response of the system is larger (increasing even more so as the damping of the system diminishes) when the excitation frequency equals the natural frequency of the system (β = 1) compared to other frequency ratios. In this case resonance occur. At decreasing frequency ratio from one (β<1) the response of the system diminishes, and the system approaches a more stiffness dominated condition. The excitation frequency is minor compared to the natural frequency of the system, and as a result no significant inertia forces develops in the system. At increasing frequency ratio from one (β>1) the response of the system also diminishes, but now the system approaches a more inertia dominated condition. The excitation frequency is large compared to the natural frequency of the system, and as a result no significant stiffness forces develops in the system. From this information it can be concluded that damping of a system is only viable in the resonance region of the system.

Furthermore, in Figure 7 the phase angle between load and response is presented as a function of frequency ratio for different damping ratios. From this figure it is seen that for all damping ratios the phase angle between load and response is 90° or $\frac{\pi}{2}$ radians for a frequency ratio equal to one. Thus, this confirms that at a phase difference of 90 ° between load and response maximum response will be achieved.
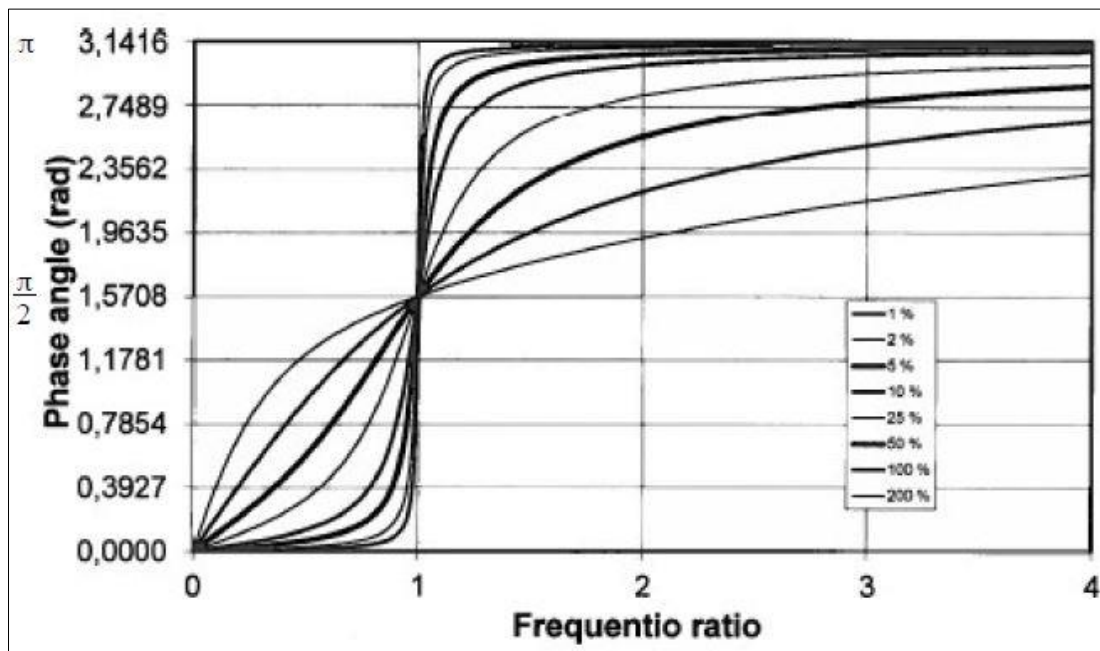
Figure 7 Phase angle between load and response as a function of the frequency ratio for given damping ratios (Larsen, 2015)

2.3.   Design of a Free Surface Tank

The dimensions of importance in the design of a free surface tank is tank length l, tank breadth b and water depth h.

Faltinsen (1990) stated that the tank breadth is in most cases chosen to be the cross-sectional breadth of the ship hull. Furthermore, Faltinsen & Timokha (2009) stated that the tank length

can be determined from the ratio $\frac{\overline{\Delta GM_T}}{\overline{GM_T}}$, where $\overline{\Delta GM_T}$ is the quasi-steady decrease (free surface correction) in $\overline{GM_T}$. Quasi-steady conditions denote that the excitation frequency is much lower than the lowest natural frequency of the water in the tank. Typical region of the ratio $\frac{\overline{\Delta GM_T}}{\overline{GM_T}}$ for free surface tanks lies between 0.15 and 0.3. By knowing this ratio, the tank length can be found. From Pettersen (2007) $\overline{\Delta GM_T}$ is defined as:

$$\overline{\Delta GM_T} = \frac{I_{tank}}{\forall_{ship}} \tag{17}$$

where I_{tank} is the area moment of the water line in the tank, and $\forall_{ship}$ is the water displacement of the ship. I_{tank} is given as:

$$I_{tank} = \frac{lb^3}{12} \tag{18}$$

As previously mentioned the water depth in the tank influence the natural periods (modes) of the water in the tank. As stated by Pettersen (2007) the dispersion relation for finite water depth is applied in equation (2) on page 9, as a free surface tank has finite water depth. This relation is defined as:

$$\omega^2 = kg\ tanh(kh) \tag{19}$$

where k and g is the wave number and acceleration of gravity respectively. The wave number is defined as:

$$k = \frac{2\pi}{\lambda} \tag{20}$$

By applying equation (3) on page 9 for the wave length λ, the wave number can be rewritten to:

$$k = \frac{\pi n}{b} \tag{21}$$

The dispersion relation can now be expressed as:

$$\omega_n^2 = \frac{\pi n}{b} g \, tanh\left(\frac{\pi n}{b} h\right) \tag{22}$$

Since shallow water conditions ($\frac{h}{b} \ll 1$) apply in a free surface tank $tanh\left(\frac{\pi n}{b} h\right) \approx \frac{\pi n}{b} h$. From this information the natural periods from equation (2) page 9 can be rewritten to:

$$T_n = \frac{2b}{\sqrt{gh} \, n} \tag{23}$$

The water depth can now be found by rearranging equation (23) to:

$$h = \frac{1}{n} \frac{1}{g} \frac{4b^2}{(T_n)^2} \tag{24}$$

Since largest dynamic and hydrostatic pressures exists at the first natural period of a free surface tank, it is always designed such that in the ships initial condition the ratio between the first natural period of the tank, and the natural period of the ship remains close to, or at 1.0, all while simultaneously satisfying shallow water conditions.

2.4. Scaling

When designing new systems, it is important to ascertain a level of guarantee that the design will perform according to what was initially intended. Therefore, among other things, experimentation with a model is performed to verify predicted design performance, discover design errors that reduce performance and improve etc. These physical models are supposed to represent full-scale systems as close as possible at a much smaller scale. However, to confirm that these experiments will produce accurate results in a scaled down version, proper knowledge about scaling law is required. By applying these laws, the proper properties of the model can be determined (Steen, 2014).

In fluid dynamics dimensional analysis can be applied to obtain a group of meaningful dimensionless quantities for relevant variables. In so doing a functional relationship between the different parameter groups can be established for all flow-governing quantities. The scaling laws are obtained by taking the ratios of the different forces (Steen, 2014).

As stated by Steen (2014) the following conditions must be satisfied to obtain similarity in the forces between model scale and full scale:

- Geometrical similarity
- Kinematic similarity
- Dynamic similarity

2.4.1. Geometrical Similarity

A constant length scale exists between structures that has geometrical similarity in model and full scale. This length scale is given as:

$$\lambda = \frac{L_F}{L_M} \tag{25}$$

where L_F and L_M are any dimensions of the model/full scale structure. Furthermore, this requirement is also applied to the surrounding environment, as model experiments would be quite pointless if a corresponding scaled environment condition for the given model could not be formed. However, this state is not easy to achieve in practical testing. For instance, in full scale a ship is exposed to an almost unrestricted extent of surrounding water. In model scale such condition is physically impossible to reproduce. Consequently, physical boundaries will always be present in model testing, and as a result, they will influence the results to some degree (Steen, 2014).

2.4.2.   Kinematic Similarity

When it comes to kinematic similarity, the velocity ratios in model scale must be equal to the velocity ratios in full scale. The implication is geometrical similarity of the flow motions in both cases. An example of kinematic similarity has been described by Steen (2014), and involves forward speed of a ship and the rotational speed of the ships propeller:

$$\frac{U_F}{n_F(2\pi R_F)} = \frac{U_M}{n_M(2\pi R_M)} \tag{26}$$

or

$$\frac{U_F}{n_F D_F} = \frac{U_M}{n_M D_M} = J_F = J_M \tag{27}$$

where U is the ship speed, n is the rate of revolution of the propeller, R is the propeller radius, D is the propeller diameter and J is the advance coefficient.

2.4.3.   Dynamic Similarity

A requirement to obtain dynamic similarity is to have equal ratio at model and full scale between the different force contributors present in the problem. As stated by Steen (2014) the following force contributors can in principle be of importance in a hydrodynamic scaling problem:

1. Inertia Forces, $F_i \propto \rho \frac{dU}{dt} L^3 = \rho \frac{dU}{dx}\frac{dx}{dt} L^3 = \rho U^2 L^2$ $\hspace{2em}$ (28)

2. Viscous Forces, $F_v \propto \mu \frac{dU}{dx} L^2 = \mu U L$ $\hspace{2em}$ (29)

3. Gravitational Forces, $F_g \propto \rho g L^3$

$$(30)$$

4. Pressure Forces, $F_p \propto p L^2$

$$(31)$$

5. Elastic forces in the fluid, $F_e \propto \varepsilon_v E_v L^2$

$$(32)$$

6. Surface Forces, $F_s \propto \sigma L$

$$(33)$$

where

L: Length

U: Velocity

ρ: Fluid density

g: Gravitational acceleration

μ: Fluid viscosity coefficient

ε_v: relative elongation

E_v: Volume elasticity

σ: Surface tension

If several of the force contributors mentioned above are of importance in a hydrodynamic scaling problem, it is in general not possible to achieve dynamic similarity between all the different force contributors simultaneously. However, in all hydrodynamic scaling problems dynamic similarity between gravity forces is possible. Hence, equality in Froude number between model and full scale must be achieved. Therefore, if such a problem presents itself one can use Froude scaling to account for other scale effects such as for instance Reynolds number (Steen, 2014).

In testing of a free surface tank surface waves generated by the motion of the tank are the main contributor to the forces present in the tank. Since the formation of surface waves is governed

by gravitational forces, it implies that for these conditions equality in Froude number for model and full scale must be achieved.

From Steen (2014) the Froude scaling law (assuming geometrical and kinematic similarity) is defined as the relation between inertia and gravity forces and given as:

$$\frac{F_i}{F_g} \propto \frac{\rho U^2 L^2}{\rho g L^3} = \frac{U^2}{gL} \tag{34}$$

Applied on model and full scale this requirement gives:

$$\frac{U_M^2}{gL_M} = \frac{U_F^2}{gL_F} \tag{35}$$

$$\frac{U_M}{\sqrt{gL_M}} = \frac{U_F}{\sqrt{gL_F}} = F_N \tag{36}$$

where F_N is the Froude number. As previously mentioned surface waves are gravity waves. Froude number equality will therefore give equality in wave resistance coefficient.

Steen (2014) mentioned that from this scaling method the following physical parameters can be derived:

Structural mass: $\qquad M_F = \frac{\rho_F}{\rho_M} \lambda^3 M_M$ $\qquad\qquad\qquad\qquad$ (37)

Force: $\qquad\qquad F_F = \frac{\rho_F}{\rho_M} \lambda^3 F_M$ $\qquad\qquad\qquad\qquad\quad$ (38)

Moment: $\qquad\quad M_F = \frac{\rho_F}{\rho_M} \lambda^4 M_M$ $\qquad\qquad\qquad\qquad\quad$ (39)

Acceleration: $\qquad a_F = a_M$ $\qquad\qquad\qquad\qquad\qquad$ (40)

Time: $\qquad\qquad t_F = \sqrt{\lambda}\ t_M$ $\qquad\qquad\qquad\qquad\qquad$ (41)

Pressure: $\qquad\quad P_F = \dfrac{\rho_F}{\rho_M}\lambda P_M$ $\qquad\qquad\qquad\qquad\qquad$ (42)

As fresh water is commonly used in model scale tests in comparison to seawater, which is usually the case in full scale, the ratio $\dfrac{\rho_F}{\rho_M}$ is included to account for differences in fluid density.

3. Experimental Setup

In this chapter the experimental setup is presented. First the rig used during the experiments is described, followed by a general description of the instrumentation applied in the setup.

3.1. The Two-Degree of Freedom Sloshing Tank Simulator

The model used during the different experiments consists of two parts; a two degree of freedom rig, and a free surface tank which is installed on top of the rig. Naturally the degrees of freedom are roll and sway, and since the rig is equipped with two electric servos, it allows for both individual and combined motion of these two. Furthermore, the rig also enables the possibility for installation of different tank configurations like a U-tube tank, but during the tests performed in this thesis a free surface tank was applied.

The free surface tank mounted on the rig was a 1:20 scale model of a full scale version. Just as for a full scale free surface tank, the coordinate system was defined as lying such that the tank rolls around the x-axis. The y-axis would then lay along the breadth of the tank. See *Figure 8* for a presentation of the model tank's coordinate system and dimensions.
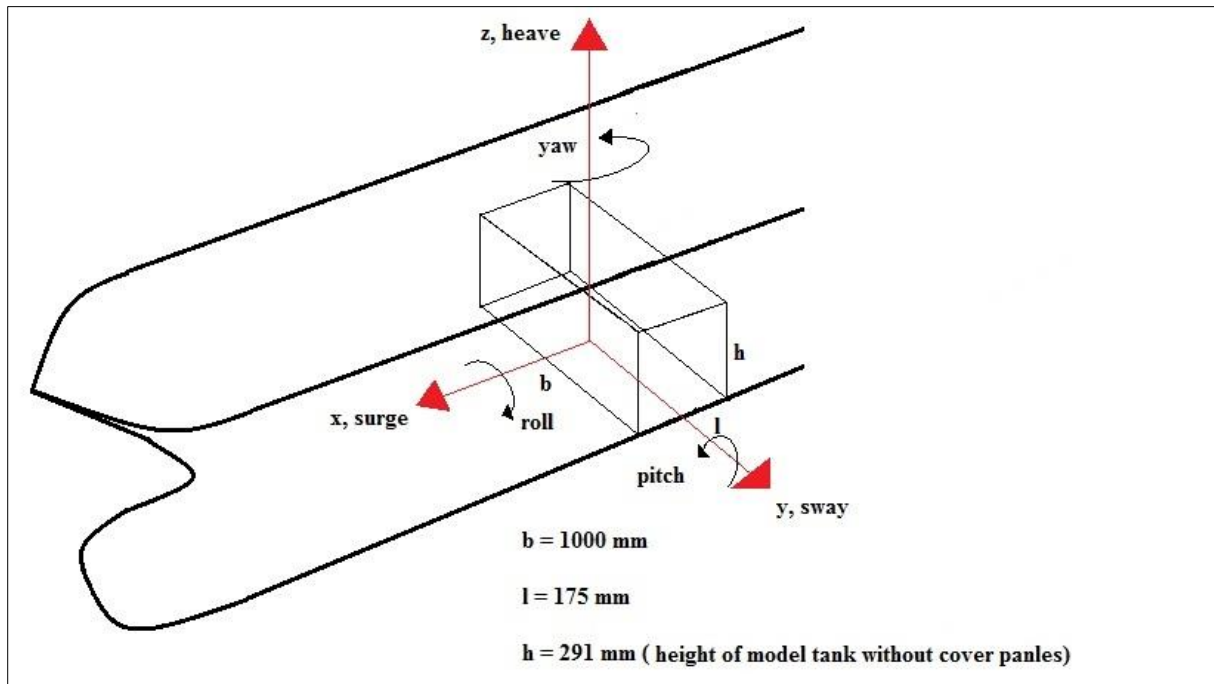
Figure 8 Definition of model tank's dimensions and coordinate system

The model tank had adjustable top covers, meaning that the tank height could be altered. However, full scale free surface tanks do not have an adjustable tank height; all the dimensions are fixed according to what was specified in the design process. Due to this fact, the tank height of the model needed to be specified. To reduce the risk for water slamming against the top covers it was decided that the tank height should be as large as possible. This would make the tank dimensions unrealistic compared to that of a real free surface tank, but in return it would reduce the risk for water slamming against the top covers during large motions. If water hits the top of the tank, not only does it lead to saturation of the damping effect, but it introduces much more complicated water motions.

Upon first arrival at the tank the top covers were not placed at their highest location, but quite close. However, as stated by Håvard Holm, since they were fixed quite firmly in that location with tape to prevent spilling of water during large motions, it was decided to use that position in the tests. With this position of the top covers the max tank height was 22cm.

There were five transducers installed on the rig; two strain gauges to measure vertical forces, one strain gauge to measure horizontal forces and finally, two displacement gauges to measure roll and sway motion respectively. As a side note the tank did allow for the use of damping grids. However, the tests performed in this thesis does not include the use of damping grids. See *Figure 9* for a presentation of the different components and finished assembly of the sloshing simulator.
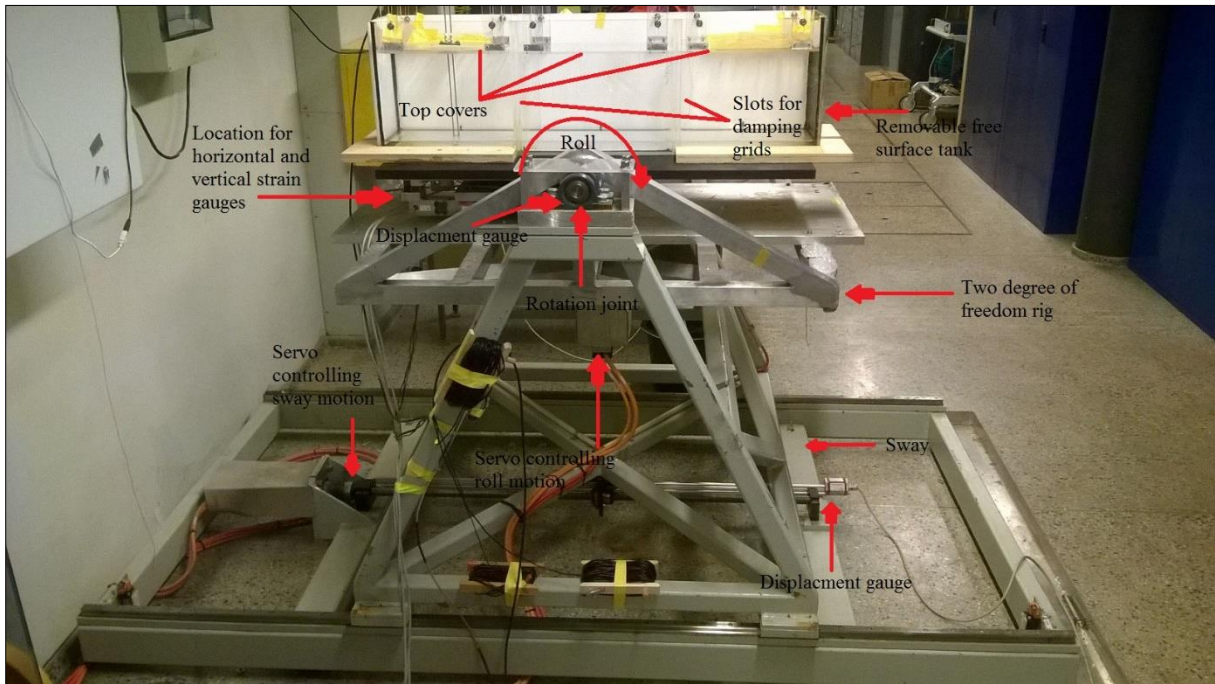
Figure 9 Finished assembly of sloshing simulator and description of different components

3.2.   Instrumentation

A typical instrumentation setup is used in the tests; this includes the model which shall be tested, transducers, a signal amplifier, an A/D converter, and computers for operation and data acquisition/ analysis. Presented in Figure 10 is the setup of the data acquisition system applied for the two degree of freedom sloshing simulator.
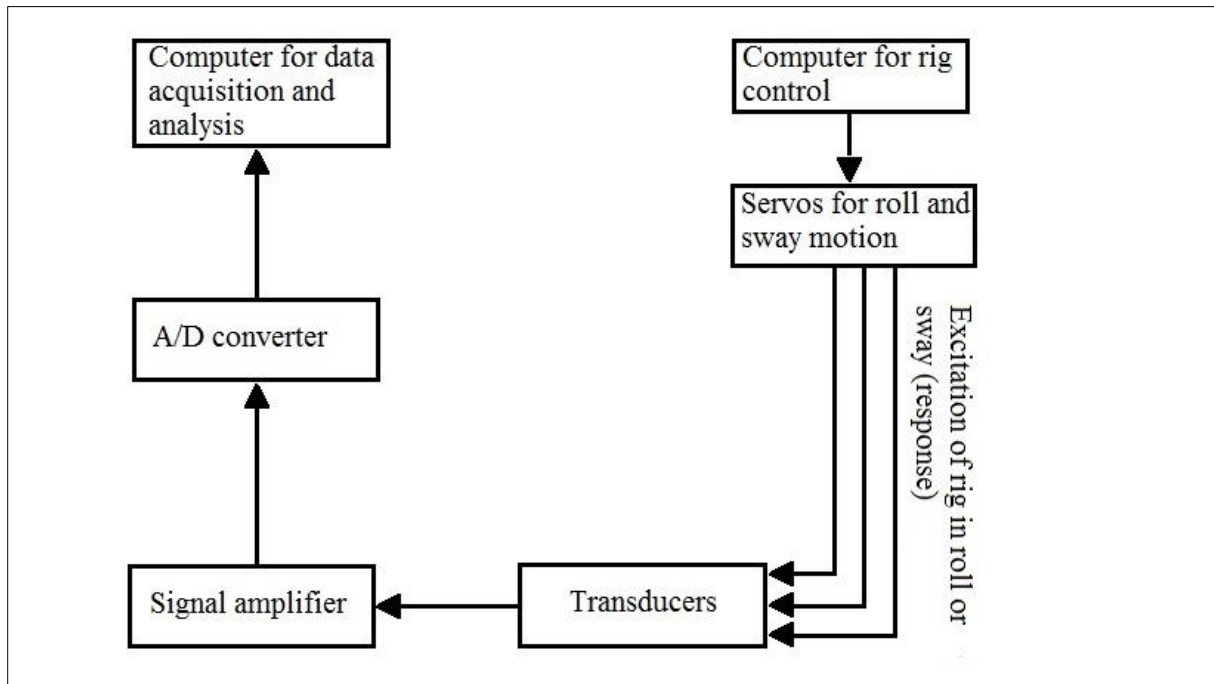
Figure 10 Schematic of the data acquisition system for the two degree of freedom sloshing simulator

The computer for rig control sends analogue signals to the rig servos. The rig then move according to what was specified by the input parameters. Then the transducers register the motions and forces present during the test and transfer them as analogue signals. Next, a signal amplifier strengthens the analogue signals from the transducers. Finally, the amplified analogue signal is converted to digital signal. These digital signals are then sent to the computer for data acquisition and can now be analyzed.

The data acquisition program is called MGCReg 4.1 or Catman and records time domain results in real time. Furthermore, in this program eight channels were established; one for time, two for roll and sway displacement, one for horizontal force, two for vertical forces, one for total vertical force (the two vertical forces added together) and one for roll moment. The channel that was applied in the experimental investigation were the one for total vertical force. Lastly, the program gives the option to store the results as different files, all from xlx files to bin files for further analysis in separate programs.

4. Experimental Preparation

In this chapter the experimental preparation will be explained. To establish a good understanding of the experimental layout, the execution strategy for the experiments is discussed. Then, to ensure trustworthy experimental results, the calibration and zeroing procedure is addressed.

4.1.   Assembling an Execution Strategy for the Experiments

As previously stated the objective in this thesis was to try to find a connection between the vertical forces and the excitation amplitude, excitation period and water filling level in pure sway motion for a roll damping tank. Hence, numerous experiments were planned and executed with the differing parameters to gain as much data as possible. Then the frequency spectrums of this data would be plotted and examined. By performing multiple experiments, it would allow for similarities to be spotted more easily should they be present.

Twenty-four main experiments were performed including two preparation tests. The first preparation test was conducted just to verify that the Matlab script was practicable (see appendix B for Matlab script), while the second test was performed to optimize the accuracy of the experimental data retrieved from each test run. See section 5.2 for a more detailed discussion of this procedure.

In the main experiments three different sway amplitudes were tested, eight different water levels, and seventeen different excitation periods. Each experiment had a defined sway amplitude, and water filling level, which were tested with seventeen different excitation frequencies. This corresponded to a total amount of twenty-four main experiments. The sway amplitude varied from 4mm to 8mm, the water filling level varied from 16cm to 2cm (shallow

water condition is valid), and the excitation period from -2 to +2 seconds from the resonance period (full scale). Furthermore, the sway amplitude varied by 2mm each time, the water filling level by 2cm, and the excitation period by 0.25s from the full scale resonance period. Presented in Figure 11 is a matrix of the different test combinations.
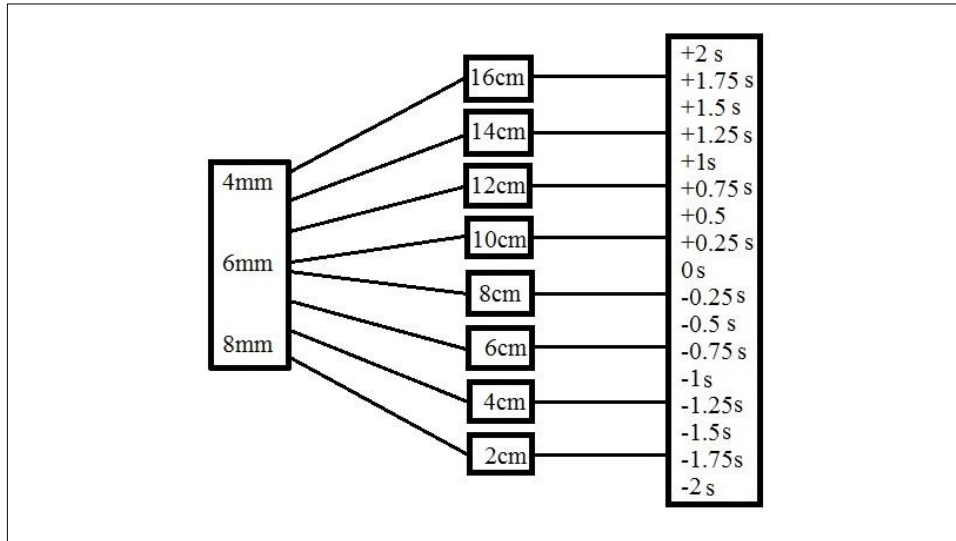
Figure 11 Matrix of test combinations

In order to find the different model scale excitation periods for each water height, the water heights corresponding full scale natural period first had to be calculated. Mentioned earlier in the thesis, the model tank was a 1:20 scale version of the full scale tank. Stated in chapter 2.3 the natural periods of a roll damping tank if shallow water conditions apply was defined as:

$$T_n = \frac{2b}{\sqrt{gh}\, n} \tag{43}$$

Only the first natural period is of interest, as this condition gives the largest dynamic and hydrostatic pressures. Hence, by applying equation (53), the full scale resonance period at mode 1 for the different water heights could be calculated. Thereafter, the corresponding full scale excitation periods, ranging from -2 to +2 seconds from the resonance period, could be found. Finally, by then applying equation (41) on page 25 the model scale excitation periods for each water height could be attained. It should be noted that the program for rig control

required an excitation frequency defined in hertz. Therefore, the model scale excitation periods needed to be elevated by minus one before they were implemented into the program. Presented below is a demonstration of the calculation procedure explained above at a water filling level of 12 cm, and excitation period at 1 s above resonance.

$$T_{1\ full\ scale} = \frac{2 * 1m * 20}{\sqrt{9.81\ m/s^2 * 0.12m * 20 * 1}} = 8.24\ s \tag{44}$$

$$T_{excitation\ full\ scale} = T_{1\ full\ scale} + 1 = 9.24\ s \tag{45}$$

$$T_{excitation\ full\ scale} = \sqrt{\lambda} * T_{excitation\ model\ scale} \tag{46}$$

$$T_{excitation\ model\ scale} = \frac{9.24\ s}{\sqrt{20}} = 2.07\ s \tag{47}$$

$$f_{excitation\ model\ scale} = \frac{1}{2.07\ s} = 0.484\ Hz \tag{48}$$

This procedure was applied for all periods and water heights. However, to save time, the calculations were performed in excel. Shown in Table 1 is a presentation of the final excel setup which was applied for each experiment. See appendix A for a complete list of tables of all the main experiments performed.

Table 1 Excel setup applied for each main experiment. Three different experiments are demonstrated in this table

									R								
Waterfilling level [m]	0,12																
Excitation amplitude pure sway [mm]	4 (7)	6(8)	8 (9)														
Full scale resonance period: T_f [s]	8,24																
Model scale resonance period: T_m [s]	1,84																
y	-2	-1,75	-1,5	-1,25	-1	-0,75	-0,5	-0,25	0	0,25	0,5	0,75	1	1,25	1,5	1,75	2
Range of excitation period full scale : T_f-y [s]	6,24	6,49	6,74	6,99	7,24	7,49	7,74	7,99	8,24	8,49	8,74	8,99	9,24	9,49	9,74	9,99	10,24
Range of excitation period model scale: T_f-y/20^0,5 [s]	1,40	1,45	1,51	1,56	1,62	1,68	1,73	1,79	1,84	1,90	1,96	2,01	2,07	2,12	2,18	2,23	2,29
Range of excitation frequency model scale [Hz]	0,716	0,689	0,663	0,639	0,617	0,597	0,578	0,559	0,542	0,527	0,511	0,497	0,484	0,471	0,459	0,447	0,437

4.2. Calibration and Zeroing

As for every model experiment a calibration of the measuring equipment is necessary to ensure trustworthy results. The transducers for the sloshing tank simulator was calibrated by MARINTEK engineers before they were initially installed on the rig. This was done by measuring their output for a given response, and then calculate a calibration factor which was implemented in to the measurement program (Catman in this instance).

If the transducers required recalibration after initial installation the transducers would need to be disassembled from the rig again. However, as stated by the MARINTEK engineers these transducers have been under heavy use earlier, and they have always projected little to zero deviation with measured results (digital force gauge) during inspection of the accuracy of their initial calibration. Furthermore, it was also stated that the transducers used in this model were of the sturdy type; for them to require recalibration they would have to be subjected to a large amount of force in the form of a hard knock etc. Hence, a recalibration was deemed unnecessary. However, even though it was stated that a recalibration was unlikely to be

required, an examination of the calibration accuracy needed to be performed regardless; it is important to feel confident in the fact that the receiving results are correct.

Before any examination of the accuracy was performed, a zeroing procedure was necessary. As stated by Steen (2014), zeroing is essential to acquire the measurements absolute value. By performing a zeroing procedure, a reference level (zero level) for all measurements is defined. The output measured at this zero level is then stored and later subtracted from measurements acquired from the transducers.

The displacement gauges where the first to be examined. This was done by using the computer for rig control. The program in this computer had the option to lock the rig in different positions. This feature was applied during the examination. By defining input parameters in the program, and launching the rig, the rig would move the specified deflection and stop. This movement was then recorded in Catman and could be inspected further.

The rig's initial position in sway was at the center of the track. The displacement at that location was zero. Furthermore, the initial position for roll was off course at zero degrees. Both motions were tested individually in positive and negative direction, and with two measurements in each direction. Zeroing was also performed before each measurement. See Table 2 for the results of the inspection.

Table 2 Results from inspection of displacement gauges

Motion	Direction	Input parameters in program for rig control	Catman stated deflection
Sway [mm]	Positive	10	10.06
	Negative	-20	-20.07
	Positive	20	20.02
	Negative	-10	-10.09
Roll [deg.]	Positive	8	8.02
	Negative	-16	-16.04
	Positive	16	16.05
	Negative	-8	-8.06

For the displacement gauge measuring sway motion the result lay in the acceptable range of 0.5%. For roll the result lay in the acceptable range of 0.4%. Both these results are quite good, and shows that a recalibration of the displacement transducers is not required.

To examine the accuracy of the strain gauges a digital force gauge was applied. The digital gauge was pushed against the plate holding the tank. To get the horizontal forces the gauge had to be pushed horizontally against the plate. This was performed on each side of the plate to record both positive and negative forces in Catman. As before, two measurements on each side. The same principle was performed for the vertical forces. However, instead of pushing horizontally, be pressure was applied vertically. As earlier, zeroing was also performed before each measurement. See Table 3 for the results of the inspection.

Table 3 Results from inspection of strain gauges

	Plate location	Measured force from digital force gauge	Measured force in Catman
Horizontal force [N]	Catman positive side	22.82	23.11
		73.25	73.52
	Catman negative side	26.43	-25.67
		71.27	-73.04
Vertical force tot [N]	Catman positive side	44.56	44.39
		93.48	94.17
	Catman negative side	45.52	-44.89
		93.21	-92.68

For the strain gauge measuring horizontal force the result lay in an acceptable range of approximately equal to 2%. For the strain gauges measuring vertical forces (the values from the two gauges were added together to give total vertical force) the result lay in an acceptable range of approximately equal to 1%. These results are also very good. Hence, a recalibration of the strain transducers was not required.

5. Pre-Processing of Experimental Data

In this chapter the pre-process of the experimental data is discussed. This involves filtering of the data to ensure that it is free from unwanted noise polluting the results, and an evaluation of the accuracy of the experimental data to further increase the trustworthiness of the results.

5.1. Filtering of Experimental Data

It exists several filtering methods, and they come in both analog and digital form. For instance, if a measured signal is polluted with noise, a filter can be applied to remove that noise. In other words; a filtering procedure will suppress this interfering signal by excluding it completely, allowing only the signals of importance to pass through (Steen, 2014).

In Catman the time domain results of the total vertical force were recorded. As there were no analogue, or digital filters present in the experimental instrumentation, Catman recorded unfiltered time domain results. Hence, before transforming these time domain plots to frequency domain for further analysis, they had to be filtered using a digital filter in Matlab. The reason for why they needed to be filtered in the first place, is due to water exhibiting non-linear behavior when exited. Thus, during excitation in sway the non-linear behavior of water led to abnormal peaks in the time domain plots of the total vertical force. These unwanted peaks were the interference, or the noise in the plots, and so they needed to be suppressed in order to acquire the important part of the plot.

When applying a filter, it is important that the appropriate filtering method is chosen. As stated by Steen (2014), the noise in a signal is usually appearing at a significantly higher frequency than the physical measuring signal. By inspecting an unfiltered time domain plot of total vertical force in pure sway this statement is confirmed. See Figure 12.
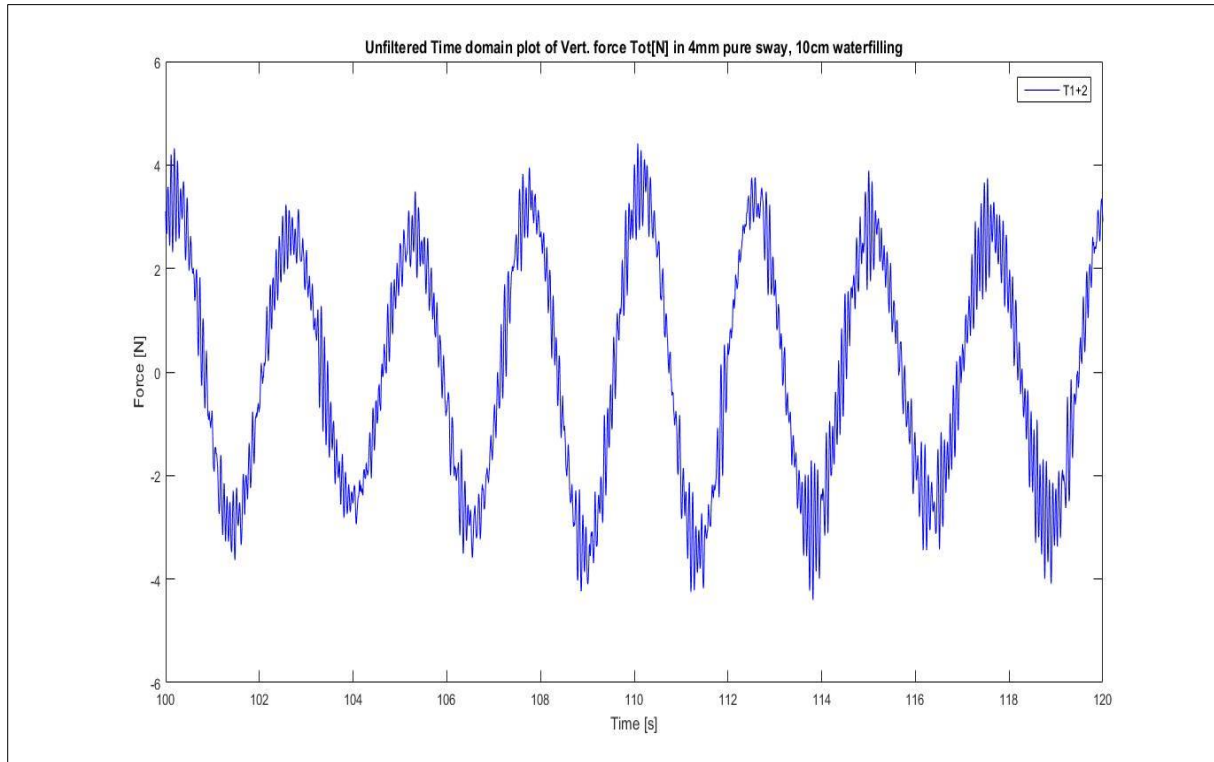
Figure 12 Unfiltered time domain plot of total vertical force showing the high frequency noise

As Figure 12 shows, the plot is indeed polluted with high frequency noise. Therefore, the correct filtering method would be a low pass filter. In a low pass filter all signals with frequency higher than a specified cut-off frequency (also known as boundary frequency) is attenuated, while signals with frequency lower than the cut-off frequency is passed. This filtering method was then implemented as a digital filter using Matlab (Steen, 2014).

As seen from the experiments in appendix A, the full scale excitation period for all water heights ranged from minus two seconds to plus two seconds from the full scale resonance period. Thus, for all water heights the model scale excitation frequency ranged between 0.9Hz and 0.2Hz (see appendix A). Therefore, the cut-off frequency could at least not be less than 0.9Hz, otherwise it would mean filtering out the actual measuring frequency. This is illustrated in Figure 13, where a cut-off frequency of 0.5Hz is applied.
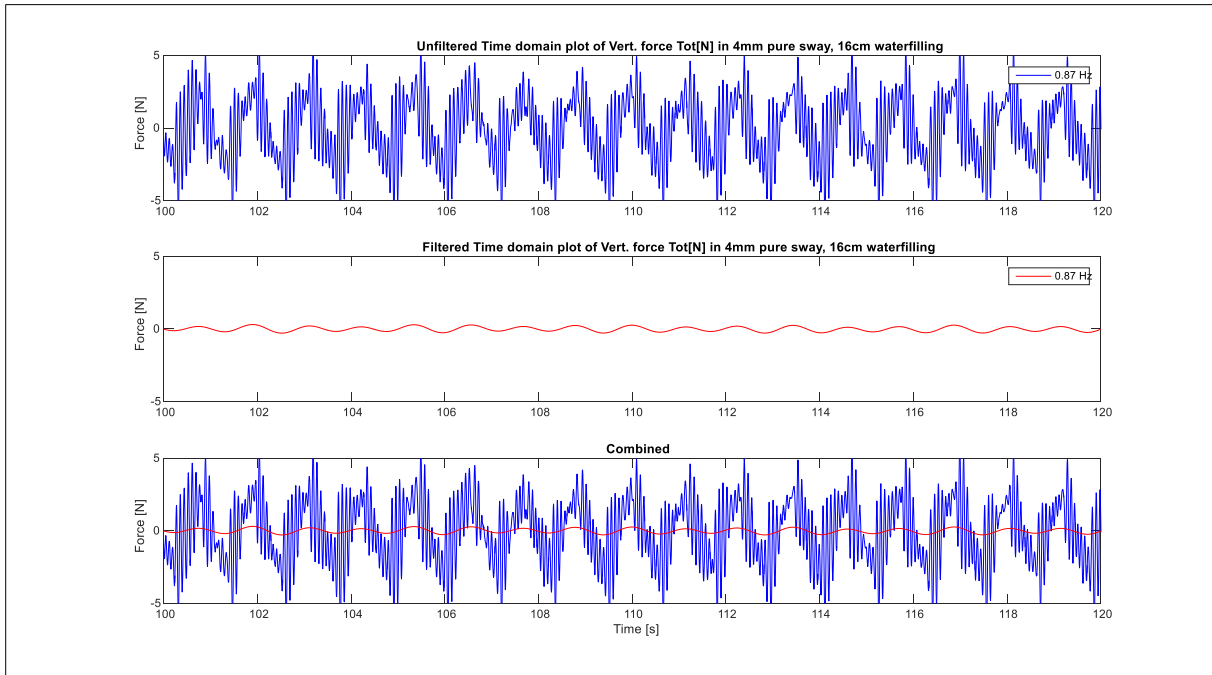
Figure 13 Result of using a cut-off frequency less than the actual measured frequency. A time domain plot of total vertical force at 4mm pure sway, 16cm water filling level, and model scale excitation frequency of 0.87 Hz is applied

The figure shows that using a cut-off frequency less than the measuring frequency will give an incomplete portrayal of the time domain plot after filtering is achieved.

Nevertheless, it was also important to define a cut-off frequency that was not too close to 0.9Hz, or too far apart. A cut-off frequency that is too far apart will fail to remove the noise completely, while a cut-off frequency too close will also affect the measuring frequency, though not as heavily as demonstrated above.

For instance, if the cut-off frequency is set at 0.9Hz, the amplitude of sinusoids for filtered time domain plots with excitation frequency far lower than this value will be smooth, and give an accurate representation of the physical measuring signal. However, this will not be the case at excitation frequencies close to this value. The amplitude of sinusoids for filtered time domain plots with excitation frequency close to this value will be smooth, but they will be an incomplete representation of the actual measured signal. This circumstance is presented well in Figure 14 and Figure 15.
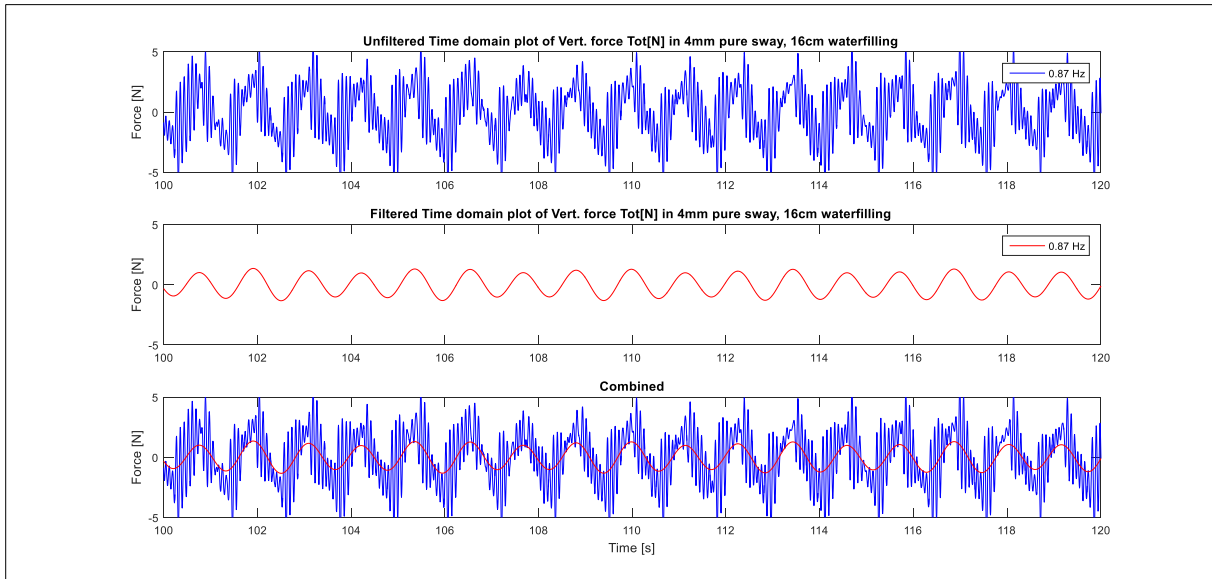
Figure 14 Result of using a cut-off frequency at 0.9Hz for a time domain plot of total vertical force at 4mm pure sway, 16cm water filling level, and model scale excitation frequency of 0.87 Hz
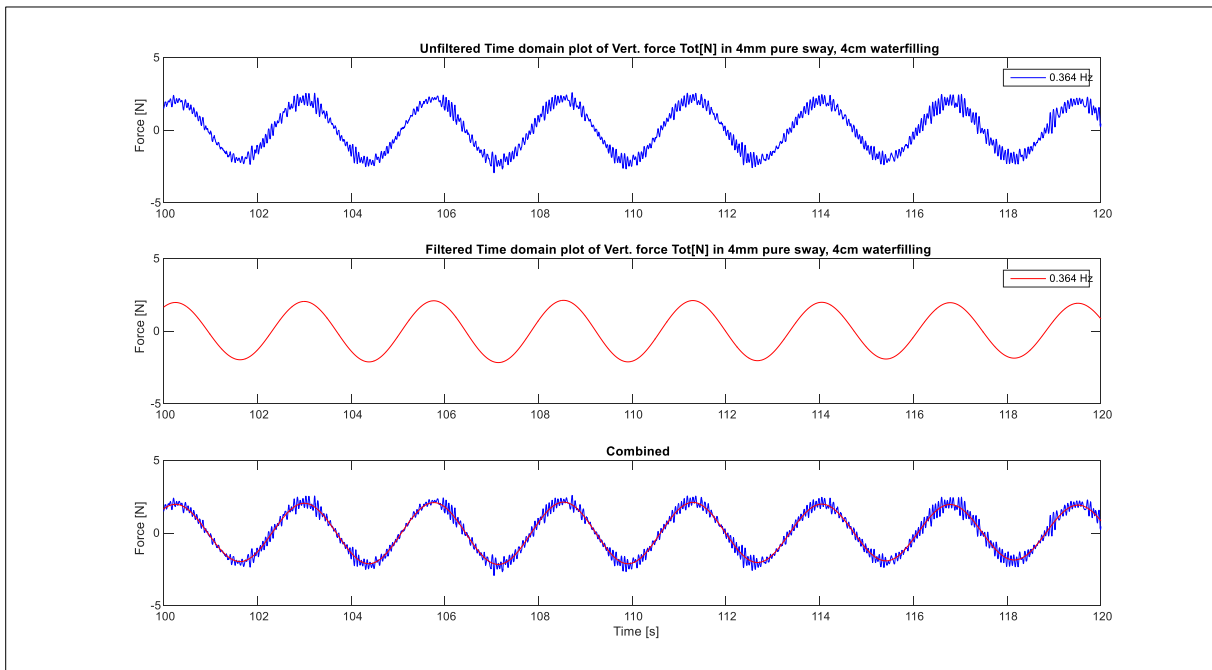
Figure 15 Result of using a cut-off frequency at 0.9Hz for a time domain plot of total vertical force at 4mm pure sway, 4cm water filling level, and model scale excitation frequency of 0.394 Hz

As seen from Figure 14, the amplitude of the filtered signal is not as large as it can be, giving an incomplete representation of the measured signal. Furthermore, the filtered signal in Figure 15 gives a good representation of the physical measured signal.

Conversely, by setting the cut-off frequency at a value higher than 0.9Hz, this time at 2.0Hz, the amplitude of sinusoids for filtered time domain plots with excitation frequency close 0.9Hz will no longer be as inaccurate as before. Instead, as a result of increasing the cut-off frequency, the amplitude of these sinusoids will now give a much more accurate representation of the physical signal, all while still retaining its smoothness. Furthermore, the amplitude of the sinusoids for filtered time domain plots with excitation frequency far lower than 0.9Hz will, as before, still retain its accurate portrayal of the physical signal, with little variation. This situation is presented in the figures below.
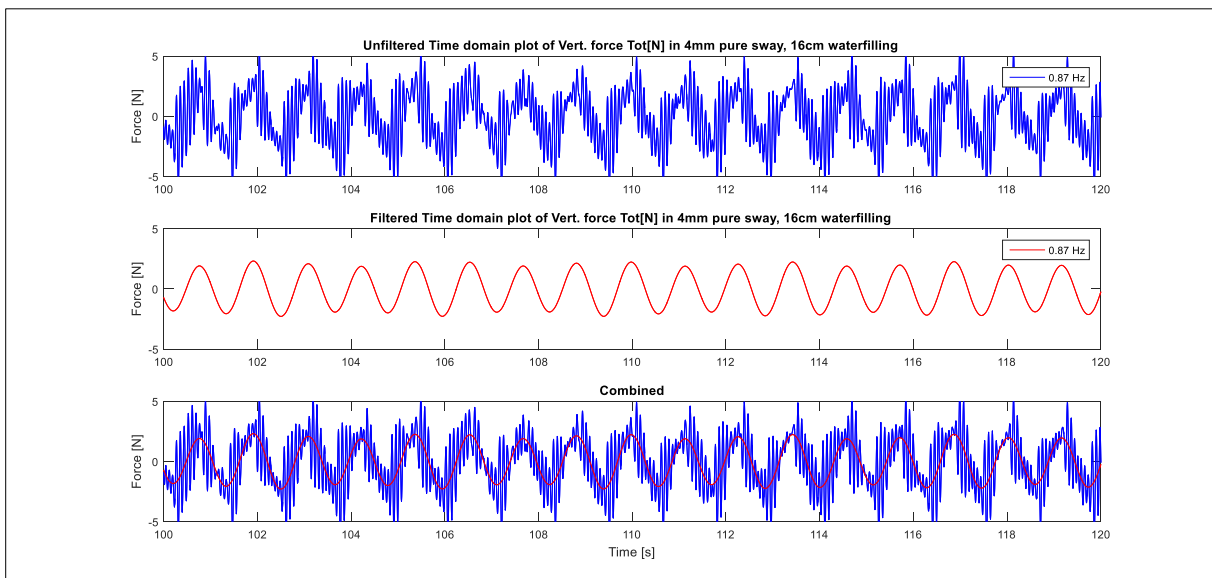
Figure 16 Result of using a cut- off frequency at 2.0Hz for a time domain plot of total vertical force at 4mm pure sway, 16cm water filling level, and model scale excitation frequency of 0.87 Hz
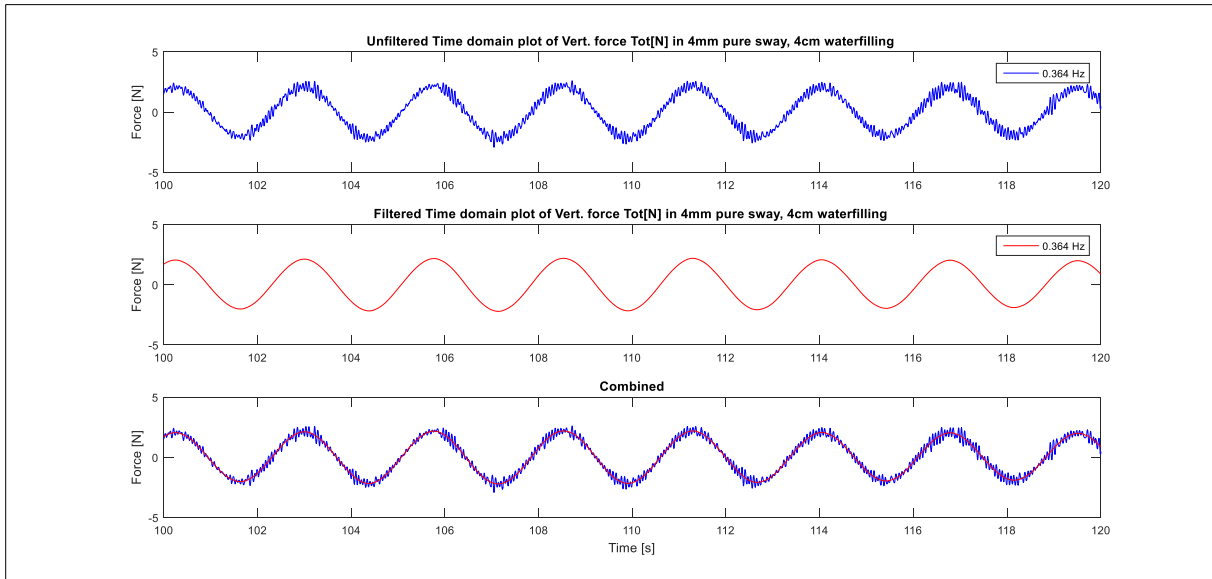
Figure 17 Result of using a cut- off frequency at 2.0Hz for a time domain plot of total vertical force at 4mm pure sway, 4cm water filling level, and model scale excitation frequency of 0.394 Hz

As seen from Figure 16, using a cut-off frequency 2.0Hz enables the filtered signal to give a much better portrayal of the actual measured signal than the previous example. Furthermore, the filtered signal in Figure 17 still retains its good representation of the physical signal with little deviation compared to the previous example. What this inspection divulges is that the farther away from the measuring frequency the cut-off frequency is, the more accurate the filtered signal becomes. Correspondingly, as the purpose of this procedure is to filter out noise, the distance cannot be too large as well. Finding this boundary can be tricky, and multiple attempts might be necessary. For this case it was concluded that a cut-off frequency of 2.0Hz gave good dependability.

5.2.   Accuracy of Experimental Data

As previously mentioned, this thesis contains an investigation on the frequency spectrums for the vertical forces that develop in pure sway of a free surface tank when varying parameters like water height, excitation frequency, and excitation amplitude. In such, it was imperative that the spectrums displayed trustworthy results. Therefore, to optimize the accuracy of the experimental data retrieved from each test run, an evaluation of the resolution of the frequency spectrums extrapolated from the time domain results were performed. This procedure was the second preparation test, as mentioned earlier

When tests are performed with the two degree of freedom sloshing rig the time domain results are recorded in Catman, and stored as bin files. In post processing these files are converted to readable results using Matlab. Matlab then stores the time domain recordings in columns, and these columns have a defined time step between them. The time step between these columns corresponds to the time step defined by the A/D converter. Reducing the time step will correspond to a larger total amount of registered data points in the time domain recordings, as the points will be closer together. Naturally, this also gives more columns in Matlab. The result is a more accurate representation of the time domain plot, and hence, a more accurate frequency plot resolution. Similarly, the same will happen if the length of the run is increased. It will correspond to a larger total amount of registered data points, giving more columns in Matlab. Albeit, the points will not be closer together, but since the run is longer the outcome will be the same; a more accurate representation of the time domain plot, and more accurate frequency plot resolution. Hence, to optimize the accuracy of the frequency spectrums, either the time step of the recordings needed be altered, or the duration of the test run.

The time step during the measurements, otherwise known as sampling frequency, was already defined in the A/D converter, and was 0.005s, or 200Hz respectively. It was assumed that this time step was as good as it could be, and therefore was not adjusted. Consequently, to increase the accuracy of the results the length of the run had to be changed instead.

Based on the above explanation, testing with different durations meant determining which running time gave enough data points to create accurate frequency spectrum resolutions, while simultaneously be time efficient. Thus, the second preparation test was run multiple times, each time with varying duration. A water height of 10cm, a sway amplitude of 4mm, and an excitation period of 1s over the full scale resonance period was used as basis for the test. The full scale excitation period of 1s over the resonance period corresponded to a model excitation frequency of 0.446 Hz. The durations that were tested were, 2min, 5min, 10min, 30min, and 60min. Presented in Figure 18 is a frequency plot of total vertical force for the different durations tested, and their respective peak values in Table 4.
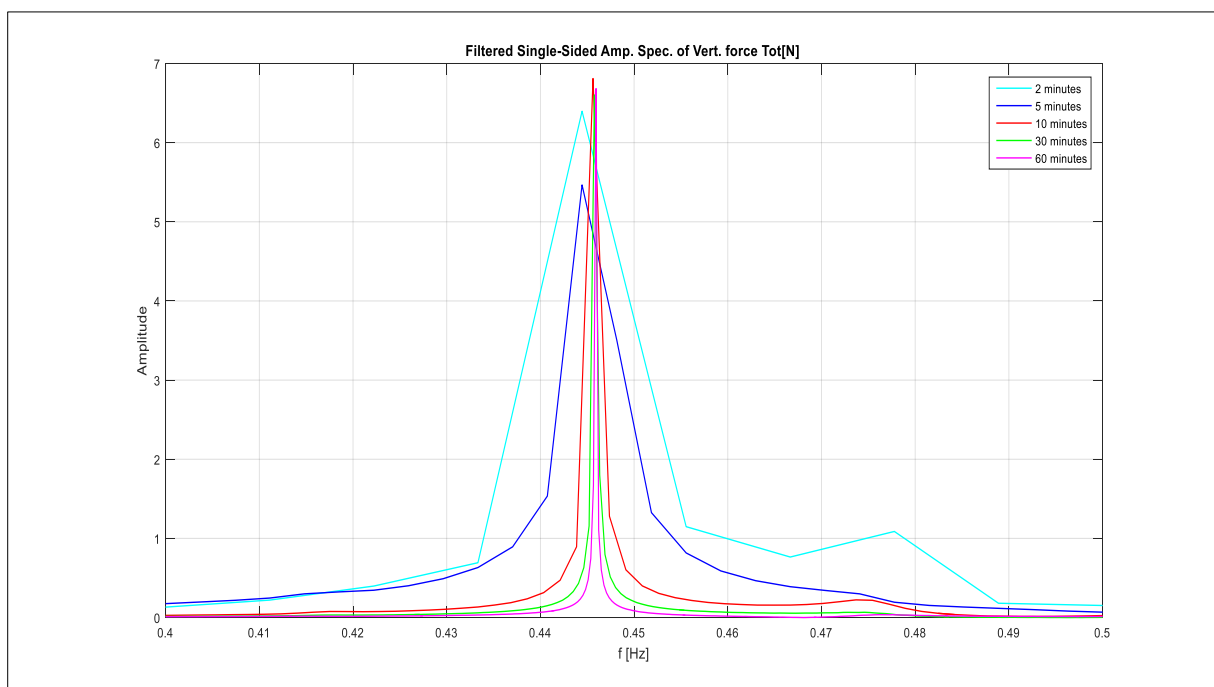
Figure 18 Frequency plot of different durations

Table 4 Table containing max amplitude and respective frequency to the different durations for total vertical force

Duration	Max amp/Freq.
2 minutes	6.448/0.4444
5 minutes	5.512/0.4444
10 minutes	6.874/0.4456
30 minutes	6.665/0.4458
60 minutes	6.745/0.4459

As seen from Figure 18 the frequency spectrum for a two-minute duration run had larger spacing between the data points compared to the rest, resulting in a poor frequency domain resolution. This is a direct result of the small duration time. From Table 4 this statement is confirmed; 0.446Hz is not included, instead a frequency at 0.4444Hz is resolved. Furthermore, a sixty-minute duration run had very little spacing between the data points, which in return gave a very good resolution of the frequency spectrum. As seen from Table 4 a frequency at 0.4459Hz is resolved which is extremely close to the wanted excitation frequency of 0.446Hz, however the length of the run in this instance is not at all time efficient. A more appropriate running time seems to be ten minutes. With a ten-minute duration the space between the data points is reduced to one thousandth of a decimal. This means that the deviation from the wanted frequency resolution will be small, which is evident in both Figure 18, and in Table 4; the resolved excitation frequency is 0.4456Hz, which is very close to the wanted resolution. Additionally, the length of the run was adequate. Ten minutes was therefore accepted as a suitable running length. As mentioned earlier there were seventeen different excitation frequencies that were going to be tested for each main experiment, in other words, seventeen test runs per experiment. This meant that each experiment now had a total duration of 170 minutes, not counting the preparation time between each test run.

Another important factor that could influencing plot accuracy was whether or not the start of the time series was included in the Fast Fourier Transformation (FFT) of the time domain

results. This part of the run is unimportant, and can pollute the result if included. It is only the results after the rig has completed its initial startup, and maintains a continuous motion, that are interesting. Thus, this part of the time series was excluded from the analysis. A start point of 40 seconds after the initial start of the experiments was chosen as appropriate.

6. Post-Processing of Experimental Data

In this chapter the post-process of the experimental data is discussed. First the results of the experiment series are explained which include an analysis of all the frequency plots of the experiments. Thereafter the curve-fitting procedure is discussed. In this section curve-fitting is performed, and it is analyzed if there is a connection between the parameters and the vertical forces.

6.1.　　　Frequency Spectrum Analysis

Before the plots could be analyzed the experiments needed to be executed. As previously mentioned there were twenty-four main experiments, and each experiment had a defined sway amplitude, and water filling level, which were tested with seventeen different excitation frequencies. The first natural frequency for each water height was used as basis for the excitation frequencies. The experimental approach was to test every sway amplitude and excitation frequency at each water height, before moving on to the next water height and repeat the process. By starting at the highest water height it gave the option to drain the tank after each completed water height, rather than retrieving water and filling up every time. This procedure allowed time to be saved. Presented in the following figures are the resulting frequency spectrums for each experiment.
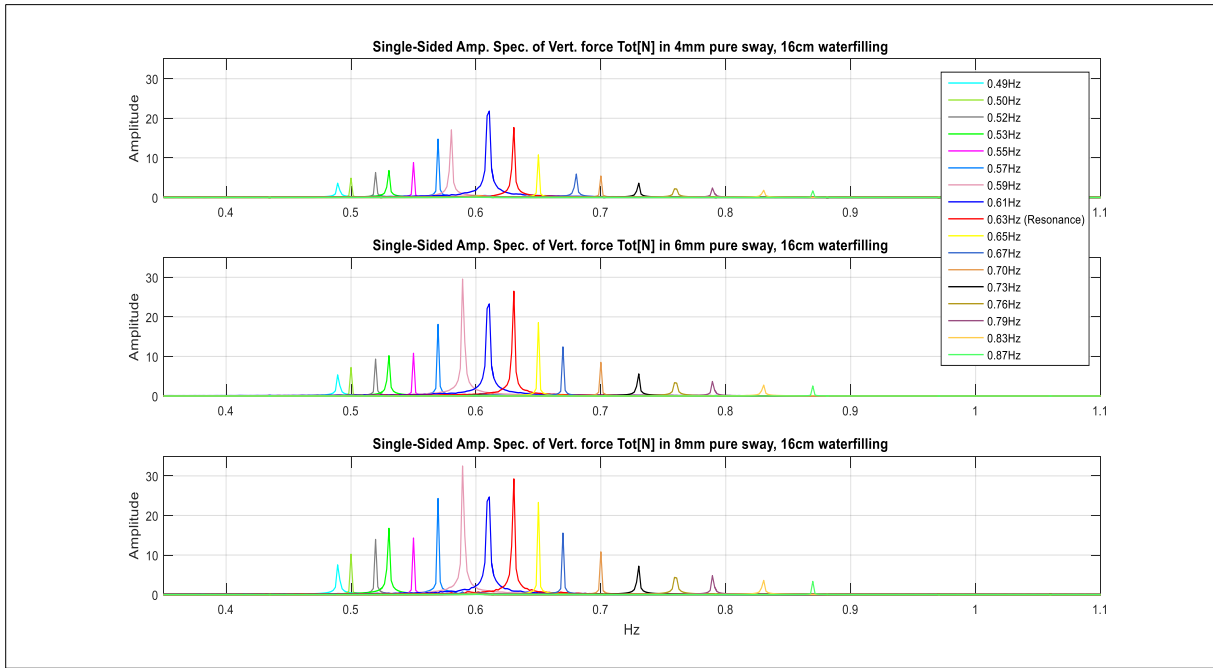
Figure 19 Experiment 1-3. Total vertical force frequency spectrums for each excitation frequency at water height 16cm, for a sway amplitude between 4-8mm
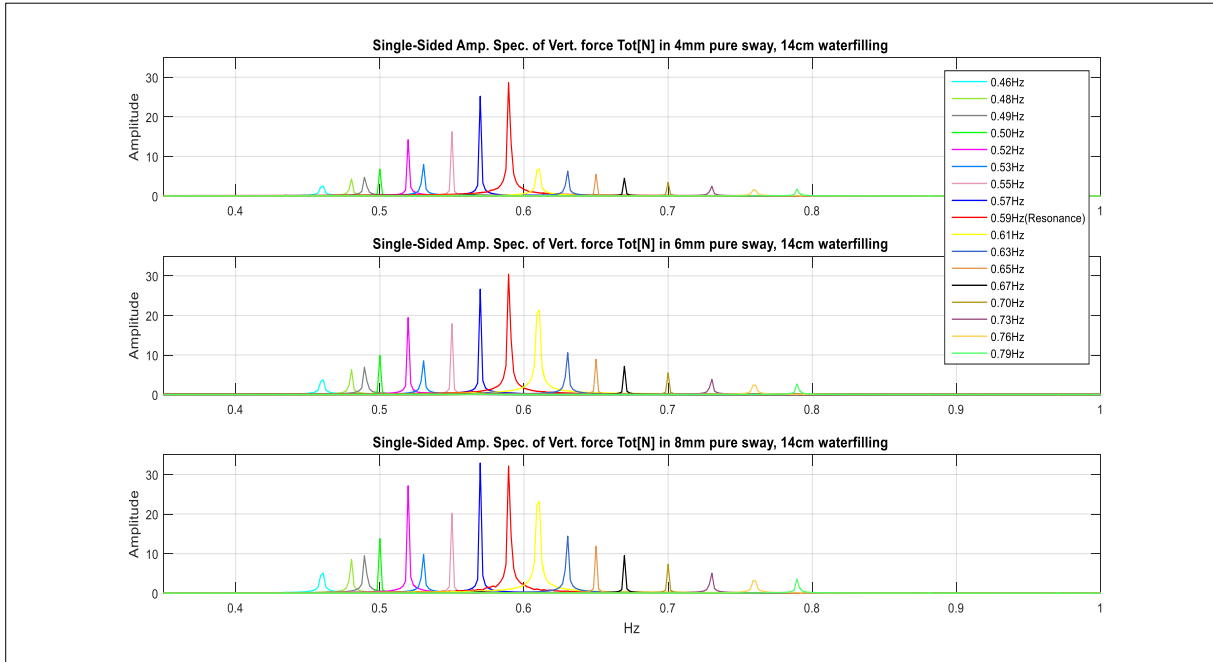
Figure 20 Experiment 4-6. Total vertical force frequency spectrums for each excitation frequency at water height 14cm, for a sway amplitude between 4-8mm
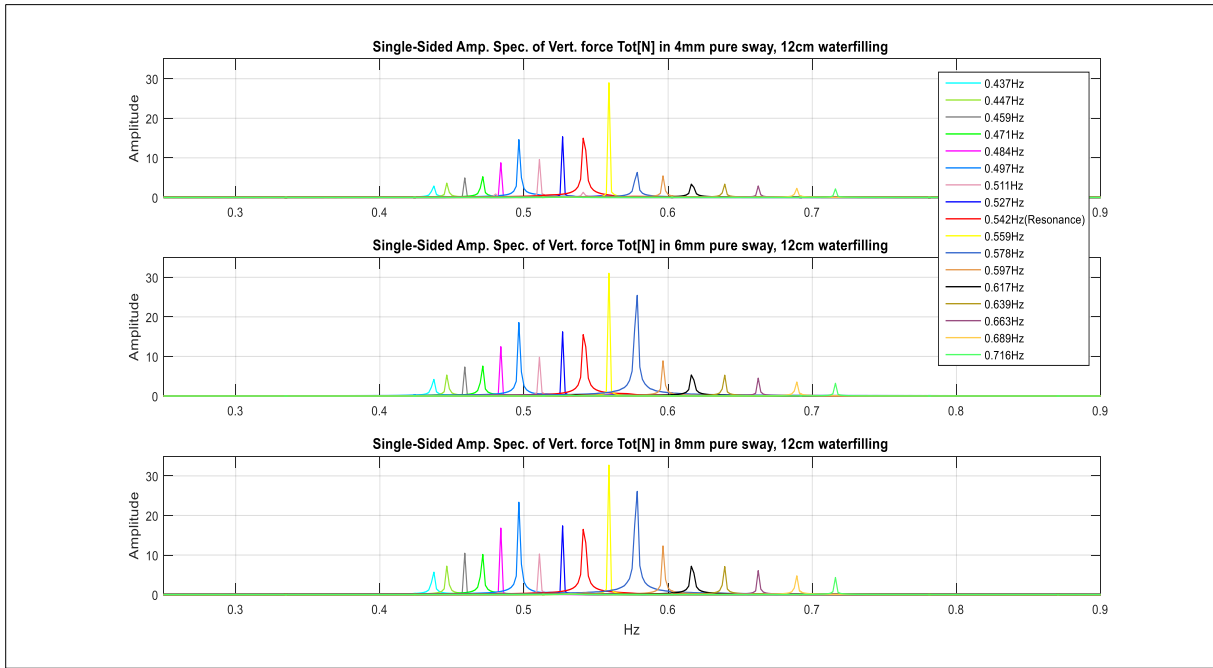
Figure 21 Experiment 7-9. Total vertical force frequency spectrums for each excitation frequency at water height 12cm, for a sway amplitude between 4-8mm
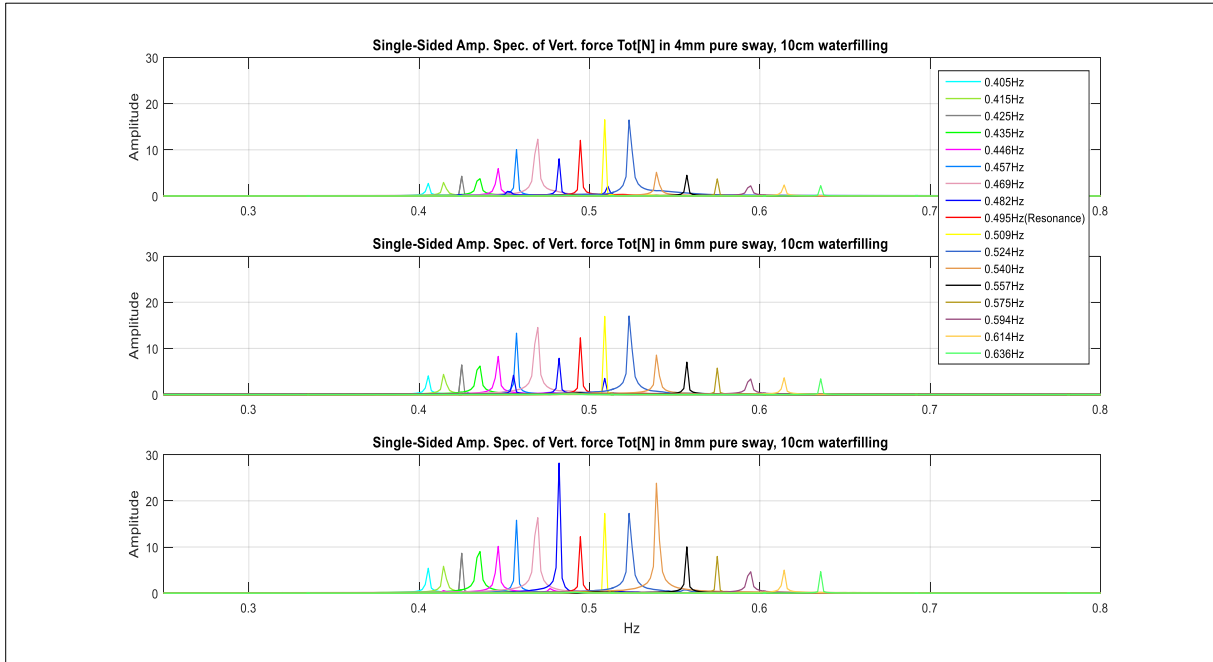
Figure 22 Experiment 10-12. Total vertical force frequency spectrums for each excitation frequency at water height 10cm, for a sway amplitude between 4-8mm
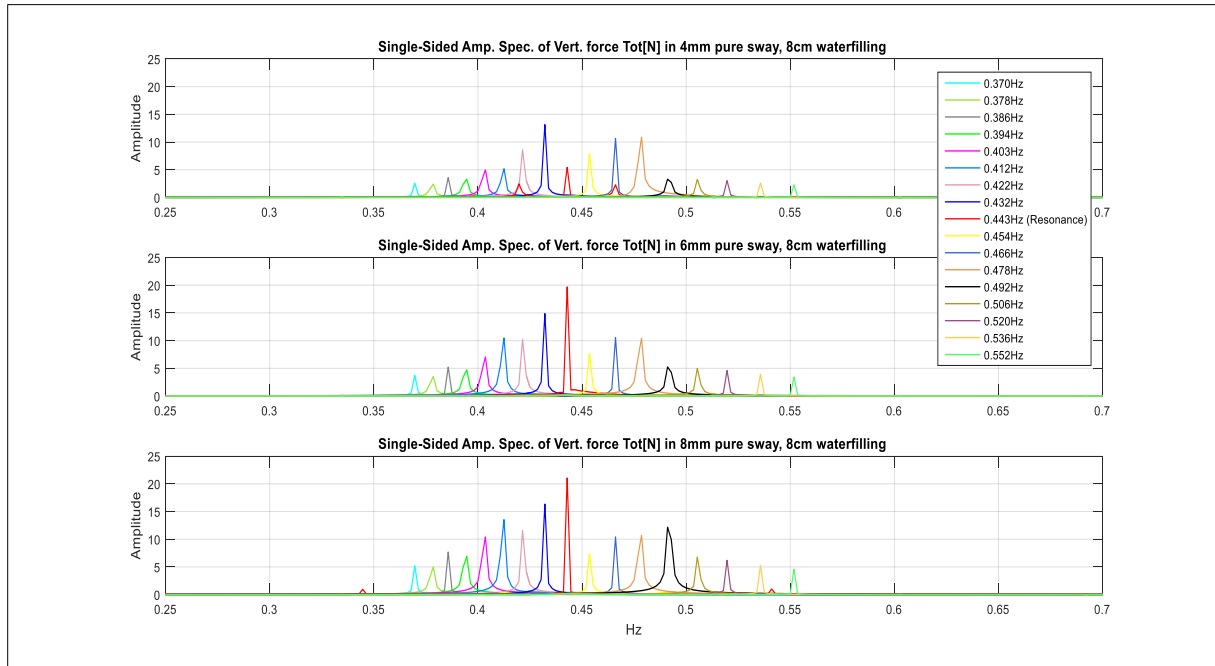
Figure 23 Experiment 13-15. Total vertical force frequency spectrums for each excitation frequency at water height 8cm, for a sway amplitude between 4-8mm
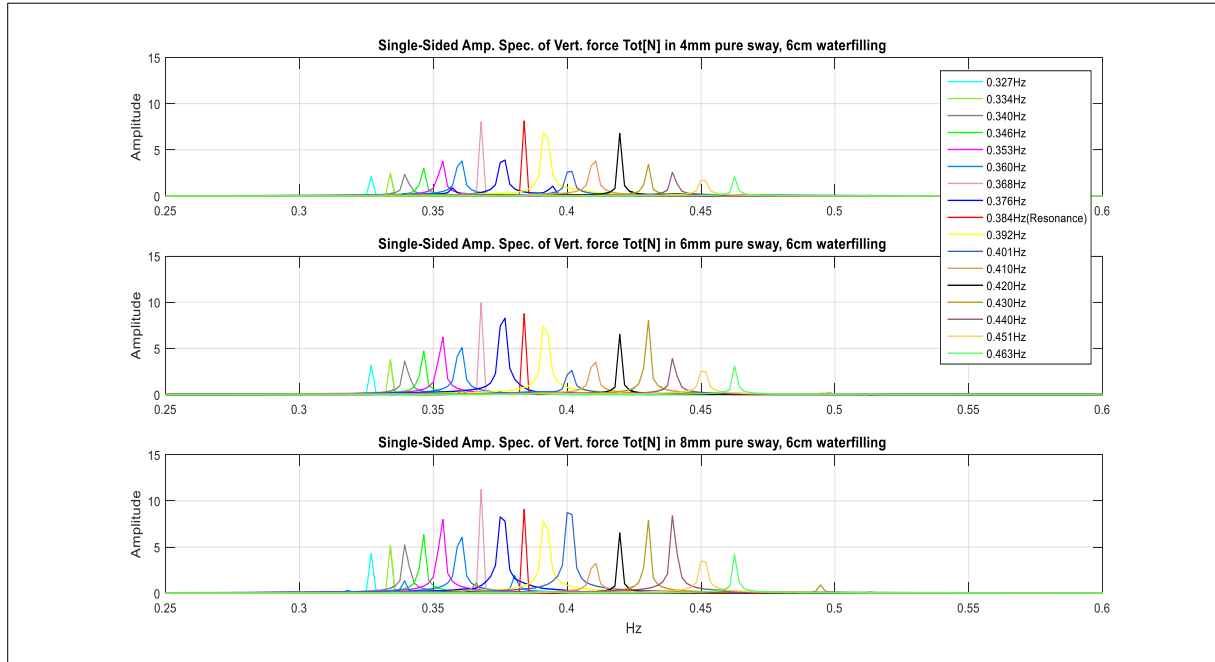
Figure 24 Experiment 16-18. Total vertical force frequency spectrums for each excitation frequency at water height 6cm, for a sway amplitude between 4-8mm
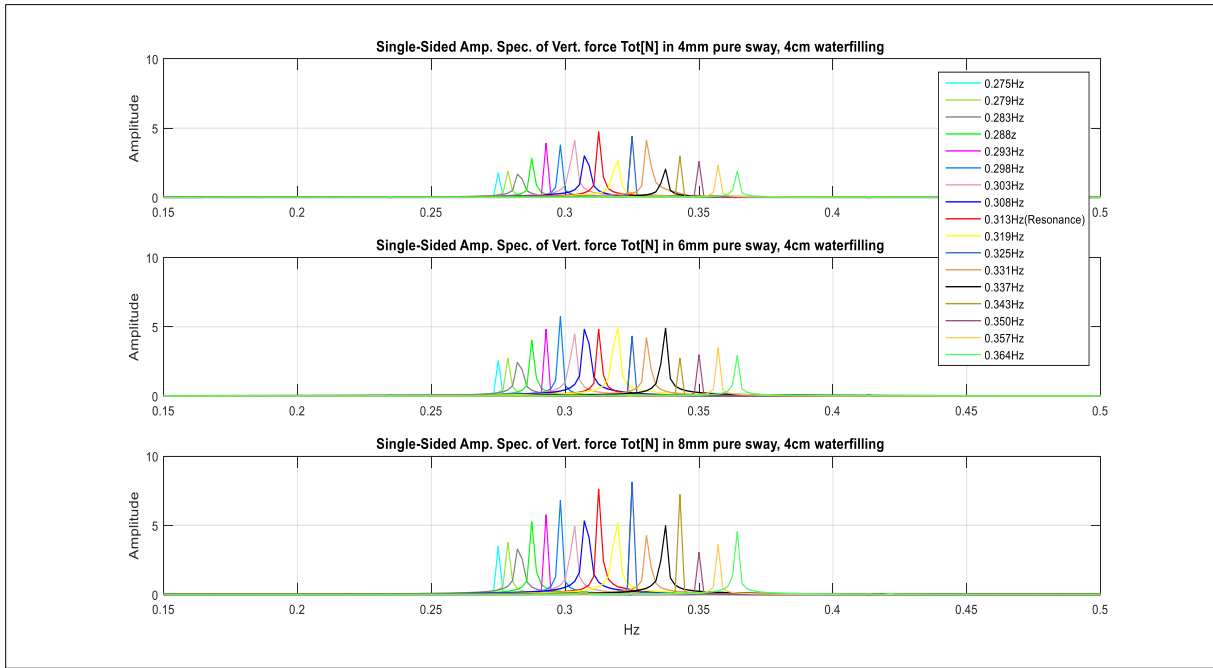
Figure 25 Experiment 19-21. Total vertical force frequency spectrums for each excitation frequency at water height 4cm, for a sway amplitude between 4-8mm
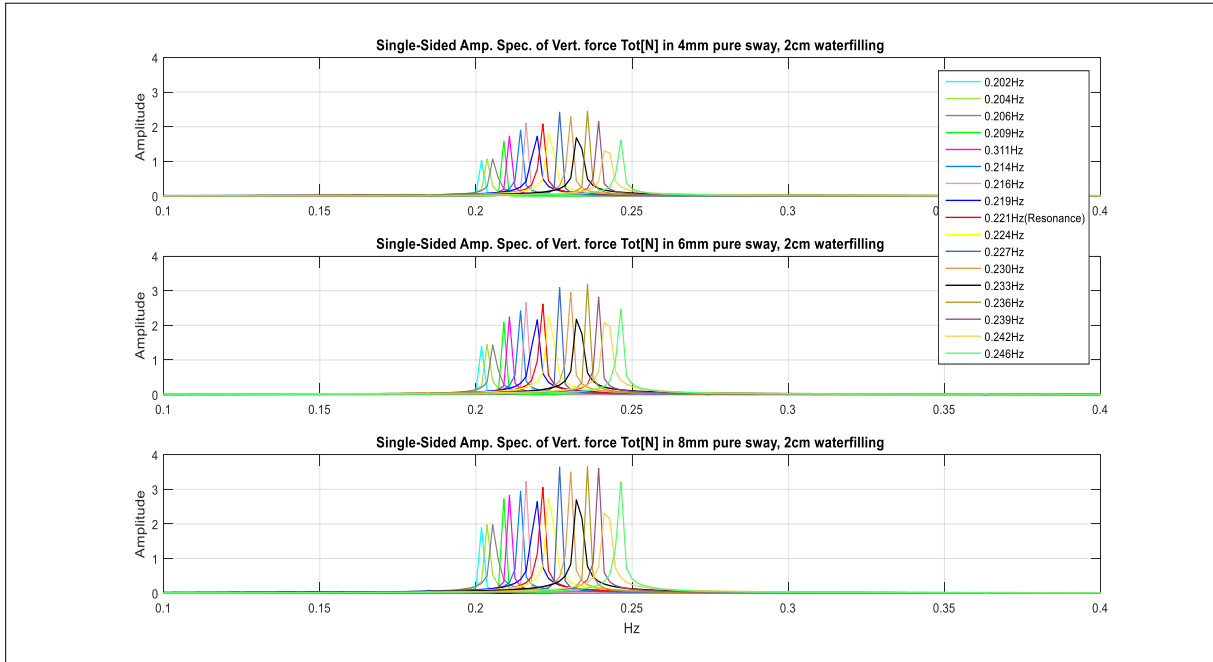
Figure 26 Experiment 22-24. Total vertical force frequency spectrums for each excitation frequency at water height 2cm, for a sway amplitude between 4-8mm

The first phenomenon that is observed in each plot, is that the amplitude of the frequency plot for the calculated resonance frequency is not the largest one. This was expected; since non-viscous fluid motions are assumed when calculating the natural frequency of the fluid in a sloshing tank, some deviations from the true natural frequency will occur. In reality, viscous effects in the fluid matter, which will influence the natural frequency. Hence, the real natural frequency will be different than the calculated one, but nonetheless, close to it.

During execution of each experiment, a number of water heights came close to maximum possible water filling level. For these water heights, some slamming of water against the top covers did occur at excitation frequencies close to resonance frequency, for 6mm and 8mm sway amplitude (no slamming at 4mm). This was precisely the case for the water heights ranging from 16cm to 12cm; at excitation frequencies around the resonance frequency, at both 6mm and 8mm sway amplitude, water slamming transpired. From 10cm to 8cm, the slamming was heavily reduced, but some slamming still occurred at the excitation frequencies closes to resonance for 6mm and 8mm sway amplitude. From 6cm to 2cm no water slamming ensued.

When water slams against the top covers in a roll damping tank, there will be a saturation of the damping effect. In the conducted experiments the damping effect is produced by the vertical forces. By observing the different experiments, it is confirmed that the damping effect is reduced due to slamming. For instance, from 12cm to 16cm water height in 6mm sway, the amplitude of the highest frequency plot is decreasing. See Figure 27.
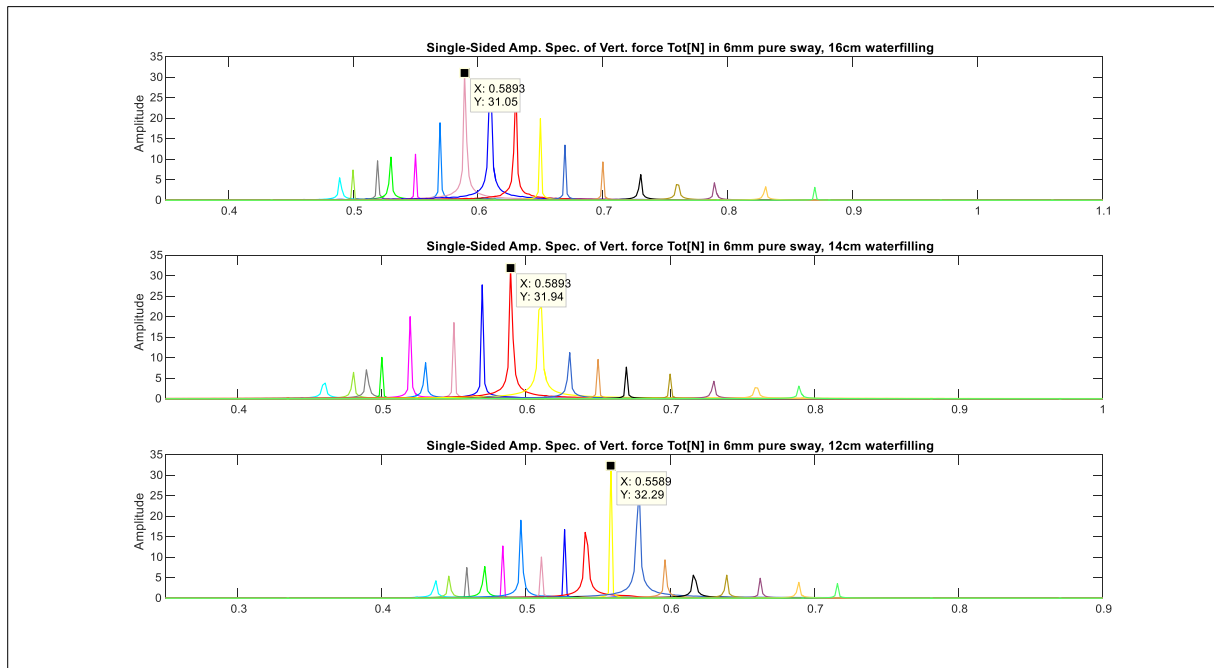
Figure 27 The effect of water slamming against the top covers

It was now established that slamming does influence the damping effect, giving lower damping at resonance. However, even though slamming occurs in some of the experiments, does it mean that these experiments can't be included in the analysis? Before this question is examined, it is investigated if a pattern exists in the different experiment data sets. If a curve shape for each experiment could be approximated, it could be concluded that a pattern in the data sets existed. To establish this approximation a linear interpolation curve-fitting procedure was performed. This procedure applied the peak values/data points for each frequency plot in every experiment to perform the procedure. Presented in the following figures are the result of interpolating linearly between each peak in every experiment.
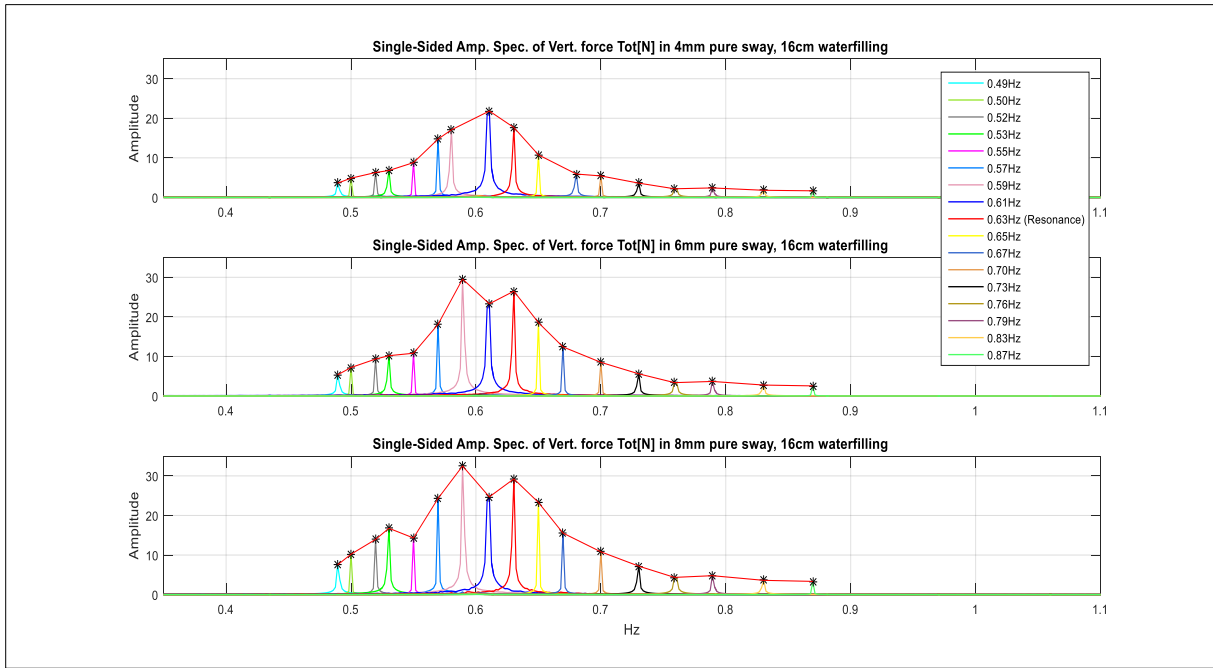
Figure 28 Linear interpolation between the peak value for each frequency plot in experiment 1-3
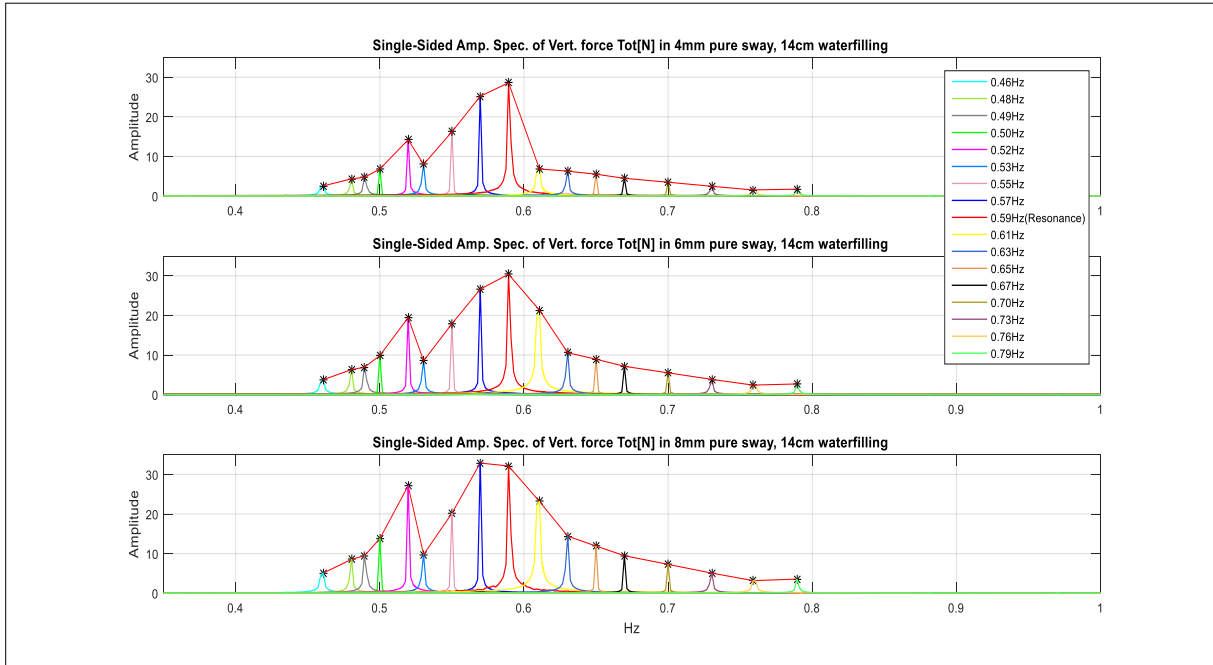
Figure 29 Linear interpolation between the peak value for each frequency plot in experiment 4-6
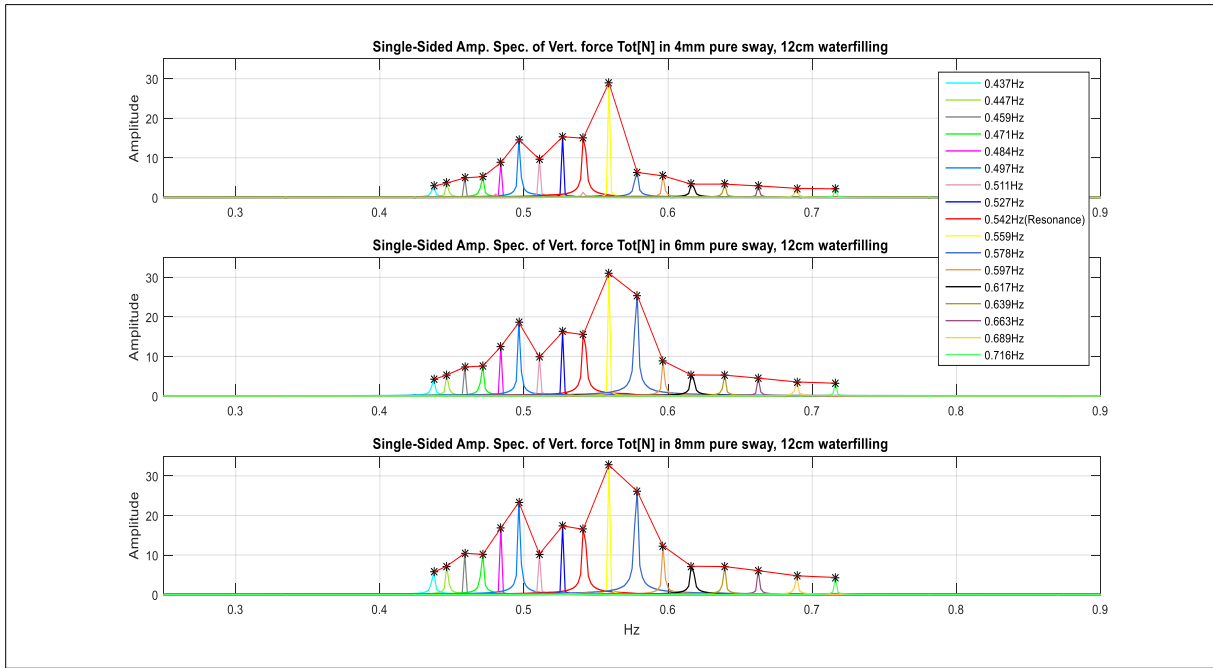
Figure 30 Linear interpolation between the peak value for each frequency plot in experiment 7-9
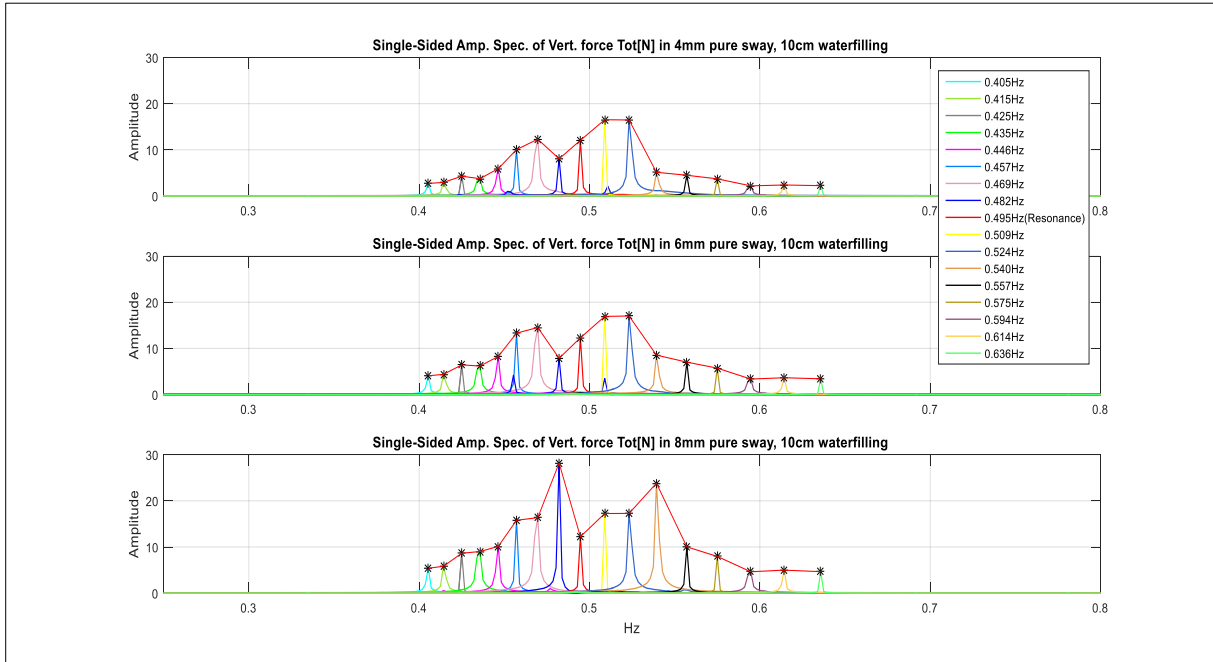
Figure 31 Linear interpolation between the peak value for each frequency plot in experiment 10-12
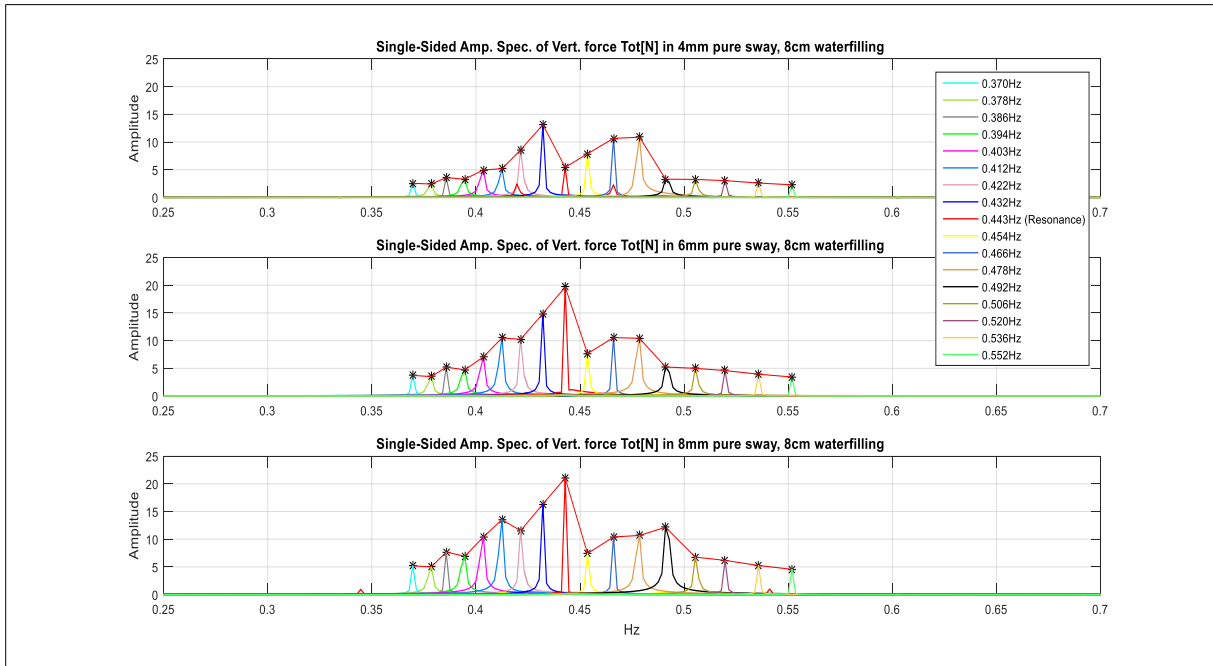
Figure 32 Linear interpolation between the peak value for each frequency plot in experiment 13-15
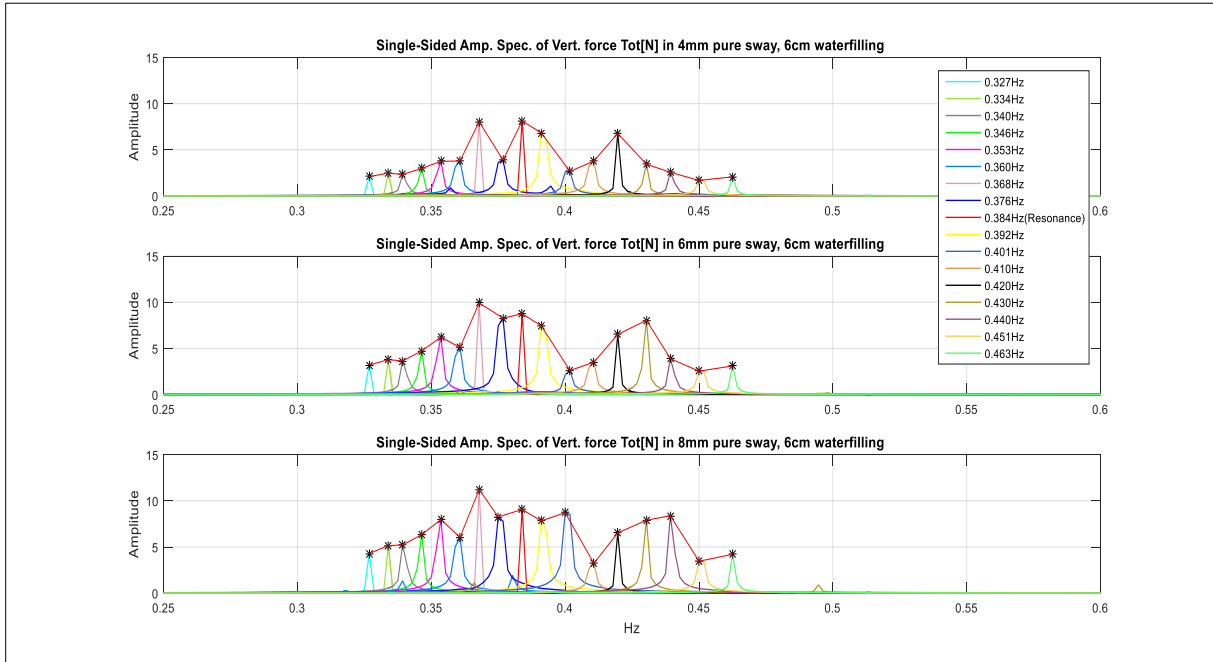
Figure 33 Linear interpolation between the peak value for each frequency plot in experiment 16-18
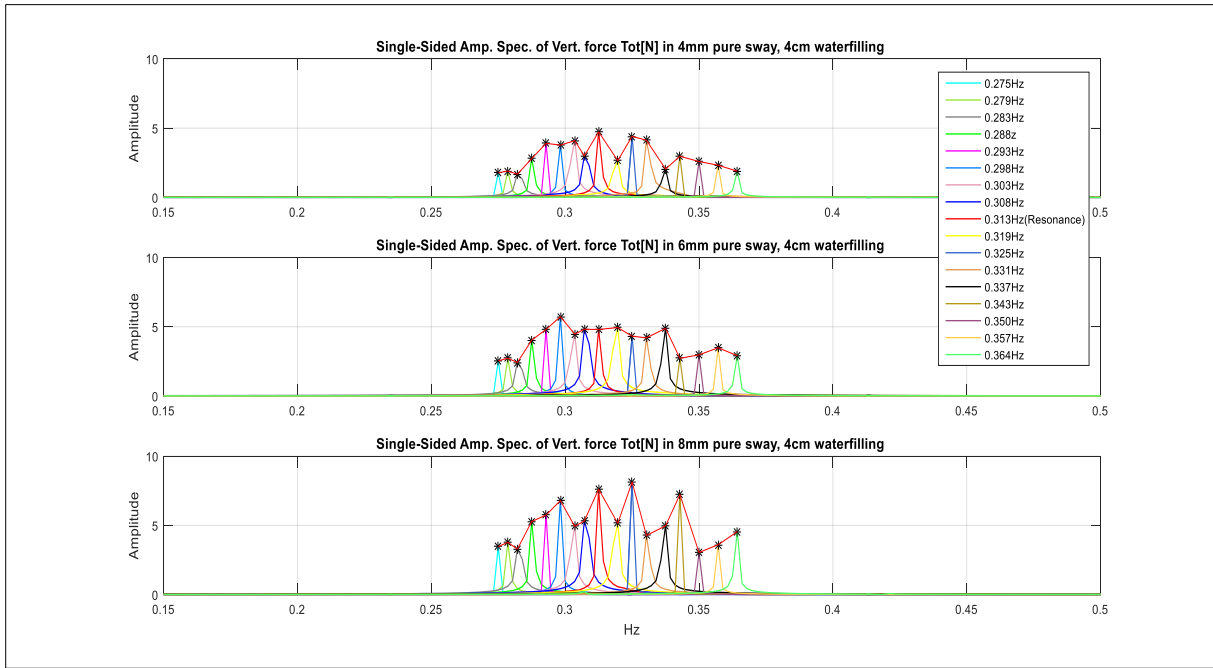
Figure 34 Linear interpolation between the peak value for each frequency plot in experiment 19-21
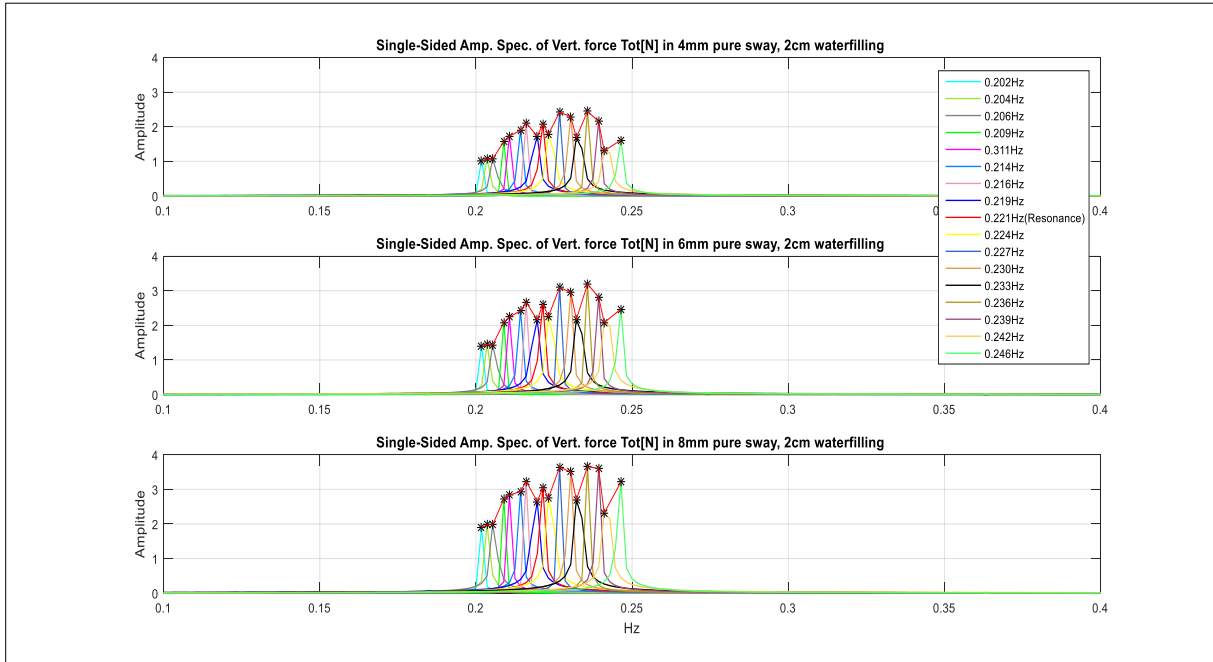
Figure 35 Linear interpolation between the peak value for each frequency plot in experiment 22-24

From the interpolation results a pattern in the data set for each experiment can clearly be seen; the data points are arranged in such a manner that a curve shape can be outlined. Furthermore, from the curve shapes outlined by this pattern a similarity in the curves at the different sway amplitudes for a defined water height can be observed. Conversely, there is a slight difference in the peak value positions in relation to other peak values in these experiments, however the variation is little (less difference between 6mm, and 8mm. Could also be due to random errors). Consequently, the general shape for these curves is not influenced by the difference. In conclusion, not only did the interpolation procedure establish that similarities between the parameters and the forces developed existed, but it found that other than leading to saturation of the damping effect, slamming didn't cause any major irregularities in the experiment results. As slamming didn't cause any major irregularities, and the objective was to find trends, the experiments where slamming occurred was not excluded from the analysis.

6.2.   Curve-Fitting Procedure

6.2.1.   Curve Estimation

Formerly, it was explained that a linear interpolation curve-fitting procedure was carried out to evaluate if the experiment data sets contained a pattern, and also to evaluate the influence of water slamming occurring in several of the experiments. If the data sets, instead of having inconsistent and random locations, had an arrangement and pattern to them, a curve could be extracted. Since this was the case it was necessary to perform a curve-fitting procedure to attempt to find an equation that represented this curve shape for each experiment well. Thereafter, the results would be plotted up against each other in a 3D plot to get a more summarized visualization, and to facilitate further evaluation of the curves. However, before attempting to find a model/equation that would represent all the data sets, it was decided to establish an early general visualization of the curve shape. Therefore, the different linear interpolation results were examined more closely, and a rough outline of this

shape was drawn. This would also allow for easier assessment of what model (linear/non-linear) would best represent said curve shape during the curve-fitting procedure. The result of the drawings is presented in the following figures.
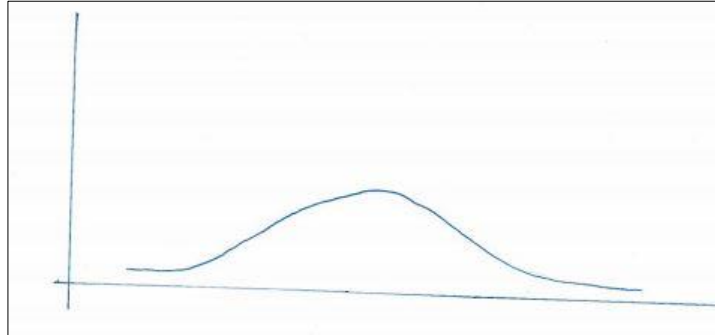
Figure 36 The curve shape for experiment 1-3
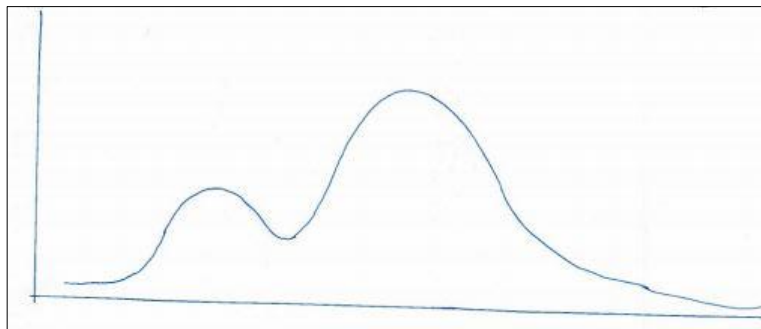
Figure 37 The curve shape for experiment 4-6 and 7-9
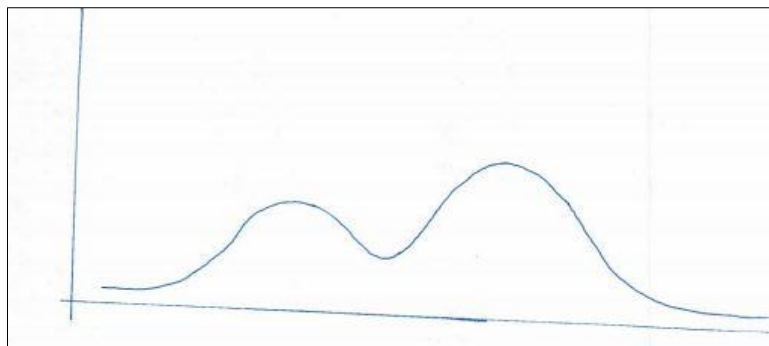
Figure 38 The curve shape for experiment 10-12
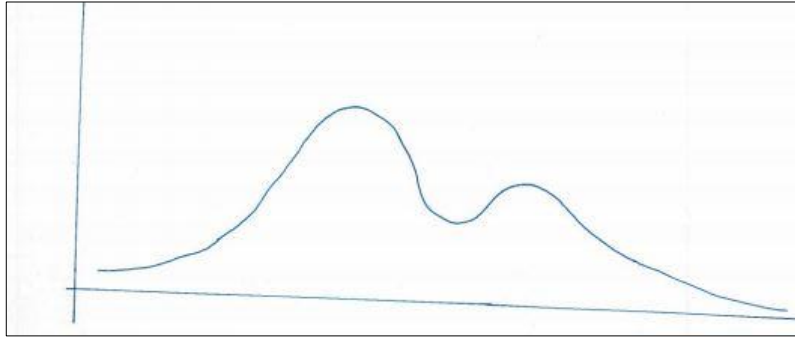
Figure 39 The curve shape for experiment 13-15
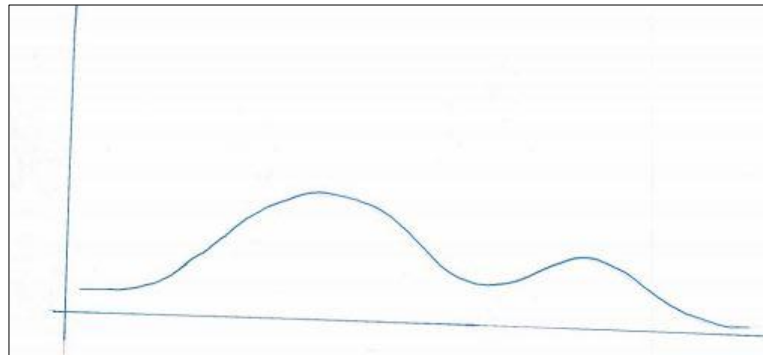
Figure 40 The curve shape for experiment 16-18
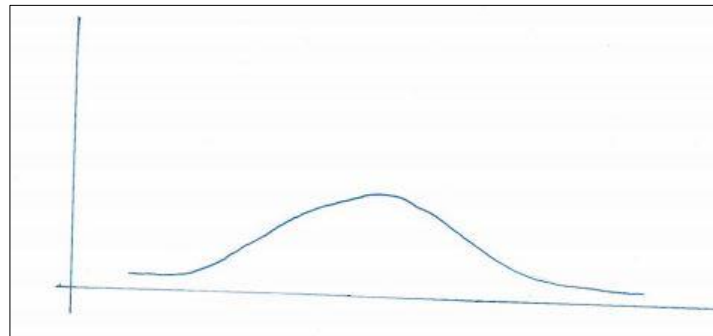
Figure 41 The curve shape for experiment 19-21 and 22-24

At most of the water heights the peak values seem to give a double peak curve shape as seen from the drawn curves, but at the water height closes to maximum filling, and water heights closes to empty, the curves seem to follow a single peak curve. Experiment 1-3 in Figure 36, with 16cm water filling level, seem to follow a single peak curve shape. In experiment 4-6, and 7-9 the peak values from each frequency plot seem to give a double peak curve shape, but with the first peak lower than the second. This is shown in Figure 37. Furthermore, in Figure 38 the same shape is visible for most of the experiments, however, the elevation of the peaks is reduced. For experiment 13-15 there is still a double peak curve shape, however, the first peak is now higher than the second. This is shown in Figure 39. For experiments 16-18 in Figure 40 it is still a double peak curve shape with reversed peak heights, but as with the curves in Figure 38, the elevation is reduced. Additionally, for these experiments it is getting more difficult to rule out the shape entirely. This is also evident in experiments 19-21, and 22-24 were it is becoming even more difficult to see a pattern. The reason for this is due to the increasing variation of the peaks, and the close proximity of the frequency plots with respect to each other (especially experiments 22-24). However, if overfitting is prevented it seems like the curves follow a similar shape like the curves in Figure 36. See Figure 41.

From the estimated drawings it is also observed that the curves are quite similar in shape at very low, and very high water levels. As stated earlier it is said that a good water level benchmark for an effective operating free surface tank is 60% of total tank volume. The counteracting roll moment developed from the first natural period at this water depth is the most optimal one. Hence, at very low water levels the damping effect diminishes to the point of being insignificant; not enough water to give an impact. Furthermore, at water depths higher than this value it is also natural to assume that performance degradation of the damping effect will occur; the damping effect given at the first natural period at these water depths will be lower than that of 60% filling. Therefore, if there is a connection between this reduced damping effect occurring at water heights close to maximum and minimum filling level, and the resulting shape of the curves, or if this is just an anomaly, is something that cannot be confirmed from these experiments alone and need to be investigated further. Nonetheless, at these water heights the results do show some tendency for this conjecture to have some validity, and hence, it might be a possibility.

6.2.2.   Matlab Curve-Fitting Toolbox

As observed so far a curve could be extracted from results. To get a more defined representation of these curves a curve-fitting procedure is performed. Curve-fitting will also contribute to the process of obtaining a more specific equation able to predict the vertical forces. Instead of performing it programmatically in the Matlab command window, it was performed interactively by using the curve-fitting toolbox in Matlab. Before it is examined what model to apply in the curve-fitting procedure, a quick summary of curve-fitting in general is discussed.

As stated on MathWorks (2016) curve-fitting implies finding the mathematical function representing a curve producing the best fit for a set of data points. It can involve interpolation, as explained in section 6.1, or smoothing, which involves finding a "smooth" function that approximately fits the data. Smoothing is the process applied in this case. The function that defines this "smooth" curve relates the response data points to the predictor data points with one or more coefficients. As stated MathWorks (2016) curve -fitting finds these coefficients by applying the principle of least squares, which minimizes the summed square of residuals. Naturally, the curve-fitting toolbox in Matlab applies this principle. According to MathWorks (2016) residuals are defined as the difference between the observed response value, and the predicted response value. In other words, if the observed response value is defined as y_i, and the predicted response value as $\hat{y}_i$, then the residual for the ith data point, r_i, is defined as:

$$r_i = y_i - \hat{y}_i \tag{49}$$

The summed square of residuals, S, is then defined as:

$$S = \sum_{i=1}^{n} r_i^2 = \sum_{i=1}^{n} (y_i - \hat{y}_i)^2 \tag{50}$$

where n is the total number of included data points.

In curve-fitting there are two types of parametric models; linear, and non-linear. General knowledge states that an equation is linear if it is linear in the variables, which means it cannot produce curvature, i.e. $y = x$. Furthermore, it said that an equation is non-linear if it is non-linear in the variables, which means that it can produce curvature, i.e. $y = x^2$. However, as stated on MathWorks (2016), in a curve-fitting procedure an equation is linear if it is linear in the coefficients/parameters, i.e. $y = ax^2$, and non-linear if it is opposite of that, i.e. $y = a^2x^2$. In other words, in a curve-fitting procedure, an equation that produces curvature can still be a linear equation as long as the coefficients are linear. Even though linear equations can model curves it has restrictions related to the curves it can model. A non-linear model covers many different forms, and therefore provides the most flexible curve-fitting functionality.

6.2.3.   Curve-Fitting Model

By looking at the drawn curves, and the subsequent peak values forming this curve shape, it seemed like a linear model would have difficulty providing the appropriate fit that was preferred. Thus, it was concluded that the curves in the experiments would be best formed by a non-linear model. There exists many option for non-linear models; exponential, rational, Fourier, Gaussian etc. As the different data sets reminded much to that of a Gaussian model, this approach was investigated. A Gauss function is defined as:

$$f(x) = a_1 e^{-\left(\frac{x-b_1}{c_1}\right)^2} \tag{51}$$

It was experimented with Gauss functions containing everything from one to multiple terms, and it was found that a Gauss function with three separate terms gave the best fit for all the experiments. The form of the Gauss function applied in the experiments was:

$$f(x) = a_1 e^{-\left(\frac{x-b_1}{c_1}\right)^2} + a_2 e^{-\left(\frac{x-b_2}{c_2}\right)^2} + a_3 e^{-\left(\frac{x-b_3}{c_3}\right)^2} \tag{52}$$

In order to achieve a good fit using the gauss function presented in equation (52) some modifications to the data sets had to be made. First, approximated end points were added in each experiment; the excitation frequency applied in every experiment was not far enough away from the resonance frequency to achieve approximate zero response. Hence, end points will contribute to a better fit. To actually verify that the response went towards zero far away from the resonance period, one of the experiments (experiment eight) was tested with full scale excitation periods at -4 seconds and +4 seconds from the resonance period. Consequently, for experiment eight this corresponded to a model scale excitation frequency of 1.054Hz and 0.365Hz respectively. Presented in Figure 42 is the results of the examination.
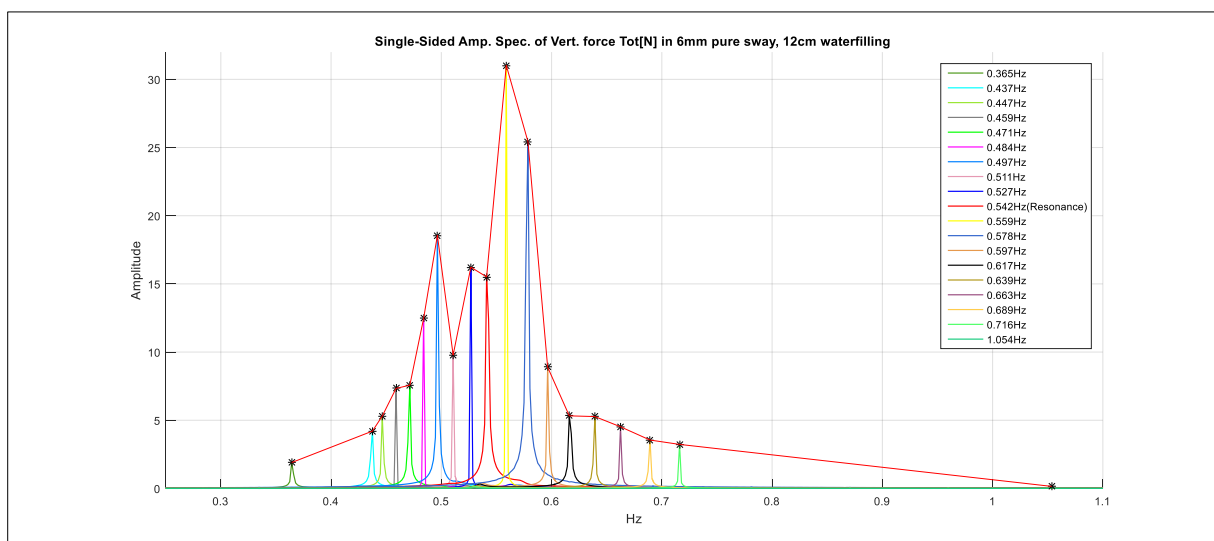
Figure 42 Experiment eight tested with excitation frequencies far away from resonance frequency to verify that response goes towards zero for these conditions

As seen from the figure, at very high and very low excitation frequencies from the resonance frequency the response decreases towards zero.

Secondly, in certain experiments some of the measured excitation frequencies, and their corresponding peak values, were on locations that deviated from the wanted curve shape. These points were excluded from the fitting process. When performing model experiments it is important to acknowledge that no physical quantity can be measured with perfect certainty. There will always be errors in the measurements, be it systematic errors, random errors, or

both. Needless to say, the results attained from the different experiments must be evaluated accordingly. This topic is discussed further in chapter 7. In any case, some error in the peak values accumulated at the different excitation frequencies in each experiment will be present; the value of each peak might not represent the average value had more tests been performed. Instead they will be a close approximate depiction. Due to this fact it allowed for some minor alterations to be made, hence the removal of some of the more extreme values, or outliers, to give a better fit.

Presented in the following figures are the curve-fitting results from using the Gaussian function in equation (52). These curve would then represent an estimate of the amplitude for the total vertical force at all other untested frequencies in the tested frequency excitation range.
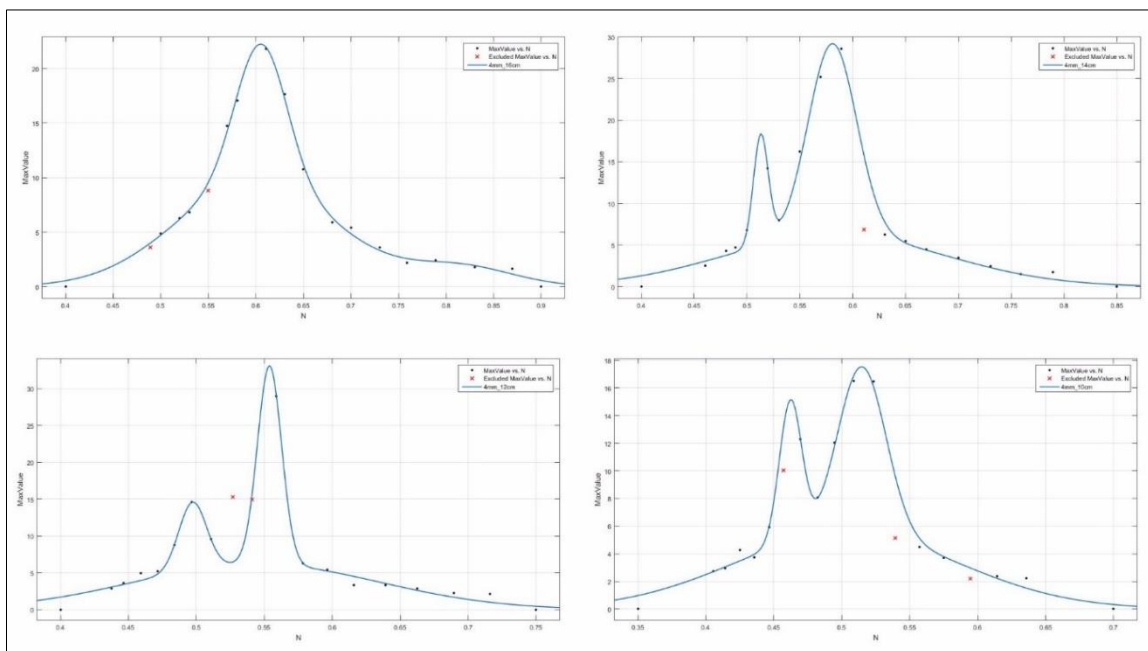
Figure 43 Curve-fitting results from 16cm-10cm water height at 4mm pure sway amplitude
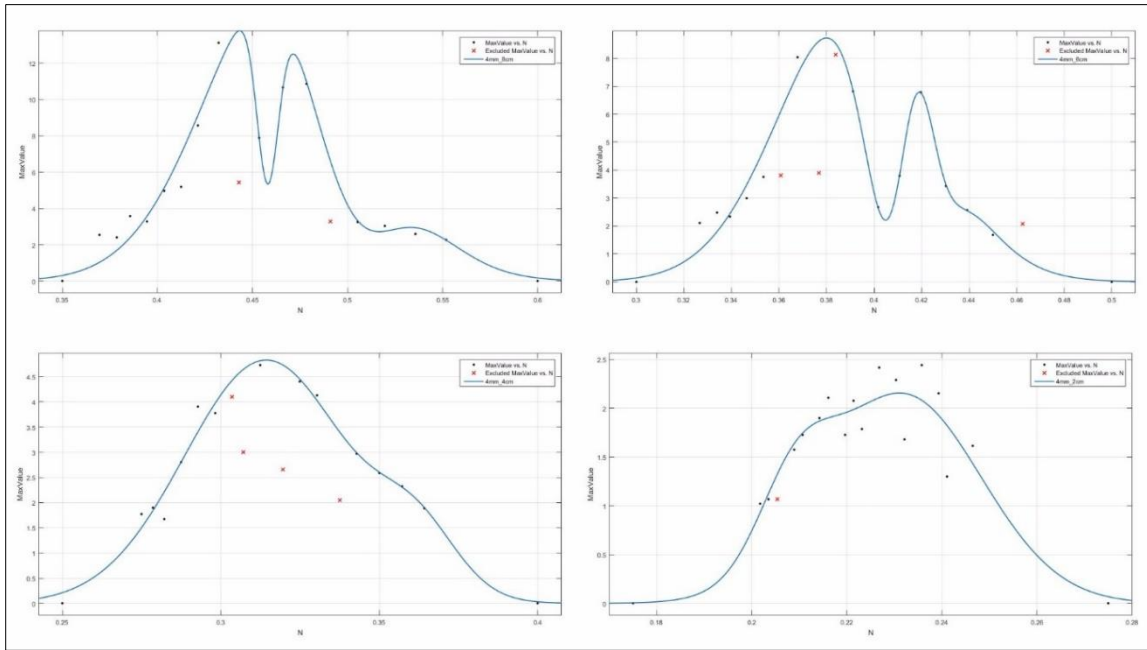
Figure 44 Curve-fitting results from 8cm-2cm water height at 4mm pure sway amplitude
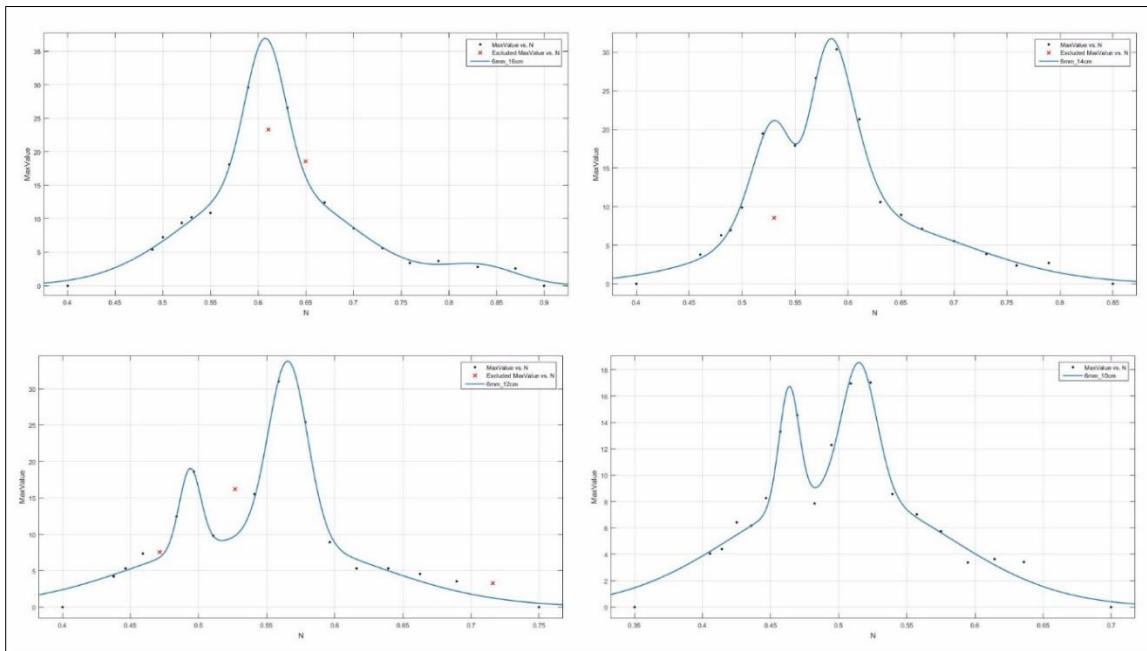
Figure 45 Curve-fitting results from 16cm-10cm water height at 6mm pure sway amplitude
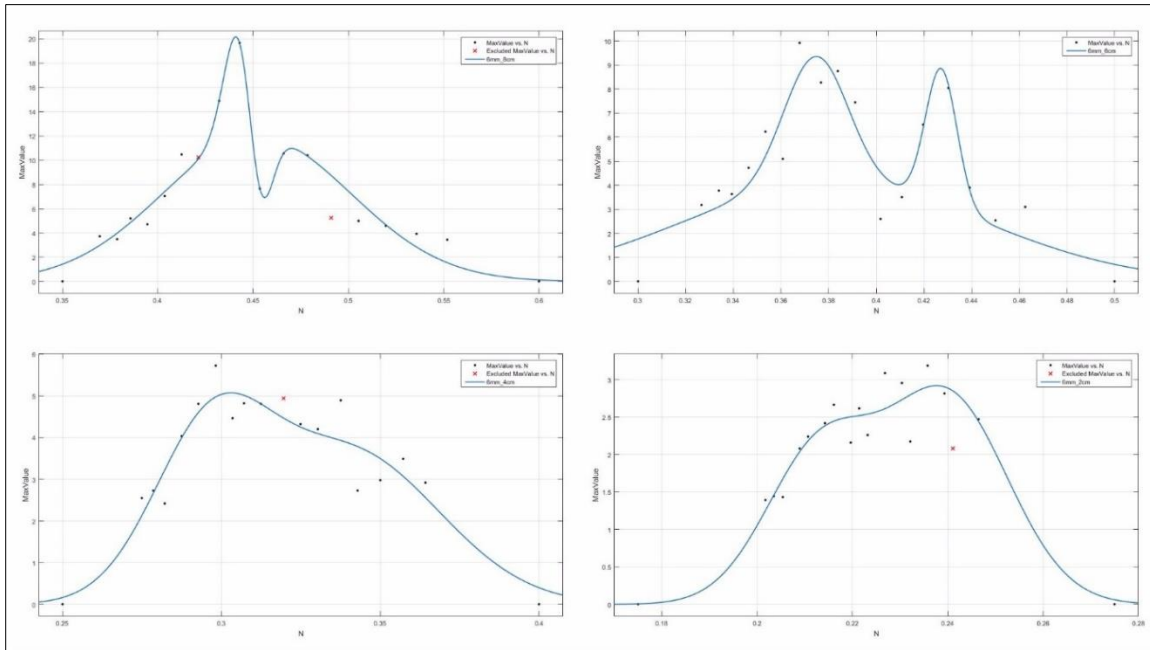
Figure 46 Curve-fitting results from 8cm-2cm water height at 6mm pure sway amplitude
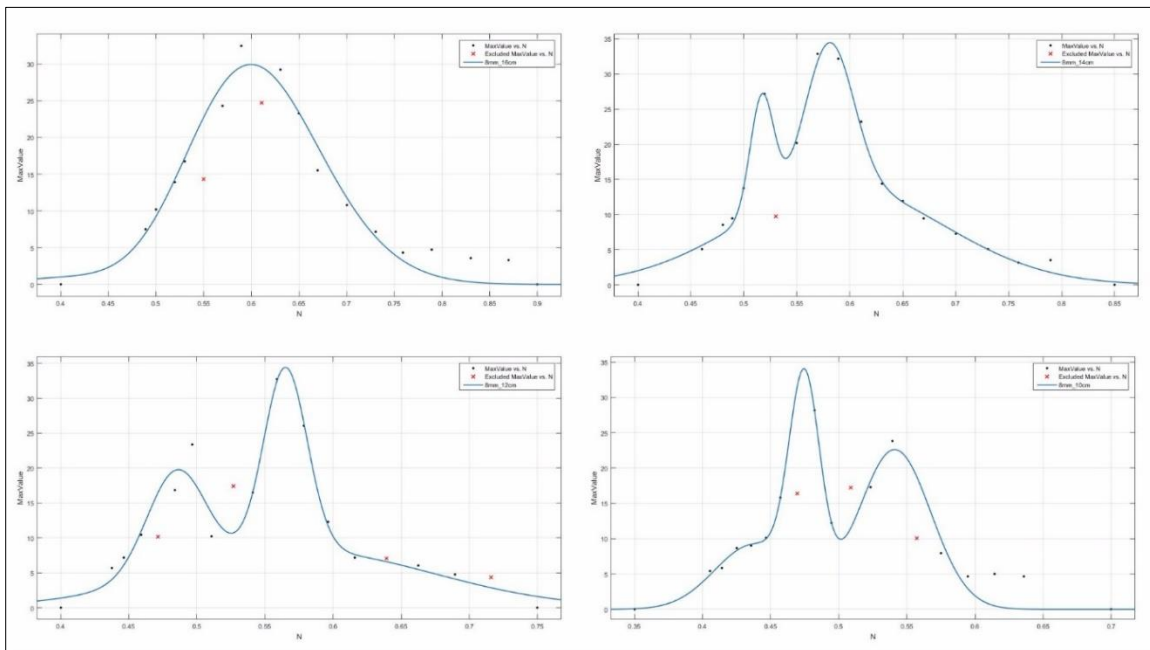
Figure 47 Curve-fitting results from 16cm-10cm water height at 8mm pure sway amplitude
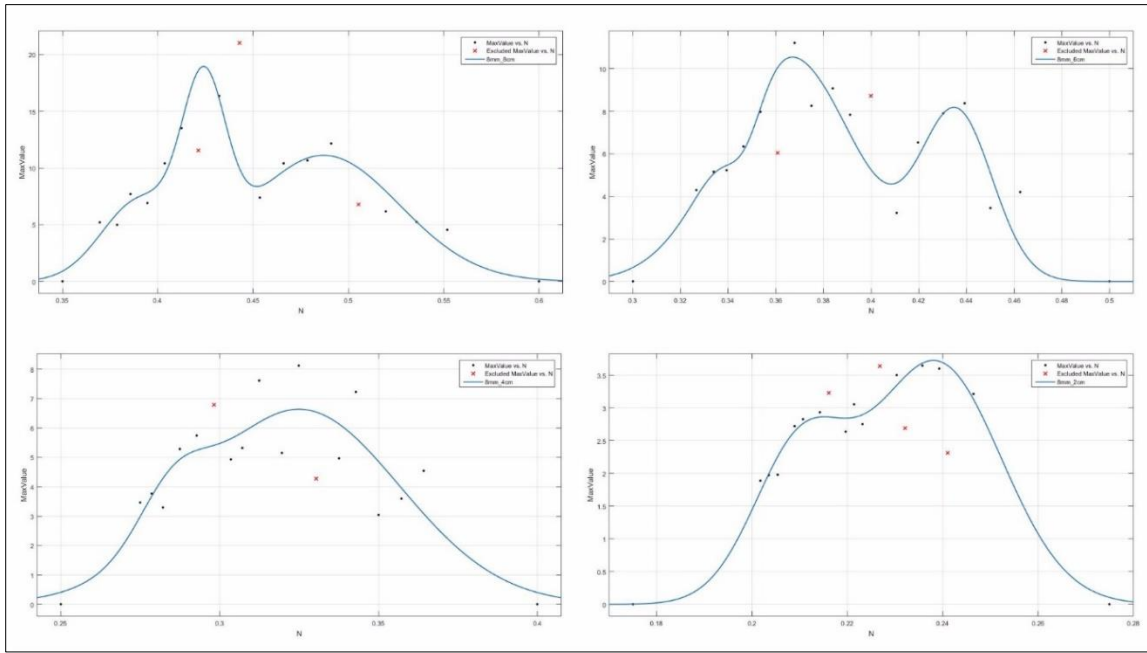
Figure 48 Curve-fitting results from 8cm-2cm water height at 8mm pure sway amplitude

The red x's in each figure represents the data points, that were excluded from the analysis. Naturally, the Gaussian model found from this curve-fitting is a function of the excitation frequency, and is therefore on the form:

$$F(f) = a_1 e^{-\left(\frac{f-b_1}{c_1}\right)^2} + a_2 e^{-\left(\frac{f-b_2}{c_2}\right)^2} + a_3 e^{-\left(\frac{f-b_3}{c_3}\right)^2} \tag{53}$$

where f is the defined as the excitation frequency, a, b and c are the Gaussian coefficients calculated by the toolbox, and F(f) is the total vertical force. The coefficients for each curve were calculated by Matlab, and can be found in appendix B.3. It can be mentioned that even though a Gaussian model was applied for this case, there were a few coefficients to consider in this particular model. It might be that other non-linear models would have given just as good a fit, but with lesser coefficients. However, as a decent fit was found this was not investigated any further.

After curve-fitting all the experiment data sets using a Gaussian function, the Gaussian curves were plotted up against each other in a 3D plot. As stated earlier plotting the curves in 3D would allow for a more summarized visualization of the results. There were three 3D plots in total,

and presented in each 3D plots are the curves for every water height at one sway excitation amplitude. The plots were extracted from the toolbox.
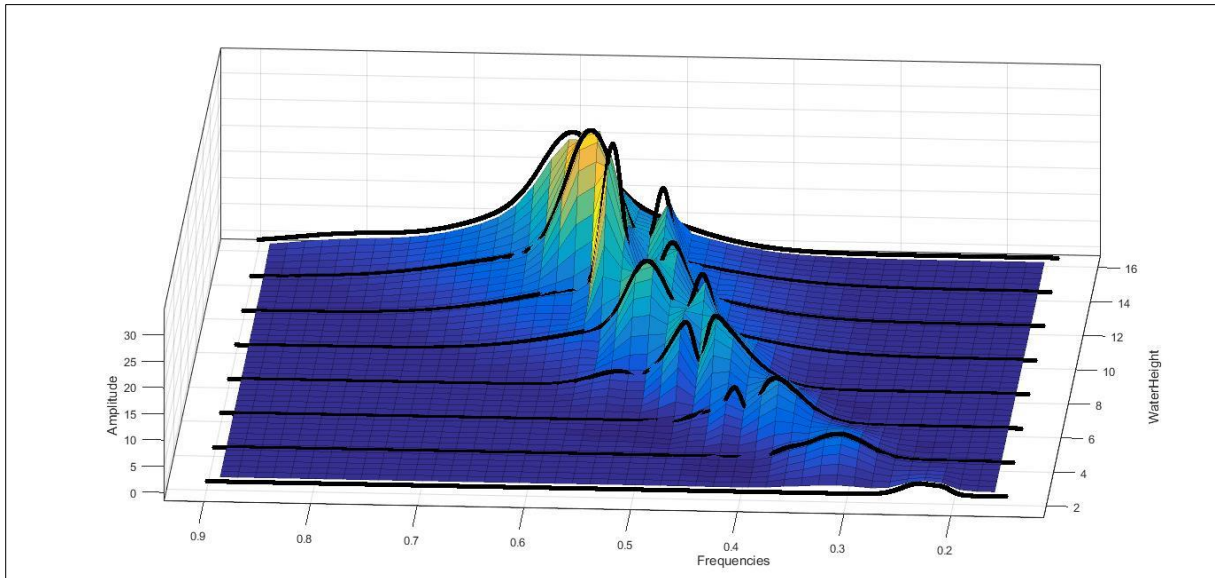
Figure 49 3D plot of Gaussian curves from 16cm-2cm in 4mm sway amplitude. Cubic interpolation is performed between each curve
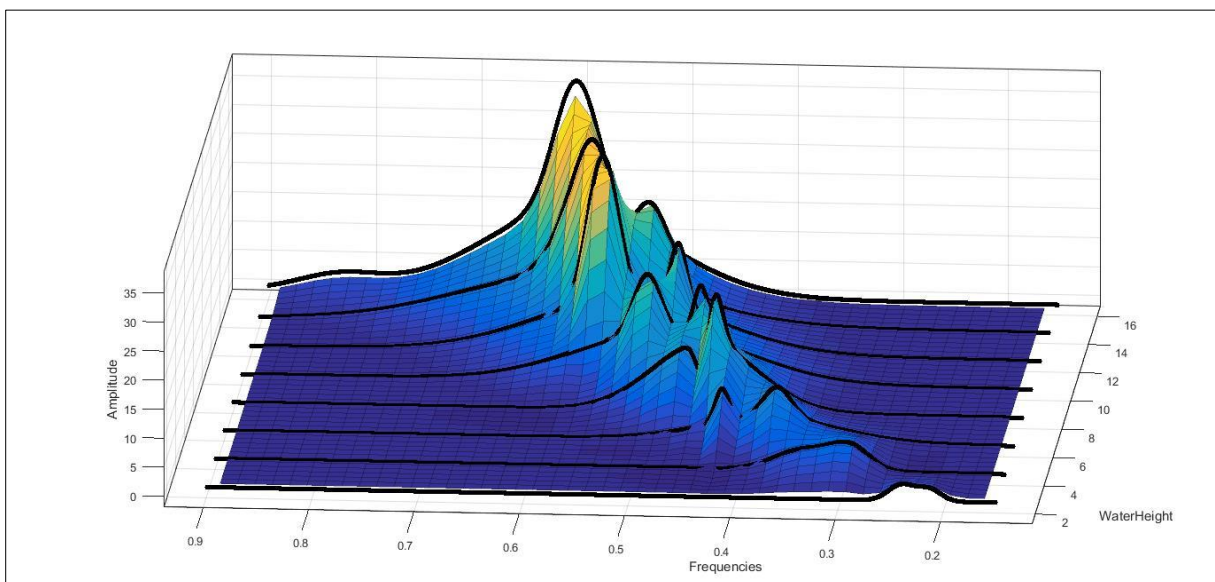
Figure 50 3D plot of Gaussian curves from 16cm-2cm in 6mm sway amplitude. Cubic interpolation is performed between each curve
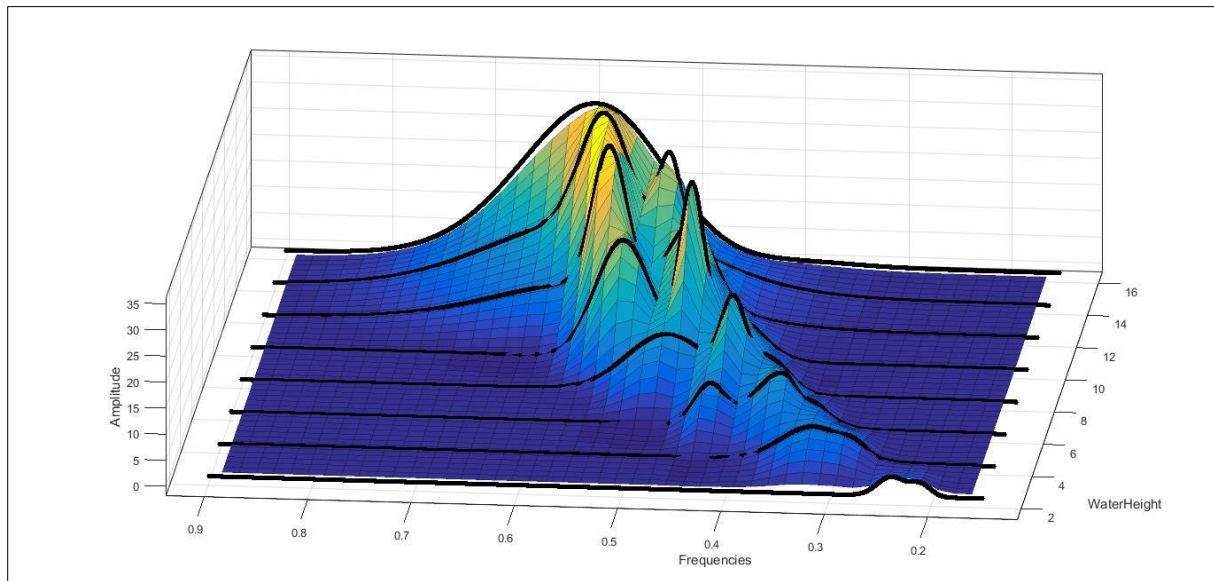
Figure 51 3D plot of Gaussian curves from 16cm-2cm in 8mm sway amplitude. Cubic interpolation is performed between each curve

As seen from the plots, at very low and very high water depth the curves are single peaked, while they are double peaked in-between. Furthermore, the similarity in the curves at the same water height for the different sway amplitudes is evident from the plots. Hence, in spite of the increasing power as a result of increasing sway amplitude, the result is that the 3D plots are quite similar to each other in terms of shape. Additionally, the 3D plots are following a curved path, which is a result of the resonance frequency changing for every new water height. Lastly, it can also be observed from the plots that the amplitude of the vertical forces seems to be largest in the range from 14cm to 12cm water height.

From these findings it can be concluded that there indeed does seem to be a similarity between the tested parameters, and the vertical forces that develop in pure sway motion of roll damping tank. However, the model found so far was a function of excitation frequency, which meant that the coefficients in the model varied each time the water height or the sway amplitude changed. In other words, the model coefficients were based on what water height and sway amplitude were present at the moment, and hence could not predict the vertical forces if these parameters were varied, without first calculating the coefficients anew. Thus, the Gaussian model gave only a partial mathematical description of the similarity; it didn't express the

70

similarities in their entirety. To get a more specific equation that better express the similarities seen in the 3D plots further investigation is necessary, however this was not accomplished in this thesis.

7. Error Analysis

When performing model experiments, it is important to acknowledge that the measured value can never give results that correspond perfectly with the expected value. For instance, if the same quantity is measured twice there is certain to be a difference between the two measured values. Hence, there will always be some level of uncertainty/error between the measured value and the expected, "true" value. According to Steen (2014) sources that contribute to such uncertainty are:

1. Scale effects
2. Incorrect modelling of structure
3. Incorrect modeling of environment
4. Instrumentation and measurements error
5. Error in analysis and interpretation of results

The points above are all sources of experimental errors that will affect the accuracy and precision of the measured values. As stated by Taylor (1999) accuracy determine how close a measured value is to the "true" value, while precision determine how well two or more measurements agree with each other. In recent years a new phenomenon has been developed to account for these experimental errors. This uncertainty analysis reduces the experimental error by considering both accuracy and precision.

According to Taylor (1999) errors that affect the accuracy of a measurement are systematic errors, while errors that affect the precision are random errors. Additionally, the degree of accuracy and precision of measured values determine whether systematic errors are present (incorrect calibration), random errors are present (not enough sample size), both, or if the accuracy and precision is so good that both errors can be "neglected". For example, high accuracy and low precision is a random error, while low accuracy and high precision is a systematic error, and so on. As stated by Steen (2014) systematic errors can arise due to for instance incorrectly calibrated measuring equipment, or zeroing neglect, while random errors can arise due to for instance mechanical vibrations, fluctuations in temperature etc.

Steen (2014) stated that for experiments where no prior proof exists that the tests give valid results, an uncertainty analysis can be very time-consuming. For instance, it requires multiple tests with different test setups, different testing facilities etc. to identify systematic errors. Additionally, in the case for random errors it requires multiple tests to reduce its effect and find an average of the results.

For the sloshing simulator at MARINTEK there exists a large database of prior experiments to verify that tests performed with the tank will produce trustworthy results given that the equipment is properly configured, and enough test samples are accumulated. Hence, in this case it was not necessary to perform an extensive uncertainty analysis involving different test setups etc. However, a routine inspection of the equipment was performed. This is explained in section 0, and involves the assessment of the calibration accuracy. Furthermore, the objective in this thesis was to find trends, and not to verify the precision of measured values. Therefore, calculating precision limits and standard deviations was not necessary. Nonetheless, to verify that some random errors will always be present, several excitation frequencies were tested a second time. See Figure 52 for the result of the inspection.
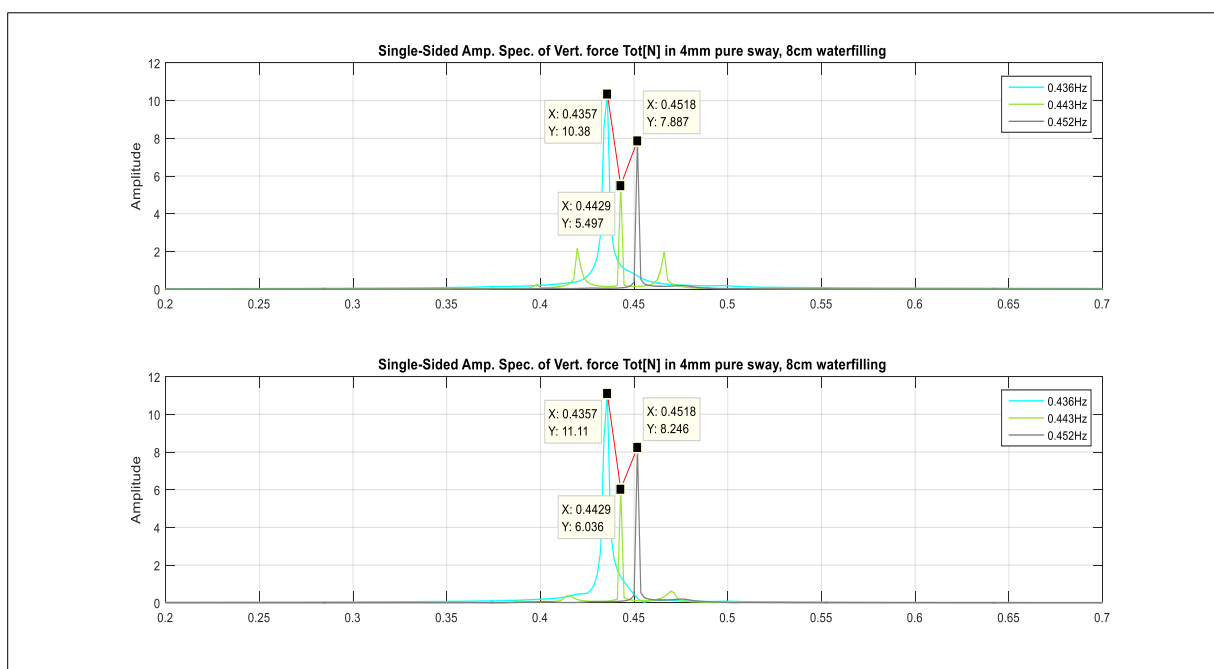
Figure 52 Verification of random errors occurring in the experiments. Three excitation frequencies at 8cm water height, and 4mm sway amplitude was run two times.

As seen from Figure 52 trends can clearly be observed. Additionally, when each specific excitation frequency in the first test is compared with the same frequency in the other test, a variation in the amplitude of the total vertical force can be observed, verifying the presence of random errors. There can be several reasons for these random errors, with viscous effects from the fluid playing one of the larger roles. The main contributor to change in viscosity is temperature; when temperature changes, so does the viscosity. As previously explained, viscous effects are also the reason for why the calculated natural frequency of the various water levels are different from the actual natural frequency. In conclusion, the viscosity of water can be an error source giving these variations in the results. Hence, this is also the reason for why some of the more extreme values in the experiments were excluded from the analysis, as explained in section 6.2.3.

8. Conclusion

In this thesis the objective was to perform experiments in pure sway motion of a model roll damping tank to try and locate a connection between the vertical forces that develop in such condition, and several influential parameters such as excitation frequency, excitation amplitude and water filling level. The frequency spectrums of the vertical forces developed at these differing parameters were instrumental in the investigation. If a connection existed an equation that, preferably, expressed the vertical forces with respect to several of the tested parameters, would be attempted found.

Twenty-four main experiments were performed, which included eight different water heights, three different sway excitation amplitudes at each water height, and seventeen different excitation frequencies at each sway amplitude for each water height, varying from the natural frequency of the given water height. To clarify, one experiment would include one specific water height and one specific sway amplitude, which were tested at seventeen different excitation frequencies and so on.

As stated earlier, the time domain results of these experiments were extracted and converted to frequency spectrums. To make it easier to evaluate if a pattern in the experimental data existed, the frequency spectrums for every excitation frequency at each water height was plotted up against each other in the same figure. Naturally, this meant that there were three figures at every water height, each with different sway amplitudes.

After every experiment had been plotted a thorough evaluation of the figures proceeded. A pattern in the figures was found by plotting the peak values for each excitation frequency, in each experiment, and drawing a line between them. As a pattern in the experiments were located it was attempted to express this pattern by an equation.

Finding a model that could represent the curves that seemed to be developed by these peak values required a curve-fitting procedure. Due to the complex curve shapes the peak values represented, it was decided to apply a non-linear model. It was found that a Gauss function of three terms would represent the curve shapes fairly well, hence it was applied as a solution in

the curve-fitting procedure. However, even though a Gaussian model gave decent curve-fittings, it didn't rule out the fact that other non-linear models could also give appropriate fittings. Nevertheless, as a non-linear model that gave good results were established, a thorough experimentation worth mentioning with other non-linear models was not conducted.

To further evaluate the curves at changing water height and sway amplitude, the curve-fitting results for every experiment was plotted up against each other in 3D. There were three 3D plots in total, and each 3D plot represented the curves for every water height at one sway excitation amplitude. From those 3D plots a clear arrangement was observed, which confirmed that a connection existed between the vertical forces and the parameters tested.

As previously mentioned, the parameters which were tested in the experiments were water height, sway amplitude and excitation frequency. Hence, since the Gauss model established so far were a function of excitation frequency, it meant that the coefficients in this model varied each time the water height or the sway amplitude changed. In other words, the model coefficients were based on what water height and sway amplitude were present at the moment, and hence could not predict the vertical forces if these parameters were varied without first calculating the coefficients anew. Strictly speaking, the model didn't express the relationship visible from the results in its entirety. Nevertheless, as an arrangement in the 3D plots was clearly visible, a model that expressed the vertical forces with more than one parameter should be possible to extract. However, finding an equation that is a function of more parameters than the excitation frequency was not accomplished in this thesis.

To summarize, in the investigation conducted during this thesis it was found that a relationship existed between the vertical forces and the parameters tested, and that this relationship could be expressed in terms of an equation. However, the function established could only model the vertical forces for varying excitation frequency, and thus, the relationship was only partially expressed; the coefficients in the equation varied each time the water height or the sway amplitude changed, hence the model could not predict the vertical forces if these parameters varied without first calculating the coefficients anew.

9. Prospect for Further Work

When it comes to prospect for further work it is, first and foremost, recommended to continue where this thesis left off; try to develop a full mathematical description of the relationship that exists between the vertical forces and the tested parameters. It was found that a Gaussian model gave decent fittings, hence it is recommended to apply this non-linear model when trying to express the relationship with more than one parameter. However, as no other non-linear models were tested another suggestion is to investigate with other such models to evaluate if a more improved overall fit can be achieved.

A possible direction to take the present problem is to acquire a two parameter model which is a function of both excitation frequency and water height. Therefore, since the 3D plots were quite similar in shape, one could attempt to extract a relationship that accounted for the power difference at each sway amplitude, and then implement this relationship into the model. This would enable the possibility to predict the vertical forces, not only for different excitation frequencies and water heights, but at different sway amplitudes as well.

As mentioned earlier when a ship rolls there is a coupling of sway and roll motion. Thus, further work could involve testing the tank in a pure roll motion to see how the forces and moments are influenced by the parameters in this state. Further investigations involving coupled sway and roll motion of the tank could also be accomplished to evaluate the forces and moments there.

Lastly, another matter which might be interesting to investigate further is the curve shape that seems to be developed by the position of the frequency spectrum peak values at water heights close to maximum and minimum filling level. At these conditions the damping effect was reduced. Hence, it would be interesting to know if there is a connection between this reduced damping effect and the position of the frequency spectrum peak values in relation to each other, or if it is just an anomaly.

References

Akyildiz, H., & Ünal, E. (2005). Experimental investigation of pressure distribution on a rectangular tank due to the liquid sloshing. Ocean Engineering., pp. 1503-1516.

Biles, H. J. (1925). Model experiments wih anti-rolling tanks. Transactions of Institution of Naval Architects.

Chu, B. T., & Ying, S. J. (1963). Thermally driven nonlinear oscillations in a pipe with traveling shock waves. Physics of Fluids., pp. 1625-1637.

Faltinsen, O. M. (1990). Sea Loads on Ships and Offshore Structures. Cambridge University Press.

Faltinsen, O. M., & Timokha, A. N. (2009). Sloshing. Cambridge University Press.

Frahm, H. H. (1911). Results of trials of the anti-rolling tanks at sea. Journal of the American Society for Naval Rngineers, pp. 571-597.

Goodrich, G. J. (1968). Developement and design of passive roll stabilisers. London: Royal Institution of Naval Architects.

Larsen, C. M. (2015). TMR 4182 Marine Dynamics compendium. Department of marine technology, NTNU.

MathWorks. (2016). se.matworks.com. Retrieved from MathWorks: http://se.mathworks.com/help/curvefit/least-squares-fitting.html

Moaleji, R., & Grieg, A. R. (2007). On the development of ship anti-roll tanks. Ocean Engineering, pp. 103-121.

Perez, T., & Blanke, M. (2012). Ship roll damping control. Annual Reviews in Control., pp. 129-147.

Pettersen, B. (2007). Marine Technology 3 - Hydrodynamics. Trondheim: NTNU.

Steen, S. (2014). Experimental methods in marine hydrodynamics. Trondheim: NTNU.

Taylor, J. R. (1999). An Introduction to Error Analysis: The Study of Uncertainties in Physical Measurements. University Science Books.

TMR 7 Experimental methods in Marine Hydrodynamics. (2015). Retrieved from http://www.ivt.ntnu.no/imt/courses/tmr7/LabTests/LabTest1/labtest1_2015.htm

Van den Bosch, J. J., & Vugts, J. H. (1966). Roll damping by free surface tanks.

Verhagen, J. H., & Van Wijngaarden, L. (1965). Non-linear oscillations of fluid in a container. Journal of Fluid Mechanics., pp. 737-751.

Appendix A: Summary of Experiments

Table 5 Experiment 1-3

Waterfilling level [m]	0,16																
Excitation amplitude pure sway [mm]	4 (1)	6(2)	8 (3)														
Full scale resonance period: T_f [s]	7,14																
Model scale resonance period: T_m [s]	1,60																
									R								
y	-2	-1,75	-1,5	-1,25	-1	-0,75	-0,5	-0,25	0	0,25	0,5	0,75	1	1,25	1,5	1,75	2
Range of excitation period full scale : T_f-y [s]	5,14	5,39	5,64	5,89	6,14	6,39	6,64	6,89	7,14	7,39	7,64	7,89	8,14	8,39	8,64	8,89	9,14
Range of excitation period model scale: T_f-y/20^0,5 [s]	1,15	1,21	1,26	1,32	1,37	1,43	1,48	1,54	1,60	1,65	1,71	1,76	1,82	1,88	1,93	1,99	2,04
Range of excitation frequency model scale [Hz]	0,87	0,83	0,79	0,76	0,73	0,70	0,67	0,65	0,63	0,61	0,59	0,57	0,55	0,53	0,52	0,50	0,49

Table 6 Experiment 4-6

Waterfilling level [m]	0,14																
Excitation amplitude pure sway [mm]	4 (4)	6(5)	8 (6)														
Full scale resonance period: T_f [s]	7,63																
Model scale resonance period: T_m [s]	1,71																
									R								
y	-2	-1,75	-1,5	-1,25	-1	-0,75	-0,5	-0,25	0	0,25	0,5	0,75	1	1,25	1,5	1,75	2
Range of excitation period full scale : T_f-y [s]	5,63	5,88	6,13	6,38	6,63	6,88	7,13	7,38	7,63	7,88	8,13	8,38	8,63	8,88	9,13	9,38	9,63
Range of excitation period model scale: T_f-y/20^0,5 [s]	1,26	1,32	1,37	1,43	1,48	1,54	1,59	1,65	1,71	1,76	1,82	1,87	1,93	1,99	2,04	2,10	2,15
Range of excitation frequency model scale [Hz]	0,79	0,76	0,73	0,70	0,67	0,65	0,63	0,61	0,59	0,57	0,55	0,53	0,52	0,50	0,49	0,48	0,46

Table 7 Experiment 7-9

										R								
Waterfilling level [m]	0,12																	
Excitation amplitude pure sway [mm]	4 (7)	6(8)	8 (9)															
Full scale resonance period: T_f [s]	8,24																	
Model scale resonance period: T_m [s]	1,84																	
γ	-2	-1,75	-1,5	-1,25	-1	-0,75	-0,5	-0,25	0	0,25	0,5	0,75	1	1,25	1,5	1,75	2	
Range of excitation period full scale : T_f-γ [s]	6,24	6,49	6,74	6,99	7,24	7,49	7,74	7,99	8,24	8,49	8,74	8,99	9,24	9,49	9,74	9,99	10,24	
Range of excitation period model scale: T_f-γ/20^0,5 [s]	1,40	1,45	1,51	1,56	1,62	1,68	1,73	1,79	1,84	1,90	1,96	2,01	2,07	2,12	2,18	2,23	2,29	
Range of excitation frequency model scale [Hz]	0,716	0,689	0,663	0,639	0,617	0,597	0,578	0,559	0,542	0,527	0,511	0,497	0,484	0,471	0,459	0,447	0,437	

Table 8 Experiment 10-12

										R								
Waterfilling level [m]	0,1																	
Excitation amplitude pure sway [mm]	4 (10)	6(11)	8 (12)															
Full scale resonance period: T_f [s]	9,03																	
Model scale resonance period: T_m [s]	2,02																	
γ	-2	-1,75	-1,5	-1,25	-1	-0,75	-0,5	-0,25	0	0,25	0,5	0,75	1	1,25	1,5	1,75	2	
Range of excitation period full scale : T_f-γ [s]	7,03	7,28	7,53	7,78	8,03	8,28	8,53	8,78	9,03	9,28	9,53	9,78	10,03	10,28	10,53	10,78	11,03	
Range of excitation period model scale: T_f-γ/20^0,5 [s]	1,57	1,63	1,68	1,74	1,80	1,85	1,91	1,96	2,02	2,08	2,13	2,19	2,24	2,30	2,35	2,41	2,47	
Range of excitation frequency model scale [Hz]	0,636	0,614	0,594	0,575	0,557	0,540	0,524	0,509	0,495	0,482	0,469	0,457	0,446	0,435	0,425	0,415	0,405	

Table 9 Experiment 13-15

Waterfilling level [m]	0,08																
Excitation amplitude pure sway [mm]	4 (13)	6(14)	8 (15)														
Full scale resonance period: T_f [s]	10,10																
Model scale resonance period: T_m [s]	2,26																
									R								
y	-2	-1,75	-1,5	-1,25	-1	-0,75	-0,5	-0,25	0	0,25	0,5	0,75	1	1,25	1,5	1,75	2
Range of excitation period full scale : T_f-y [s]	8,10	8,35	8,60	8,85	9,10	9,35	9,60	9,85	10,10	10,35	10,60	10,85	11,10	11,35	11,60	11,85	12,10
Range of excitation period model scale: T_f-y/20^0,5 [s]	1,81	1,87	1,92	1,98	2,03	2,09	2,15	2,20	2,26	2,31	2,37	2,43	2,48	2,54	2,59	2,65	2,70
Range of excitation frequency model scale [Hz]	0,552	0,536	0,520	0,506	0,492	0,478	0,466	0,454	0,443	0,432	0,422	0,412	0,403	0,394	0,386	0,378	0,370

Table 10 Experiment 16-18

Waterfilling level [m]	0,06																
Excitation amplitude pure sway [mm]	4 (16)	6(17)	8 (18)														
Full scale resonance period: T_f [s]	11,66																
Model scale resonance period: T_m [s]	2,61																
									R								
y	-2	-1,75	-1,5	-1,25	-1	-0,75	-0,5	-0,25	0	0,25	0,5	0,75	1	1,25	1,5	1,75	2
Range of excitation period full scale : T_f-y [s]	9,66	9,91	10,16	10,41	10,66	10,91	11,16	11,41	11,66	11,91	12,16	12,41	12,66	12,91	13,16	13,41	13,66
Range of excitation period model scale: T_f-y/20^0,5 [s]	2,16	2,22	2,27	2,33	2,38	2,44	2,50	2,55	2,61	2,66	2,72	2,77	2,83	2,89	2,94	3,00	3,05
Range of excitation frequency model scale [Hz]	0,463	0,451	0,440	0,430	0,420	0,410	0,401	0,392	0,384	0,376	0,368	0,360	0,353	0,346	0,340	0,334	0,327

Table 11 Experiment 19-21

									R								
Waterfilling level [m]	0,04																
Excitation amplitude pure sway [mm]	4 (19)	6(20)	8 (21)														
Full scale resonance period: T_f [s]	14,28																
Model scale resonance period: T_m [s]	3,19																
y	-2	-1,75	-1,5	-1,25	-1	-0,75	-0,5	-0,25	0	0,25	0,5	0,75	1	1,25	1,5	1,75	2
Range of excitation period full scale : T_f-y [s]	12,28	12,53	12,78	13,03	13,28	13,53	13,78	14,03	14,28	14,53	14,78	15,03	15,28	15,53	15,78	16,03	16,28
Range of excitation period model scale: T_f-y/20^0,5 [s]	2,75	2,80	2,86	2,91	2,97	3,03	3,08	3,14	3,19	3,25	3,30	3,36	3,42	3,47	3,53	3,58	3,64
Range of excitation frequency model scale [Hz]	0,364	0,357	0,350	0,343	0,337	0,331	0,325	0,319	0,313	0,308	0,303	0,298	0,293	0,288	0,283	0,279	0,275

Table 12 Experiment 22-24

									R								
Waterfilling level [m]	0,02																
Excitation amplitude pure sway [mm]	4 (22)	6(23)	8 (24)														
Full scale resonance period: T_f [s]	20,19																
Model scale resonance period: T_m [s]	4,52																
y	-2	-1,75	-1,5	-1,25	-1	-0,75	-0,5	-0,25	0	0,25	0,5	0,75	1	1,25	1,5	1,75	2
Range of excitation period full scale : T_f-y [s]	18,19	18,44	18,69	18,94	19,19	19,44	19,69	19,94	20,19	20,44	20,69	20,94	21,19	21,44	21,69	21,94	22,19
Range of excitation period model scale: T_f-y/20^0,5 [s]	4,07	4,12	4,18	4,24	4,29	4,35	4,40	4,46	4,52	4,57	4,63	4,68	4,74	4,79	4,85	4,91	4,96
Range of excitation frequency model scale [Hz]	0,246	0,242	0,239	0,236	0,233	0,230	0,227	0,224	0,221	0,219	0,216	0,214	0,211	0,209	0,206	0,204	0,202

Appendix B: Summary of the Matlab Scripts Applied in the Investigation

Presented in this appendix is the different Matlab scripts applied in the investigation. It should be noted that the script used for the conversion of Catman bin files to readable files for Matlab was a file available at NTNU's course "Experimental Methods in Marine Hydrodynamics" (2015) homepage, and thus not published in this thesis.

B.1 Matlab Script for the Extraction of Time Domain Results

In this script the time domain results were extracted, filtered and transformed into frequency domain results.

```matlab
function Data=ExtractData(catkinfile)

[a1,a2]=catman_read_5r8(catkinfile); % From NTNU. conversion script


% TIMEDOMAIN RESULTS (Unfiltered signal)


Data.time=a2(1).data(1:end);
StartPoint=min(find(Data.time>40.000));
StopPoint=min(find(Data.time>10*60.000));

Data.time=a2(1).data(StartPoint:StopPoint);
Data.Vert_Tot=a2(8).data(StartPoint:StopPoint);

% TIMEDOMAIN RESULTS (Filtered signal)


[B,A]=butter(2,0.020,'low'); % Low-pass filter using butterworth technique

Data.Filtered_time=filtfilt(B,A,Data.time);
Data.Filtered_Vert_Tot=filtfilt(B,A,Data.Vert_Tot);
```

```matlab
% APPLIES THE CORRECT NAME TO THE APPROPIATE CHANNEL

Data.name1=[ [a2(1).ChannelName] '[' [ a2(1).Unit] ']'];
Data.name8=[ [a2(8).ChannelName] '[' [ a2(8).Unit] ']'];

time=Data.time;
L=length(time);      % Signal length
if ((mod(L,2))==1) % Modulus after divison
L=L-1;
end

dT=diff(time);          % Calculates the timestep in the measurements
if var(dT)>1e-5;
    warning('If you do not appear to have a constant timestep. FFT may not
be correct ')
end

T=dT(1);                 % Timestep
Fs=1/T;                  % Sampling frequency
t = (0:L-1)*T;           % Time vector

Data.f=Fs*(0:(L/2))/L;

% CONVERTS FILTERED TIMEDOMAIN RESULTS TO FREQUENCY DOMAIN RESULTS


% Vert_Force_Tot
FFT_Filtered_Vert_Tot              =              fft(Data.Filtered_Vert_Tot-
mean(Data.Filtered_Vert_Tot));
P2 = abs(FFT_Filtered_Vert_Tot/L);
Data.Filtered_Amp_Freq_Vert_Tot = P2(1:L/2+1);
Data.Filtered_Amp_Freq_Vert_Tot(2:end-1)                               =
2*Data.Filtered_Amp_Freq_Vert_Tot(2:end-1);

end
```

B.2 Matlab Script for Experimental Evaluation

As stated earlier there were 24 main experiments. Presented in the following script is the code for experiment one. The same layout was applied for every experiment, and hence it is only necessary to present one of them. This script allows the frequency spectrums for the different excitation frequencies in each experiment to be plotted and compared. Furthermore, it also generates the peak values, as well as applying linear interpolation between them. Lastly, it can be noted that the script for plotting the time domain results during filtering also followed the same layout, however, instead of plotting with respect to "f", it was plotted with respect to "time".

```matlab
% EXPERIMENT1 IN PURE SWAY WITH 4mm EXCITATION AMP., 16cm WATER FILLING AND
% 10 MIN DURATION

% 16CM WATER TESTS CATMAN FILES

file1='Test1(16cm)T1+2.bin';
file2='Test1(16cm)T1+1,75.bin';
file3='Test1(16cm)T1+1,5.bin';
file4='Test1(16cm)T1+1,25.bin';
file5='Test1(16cm)T1+1.bin';
file6='Test1(16cm)T1+0,75.bin';
file7='Test1(16cm)T1+0,5.bin';
file8='Test1(16cm)T1+0,25.bin';
file9='Test1(16cm)T1.bin';
file10='Test1(16cm)T1-0,25.bin';
file11='Test1(16cm)T1-0,5.bin';
file12='Test1(16cm)T1-0,75.bin';
file13='Test1(16cm)T1-1.bin';
file14='Test1(16cm)T1-1,25.bin';
file15='Test1(16cm)T1-1,5.bin';
file16='Test1(16cm)T1-1,75.bin';
file17='Test1(16cm)T1-2.bin';

% GENERAL GUIDE FOR PLOTTING FREQUENCY SPECTRUMS, GENERATING PEAK VALUES
% AND APPLYING LINEAR INTERPOLATION

Data1=ExtractData(file1);
Data2=ExtractData(file2);
Data3=ExtractData(file3);
Data4=ExtractData(file4);
Data5=ExtractData(file5);
Data6=ExtractData(file6);
Data7=ExtractData(file7);
Data8=ExtractData(file8);
Data9=ExtractData(file9);
```

86

```
Data10=ExtractData(file10);
Data11=ExtractData(file11);
Data12=ExtractData(file12);
Data13=ExtractData(file13);
Data14=ExtractData(file14);
Data15=ExtractData(file15);
Data16=ExtractData(file16);
Data17=ExtractData(file17);


% Plotting Vert_Force_Tot frequency spectrums

figure(1)
hold on
subplot(311),plot(Data1.f,Data1.Filtered_Amp_Freq_Vert_Tot,'c','LineWidth',
1);
hold on
subplot(311),plot(Data2.f,Data2.Filtered_Amp_Freq_Vert_Tot,'Color',[0.6 0.9
0.2],'LineWidth',1);
hold on
subplot(311),plot(Data3.f,Data3.Filtered_Amp_Freq_Vert_Tot,'Color',[0.5 0.5
0.5],'LineWidth',1);
hold on
subplot(311),plot(Data4.f,Data4.Filtered_Amp_Freq_Vert_Tot,'g','LineWidth',
1);
hold on
subplot(311),plot(Data5.f,Data5.Filtered_Amp_Freq_Vert_Tot,'m','LineWidth',
1);
hold on
subplot(311),plot(Data6.f,Data6.Filtered_Amp_Freq_Vert_Tot,'Color',[0    0.5
1],'LineWidth',1);
hold on
subplot(311),plot(Data7.f,Data7.Filtered_Amp_Freq_Vert_Tot,'Color',[0.9 0.6
0.7],'LineWidth',1);
hold on
subplot(311),plot(Data8.f,Data8.Filtered_Amp_Freq_Vert_Tot,'Color',[0     0
1],'LineWidth',1);
hold on
subplot(311),plot(Data9.f,Data9.Filtered_Amp_Freq_Vert_Tot,'Color',[1     0
0],'LineWidth',1);
hold on
subplot(311),plot(Data10.f,Data10.Filtered_Amp_Freq_Vert_Tot,'Color',[1    1
0],'LineWidth',1);
hold on
subplot(311),plot(Data11.f,Data11.Filtered_Amp_Freq_Vert_Tot,'Color',[0.2
0.4 0.8],'LineWidth',1);
hold on
subplot(311),plot(Data12.f,Data12.Filtered_Amp_Freq_Vert_Tot,'Color',[0.9
0.6 0.3],'LineWidth',1);
hold on
subplot(311),plot(Data13.f,Data13.Filtered_Amp_Freq_Vert_Tot,'k','LineWidth
',1);
hold on
subplot(311),plot(Data14.f,Data14.Filtered_Amp_Freq_Vert_Tot,'Color',[0.7
0.6 0.1],'LineWidth',1);
hold on
subplot(311),plot(Data15.f,Data15.Filtered_Amp_Freq_Vert_Tot,'Color',[0.6
0.3 0.5],'LineWidth',1);
hold on
```

```matlab
subplot(311),plot(Data16.f,Data16.Filtered_Amp_Freq_Vert_Tot,'Color',[1  0.8
0.3],'LineWidth',1);
hold on
subplot(311),plot(Data17.f,Data17.Filtered_Amp_Freq_Vert_Tot,'Color',[0.3 1
0.4],'LineWidth',1);
legend('0.49Hz','0.50Hz','0.52Hz','0.53Hz','0.55Hz','0.57Hz','0.59Hz','0.61
Hz','0.63Hz
(Resonance)','0.65Hz','0.67Hz','0.70Hz','0.73Hz','0.76Hz','0.79Hz','0.83Hz'
,'0.87Hz');
title('Single-Sided Amp. Spec. of Vert. force Tot[N] in 4mm pure sway, 16cm
waterfilling');
ylabel('Amplitude');

% Generating peak values and applying linear interpolation

subplot(311),plot(0.4,0,'*','color','k'); % Added endpoint
MaxValue(1)=0;
N(1)=0.4;
hold on
[maxvalue, n]=max(Data1.Filtered_Amp_Freq_Vert_Tot);
subplot(311),plot(Data1.f(n),maxvalue,'*','color','k');
MaxValue(2)=maxvalue;
N(2)=Data1.f(n);
hold on
[maxvalue, n]=max(Data2.Filtered_Amp_Freq_Vert_Tot);
subplot(311),plot(Data2.f(n),maxvalue,'*','color','k');
MaxValue(3)=maxvalue;
N(3)=Data2.f(n);
hold on
[maxvalue, n]=max(Data3.Filtered_Amp_Freq_Vert_Tot);
subplot(311),plot(Data3.f(n),maxvalue,'*','color','k');
MaxValue(4)=maxvalue;
N(4)=Data3.f(n);
hold on
[maxvalue, n]=max(Data4.Filtered_Amp_Freq_Vert_Tot);
subplot(311),plot(Data4.f(n),maxvalue,'*','color','k');
MaxValue(5)=maxvalue;
N(5)=Data4.f(n);
hold on
[maxvalue, n]=max(Data5.Filtered_Amp_Freq_Vert_Tot);
subplot(311),plot(Data5.f(n),maxvalue,'*','color','k');
MaxValue(6)=maxvalue;
N(6)=Data5.f(n);
hold on
[maxvalue, n]=max(Data6.Filtered_Amp_Freq_Vert_Tot);
subplot(311),plot(Data6.f(n),maxvalue,'*','color','k');
MaxValue(7)=maxvalue;
N(7)=Data6.f(n);
hold on
[maxvalue, n]=max(Data7.Filtered_Amp_Freq_Vert_Tot);
subplot(311),plot(Data7.f(n),maxvalue,'*','color','k');
MaxValue(8)=maxvalue;
N(8)=Data7.f(n);
hold on
[maxvalue, n]=max(Data8.Filtered_Amp_Freq_Vert_Tot);
subplot(311),plot(Data8.f(n),maxvalue,'*','color','k');
MaxValue(9)=maxvalue;
N(9)=Data8.f(n);
```

```matlab
hold on
[maxvalue, n]=max(Data9.Filtered_Amp_Freq_Vert_Tot);
subplot(311),plot(Data9.f(n),maxvalue,'*','color','k');
MaxValue(10)=maxvalue;
N(10)=Data9.f(n);
hold on
[maxvalue, n]=max(Data10.Filtered_Amp_Freq_Vert_Tot);
subplot(311),plot(Data10.f(n),maxvalue,'*','color','k');
MaxValue(11)=maxvalue;
N(11)=Data10.f(n);
hold on
[maxvalue, n]=max(Data11.Filtered_Amp_Freq_Vert_Tot);
subplot(311),plot(Data11.f(n),maxvalue,'*','color','k');
MaxValue(12)=maxvalue;
N(12)=Data11.f(n);
hold on
[maxvalue, n]=max(Data12.Filtered_Amp_Freq_Vert_Tot);
subplot(311),plot(Data12.f(n),maxvalue,'*','color','k');
MaxValue(13)=maxvalue;
N(13)=Data12.f(n);
hold on
[maxvalue, n]=max(Data13.Filtered_Amp_Freq_Vert_Tot);
subplot(311),plot(Data13.f(n),maxvalue,'*','color','k');
MaxValue(14)=maxvalue;
N(14)=Data13.f(n);
hold on
[maxvalue, n]=max(Data14.Filtered_Amp_Freq_Vert_Tot);
subplot(311),plot(Data14.f(n),maxvalue,'*','color','k');
MaxValue(15)=maxvalue;
N(15)=Data14.f(n);
hold on
[maxvalue, n]=max(Data15.Filtered_Amp_Freq_Vert_Tot);
subplot(311),plot(Data15.f(n),maxvalue,'*','color','k');
MaxValue(16)=maxvalue;
N(16)=Data15.f(n);
hold on
[maxvalue, n]=max(Data16.Filtered_Amp_Freq_Vert_Tot);
subplot(311),plot(Data16.f(n),maxvalue,'*','color','k');
MaxValue(17)=maxvalue;
N(17)=Data16.f(n);
hold on
[maxvalue, n]=max(Data17.Filtered_Amp_Freq_Vert_Tot);
subplot(311),plot(Data17.f(n),maxvalue,'*','color','k');
MaxValue(18)=maxvalue;
N(18)=Data17.f(n);
hold on
MaxValue(19)=0;
subplot(311),plot(0.9,0,'*','color','k'); % Added endpoint
N(19)=0.9;

K=[N;MaxValue]';
K=sortrows(K,1);
subplot(311),plot(K(:,1),K(:,2),'r');
title('Single-Sided Amp. Spec. of Vert. force Tot[N] in 4mm pure sway, 16cm
waterfilling');
ylabel('Amplitude');
xlim([0.35 1.10]);
ylim([0 35]);
```

B.3 Matlab Script to Generate 3D Plots in CF-Tool

The following script represents the code used for generating the 3D plots in the CF-tool. Additionally, the coefficients presented are the coefficients extracted from the CF-tool during the curve-fitting procedure of the experimental data.

```
% 3D PLOT OF GAUSSIAN CURVE FITTING FOR ALL WATER HEIGHTS AT 4MM SWAY AMPLITUDE

Frequencies = linspace(0.15,0.9,6000);
WaterHeight=fliplr([2 4 6 8 10 12 14 16]);

        a1 =        9.632;
        b1 =        0.5993;
        c1 =        0.1175;
        a2 =        1.792;
        b2 =        0.8155;
        c2 =        0.07807;
        a3 =        12.63;
        b3 =        0.6056;
        c3 =        0.03792;

Gauss1_16cm =    a1*exp(-((Frequencies-b1)/c1).^2)  + a2*exp(-((Frequencies-
b2)/c2).^2) + a3*exp(-((Frequencies-b3)/c3).^2);

        a1 =        6.142;
        b1 =        0.5836;
        c1 =        0.1477;
        a2 =        23.06;
        b2 =        0.5809;
        c2 =        0.03231;
        a3 =        13.21;
        b3 =        0.513;
        c3 =        0.009901;

Gauss1_14cm=   a1*exp(-((Frequencies-b1)/c1).^2)   +   a2*exp(-((Frequencies-
b2)/c2).^2) + a3*exp(-((Frequencies-b3)/c3).^2);

        a1 =        26.98;
        b1 =        0.5538;
        c1 =        0.01255;
        a2 =        9.196;
        b2 =        0.4972;
        c2 =        0.01443;
        a3 =        6.197;
        b3 =        0.5444;
        c3 =        0.1275;
```

```
Gauss1_12cm=    a1*exp(-((Frequencies-b1)/c1).^2)  +  a2*exp(-((Frequencies-
b2)/c2).^2) + a3*exp(-((Frequencies-b3)/c3).^2);

        a1 =        12.12;
        b1 =       0.5148;
        c1 =      0.02505;
        a2 =        10.18;
        b2 =       0.4623;
        c2 =      0.01164;
        a3 =        5.469;
        b3 =       0.5034;
        c3 =       0.1167;


Gauss1_10cm=    a1*exp(-((Frequencies-b1)/c1).^2)  +  a2*exp(-((Frequencies-
b2)/c2).^2) + a3*exp(-((Frequencies-b3)/c3).^2);

        a1 =        18.17;
        b1 =       0.4708;
        c1 =      0.05979;
        a2 =       -10.15;
        b2 =       0.4985;
        c2 =      0.03218;
        a3 =       -9.941;
        b3 =        0.458;
        c3 =     0.008146;


Gauss1_8cm=    a1*exp(-((Frequencies-b1)/c1).^2)  +  a2*exp(-((Frequencies-
b2)/c2).^2) + a3*exp(-((Frequencies-b3)/c3).^2);

        a1 =         10.2;
        b1 =       0.3926;
        c1 =      0.04446;
        a2 =        -9.91;
        b2 =       0.4107;
        c2 =      0.01875;
        a3 =        7.874;
        b3 =       0.4176;
        c3 =      0.01041;


Gauss1_6cm=    a1*exp(-((Frequencies-b1)/c1).^2)  +  a2*exp(-((Frequencies-
b2)/c2).^2) + a3*exp(-((Frequencies-b3)/c3).^2);

        a1 =            0;
        b1 =        62.49;
        c1 =        9.757;
        a2 =        1.186;
        b2 =        0.362;
        c2 =      0.01799;
        a3 =        4.828;
        b3 =       0.3143;
        c3 =      0.03637;


Gauss1_4cm=    a1*exp(-((Frequencies-b1)/c1).^2)  +  a2*exp(-((Frequencies-
b2)/c2).^2) + a3*exp(-((Frequencies-b3)/c3).^2);

        a1 =        2.145;
        b1 =       0.2317;
```

91

```matlab
        c1 =      0.02334;
        a2 =            0;
        b2 =       0.2299;
        c2 =    2.694e-05;
        a3 =        0.806;
        b3 =        0.209;
        c3 =      0.01082;


Gauss1_2cm=a1*exp(-((Frequencies-b1)/c1).^2)     +     a2*exp(-((Frequencies-
b2)/c2).^2) + a3*exp(-((Frequencies-b3)/c3).^2);


Amplitude=[Gauss1_16cm;Gauss1_14cm;Gauss1_12cm;Gauss1_10cm;Gauss1_8cm;Gauss
1_6cm;Gauss1_4cm;Gauss1_2cm]';


h1=mesh(Amplitude,'linewidth',1);
set(h1,'XData',WaterHeight);
set(h1,'YData',Frequencies);

xlabel('Waterheight');
ylabel('Frequencies');
zlabel('Amplitude');


% 3D PLOT OF GAUSSIAN CURVE FITTING FOR ALL WATER HEIGHTS AT 6MM SWAY AMPLITUDE

x = linspace(0.15,0.9,6000);

        a1 =        2.702;
        b1 =       0.8326;
        c1 =      0.05558;
        a2 =        21.91;
        b2 =       0.6074;
        c2 =      0.02949;
        a3 =           15;
        b3 =       0.6096;
        c3 =       0.1216;


Gauss2_16cm=a1*exp(-((x-b1)./c1).^2)+a2*exp(-((x-b2)./c2).^2)+a3*exp(-((x-
b3)./c3).^2);


        a1 =        38.73;
        b1 =       0.5619;
        c1 =      0.04506;
        a2 =       -26.62;
        b2 =       0.5557;
        c2 =      0.02423;
        a3 =        8.327;
        b3 =       0.6063;
        c3 =       0.1453;


Gauss2_14cm=a1*exp(-((x-b1)./c1).^2)+a2*exp(-((x-b2)./c2).^2)+a3*exp(-((x-
b3)./c3).^2);


        a1 =        9.338;
        b1 =       0.5426;
```

92

```
        c1 =      0.1219;
        a2 =       24.79;
        b2 =      0.5656;
        c2 =     0.02016;
        a3 =       11.11;
        b3 =      0.4937;
        c3 =     0.01106;
Gauss2_12cm=a1*exp(-((x-b1)./c1).^2)+a2*exp(-((x-b2)./c2).^2)+a3*exp(-((x-
b3)./c3).^2);


        a1 =       8.589;
        b1 =      0.5013;
        c1 =      0.1137;
        a2 =       9.053;
        b2 =      0.4636;
        c2 =     0.01027;
        a3 =       10.08;
        b3 =       0.515;
        c3 =     0.01801;

Gauss2_10cm=a1*exp(-((x-b1)./c1).^2)+a2*exp(-((x-b2)./c2).^2)+a3*exp(-((x-
b3)./c3).^2);


        a1 =       13.57;
        b1 =      0.4456;
        c1 =     0.01225;
        a2 =      -13.38;
        b2 =      0.4524;
        c2 =    0.009552;
        a3 =       11.93;
        b3 =      0.4519;
        c3 =     0.06992;

Gauss2_8cm=a1*exp(-((x-b1)./c1).^2)+a2*exp(-((x-b2)./c2).^2)+a3*exp(-((x-
b3)./c3).^2);


        a1 =       5.316;
        b1 =      0.3746;
        c1 =     0.01894;
        a2 =       4.062;
        b2 =      0.3818;
        c2 =     0.08954;
        a3 =       5.714;
        b3 =      0.4272;
        c3 =    0.009331;

Gauss2_6cm=a1*exp(-((x-b1)./c1).^2)+a2*exp(-((x-b2)./c2).^2)+a3*exp(-((x-
b3)./c3).^2);


        a1 =        3.75;
        b1 =      0.2963;
        c1 =     0.02549;
        a2 =       3.669;
        b2 =        0.34;
        c2 =     0.04021;
        a3 =           0;
        b3 =      0.3193;
```

```
        c3 =    0.0001949;

Gauss2_4cm=a1*exp(-((x-b1)./c1).^2)+a2*exp(-((x-b2)./c2).^2)+a3*exp(-((x-
b3)./c3).^2);



        a1 =       2.769;
        b1 =      0.2398;
        c1 =     0.01799;
        a2 =           0;
        b2 =      0.2289;
        c2 =   0.0001657;
        a3 =       2.028;
        b3 =      0.2131;
        c3 =     0.01596;


Gauss2_2cm=a1*exp(-((x-b1)./c1).^2)+a2*exp(-((x-b2)./c2).^2)+a3*exp(-((x-
b3)./c3).^2);


Amplitude=[Gauss2_16cm;Gauss2_14cm;Gauss2_12cm;Gauss2_10cm;Gauss2_8cm;Gauss
2_6cm;Gauss2_4cm;Gauss2_2cm]';


h2=mesh(Amplitude,'linewidth',1);
Frequencies=x;
WaterHeight=fliplr([2 4 6 8 10 12 14 16]);
set(h2,'XData',WaterHeight);
set(h2,'YData',Frequencies);

xlabel('Waterheight');
ylabel('Frequencies');
zlabel('Amplitude');



% 3D PLOT OF GAUSSIAN CURVE FITTING FOR ALL WATER HEIGHTS AT 8MM SWAY AMPLITUDE

x = linspace(0.15,0.9,6000);

        a1 =           0;
        b1 =      0.5776;
        c1 =    0.001223;
        a2 =       37.53;
        b2 =      0.5726;
        c2 =      0.1191;
        a3 =      -16.78;
        b3 =      0.5088;
        c3 =     0.08741;

Gauss3_16cm=a1*exp(-((x-b1)./c1).^2)+a2*exp(-((x-b2)./c2).^2)+a3*exp(-((x-
b3)./c3).^2);

        a1 =       20.69;
        b1 =      0.5809;
        c1 =     0.03208;
        a2 =       16.46;
        b2 =       0.517;
```

94

```
        c2 =      0.01561;
        a3 =        13.85;
        b3 =       0.5916;
        c3 =       0.1382;




Gauss3_14cm=a1*exp(-((x-b1)./c1).^2)+a2*exp(-((x-b2)./c2).^2)+a3*exp(-((x-
b3)./c3).^2);


        a1 =        26.42;
        b1 =       0.5649;
        c1 =      0.02257;
        a2 =        8.051;
        b2 =        0.579;
        c2 =        0.135;
        a3 =        14.78;
        b3 =       0.4849;
        c3 =      0.03067;

Gauss3_12cm=a1*exp(-((x-b1)./c1).^2)+a2*exp(-((x-b2)./c2).^2)+a3*exp(-((x-
b3)./c3).^2);


        a1 =        29.13;
        b1 =       0.4748;
        c1 =      0.01586;
        a2 =         22.6;
        b2 =       0.5411;
        c2 =      0.03753;
        a3 =        9.156;
        b3 =       0.4376;
        c3 =      0.04049;

Gauss3_10cm=a1*exp(-((x-b1)./c1).^2)+a2*exp(-((x-b2)./c2).^2)+a3*exp(-((x-
b3)./c3).^2);


        a1 =         14.2;
        b1 =       0.4241;
        c1 =       0.0162;
        a2 =        6.715;
        b2 =         0.39;
        c2 =      0.02806;
        a3 =        11.12;
        b3 =       0.4869;
        c3 =      0.05648;

Gauss3_8cm=a1*exp(-((x-b1)./c1).^2)+a2*exp(-((x-b2)./c2).^2)+a3*exp(-((x-
b3)./c3).^2);


        a1 =       -2.327;
        b1 =        0.347;
        c1 =      0.01088;
        a2 =        10.65;
        b2 =       0.3651;
        c2 =      0.03903;
        a3 =        7.766;
        b3 =       0.4359;
        c3 =      0.02129;
```

```matlab
Gauss3_6cm=a1*exp(-((x-b1)./c1).^2)+a2*exp(-((x-b2)./c2).^2)+a3*exp(-((x-
b3)./c3).^2);
```

```
        a1 =              0;
        b1 =        0.3311;
        c1 =     0.0002884;
        a2 =         1.687;
        b2 =         0.285;
        c2 =       0.01491;
        a3 =         6.635;
        b3 =         0.325;
        c3 =       0.04477;
```

```matlab
Gauss3_4cm=a1*exp(-((x-b1)./c1).^2)+a2*exp(-((x-b2)./c2).^2)+a3*exp(-((x-
b3)./c3).^2);
```

```
        a1 =              0;
        b1 =        0.2271;
        c1 =      0.000507;
        a2 =         3.689;
        b2 =        0.2387;
        c2 =       0.01926;
        a3 =         2.318;
        b3 =        0.2101;
        c3 =       0.01397;
```

```matlab
Gauss3_2cm=a1*exp(-((x-b1)./c1).^2)+a2*exp(-((x-b2)./c2).^2)+a3*exp(-((x-
b3)./c3).^2);

Amplitude=[Gauss3_16cm;Gauss3_14cm;Gauss3_12cm;Gauss3_10cm;Gauss3_8cm;Gauss
3_6cm;Gauss3_4cm;Gauss3_2cm]';

h3=mesh(Amplitude,'linewidth',1);
Frequencies=x;
WaterHeight=fliplr([2 4 6 8 10 12 14 16]);
set(h3,'XData',WaterHeight);
set(h3,'YData',Frequencies);

xlabel('Waterheight');
ylabel('Frequencies');
zlabel('Amplitude');
```